

# **Drone adaptation and configuration to sensor apparatus for on-site, real-time digitalised water quality test application**

Report  
to the Water Research Commission

by

Kousar B. Hoorzook<sup>1</sup>, Atheesha Singh<sup>1</sup>, Ismail Lavangee<sup>2</sup>, Willem Perold<sup>3</sup>, Leon Dicks<sup>3</sup> and Tobias G. Barnard<sup>1</sup>

<sup>1</sup> University of Johannesburg

<sup>2</sup> Drobotics

<sup>3</sup> University of Stellenbosch

WRC report no. 3180/1/24

ISBN 978-0-6392-0677-6

January 2025



**Obtainable from**

Water Research Commission  
Bloukrans Building, Lynnwood Bridge Office Park  
4 Daventry Street  
Lynnwood Manor  
PRETORIA

[hendrickm@wrc.org.za](mailto:hendrickm@wrc.org.za) or download from [www.wrc.org.za](http://www.wrc.org.za)

This is the final report of WRC project no. C2022/2023-00916.

**DISCLAIMER**

This report has been reviewed by the Water Research Commission (WRC) and approved for publication. Approval does not signify that the contents necessarily reflect the views and policies of the WRC, nor does mention of trade names or commercial products constitute endorsement or recommendation for use.

## EXECUTIVE SUMMARY

---

This report describes the development of an integrated water quality test platform that will expand the University of Johannesburg (UJ) mobile laboratory systems with new DronePort system technologies. This system can support various applications for tasks related to water quality testing protocols used to evaluate bacterial, chemical, metal and other content in water as well as expanding its scope in tasks related to security and resource management surveillance, mapping and other defined aerial imagery scopes. The mobile laboratory system provides for multiple test/analytical equipment and consumables to conduct onsite remote water quality tests and analysis. The DronePort technology embedded in the proposed mobile laboratory system supports drone operations for digitalized testing using test probes inserted directly into a water source. The drone operations will also be capacitated to conduct all photogrammetry-related operations as defined within the scope of water resource management. The integrated system will also be capacitated to record, up/download data between drone and laboratory, test apparatus and laboratory via winch-installed universal recorder, laboratory to private cloud.

The participation of UJ in the WRC-sponsored drone adaptation and configuration to sensor apparatus for on-site, real-time digitalised water quality test application project provides a conduit within which it may achieve its objective for creation of an integrated water quality test platform. The title of this WRC-sponsored project also succinctly captures the UJ scope of operations.

Another serious motivation and consideration is that the cutting edge and innovative technologies being piloted involve both bio nanosensors and digital probes launched off drone platform.

The success of the pilot study is contingent on integration of the Stellenbosch University (SUN) digital bacterial probe to Drobotics drone-adapted launch platform configured to relay probe binary data received in real-time from water surface-deployed probes to universal recorders installed and integrated onto the launch platform, further configured to relay data via radio communication in real-time to a command-and-control unit installed in an UJ Mobile Laboratory.

Extensive studies and research related to drones in various applications within water resource management processes were conducted. There is almost no information related to the use of drones in the deployment of digital probes, and nothing related to launch using either sling or winch/hoist systems. The only recorded launch of digital probes from a drone platform involved multiple attached probes directly under drone that was configured as a flotation platform. The recorded use of a sling is for the launch of water samplers in the collection of water, as well as the deployment of sonar beam apparatus. Therefore, the scope of operations developed a hypothesis that a sling and/or winch/hoist system should be best suited as a launch platform for probe insertion into a water source for water quality test processes.

Research was also conducted on Unmanned Aerial Vehicle (UAV) adapted or installed winch systems. There are numerous available off-the-shelf drone adapted winch/hoist system, however, almost all of them in various configurations are designed for transport of parcels/packages from point to point. The scope requires for a more integrated approach in the transport/launch of probe in that it requires release/deploy, stable hover ability and lift, encompassing real-time data received and record.

After consideration of multiple case studies on the use of a drone platform for water resource management, it was resolved to design and build our own integrated drone-adapted winch system as opposed to acquiring and reconfiguring a generic off-the-shelf system. The Drobotics winch/hoist system is designed and configured to launch digital water quality test probes.

Conventional bacterial diagnostics using classic or standard culturing techniques, while inexpensive, require trained technicians in a laboratory setting and a minimum of 24 hours to complete. Faster techniques such as enzyme-linked immune assays and polymerase chain reaction (PCR)-based methodologies are expensive and often require multiple enrichment and purification steps. A recent technological development that is vastly simplifying bacterial detection is the new category of integrated systems collectively known as biosensors/digital probes. Biosensors utilise biological recognition elements specific to the target bacteria and integrate them with optical, electrochemical, or piezoelectric sensors for signal detection.

The digital water quality test probe will detect *Escherichia coli* (*E. coli*) used as indicator/index organisms in general health-related water quality testing. Such *E. coli* is generally enumerated, isolated, and characterised using culture and colony counting methods, PCR, and immunology-based methods and are the most common tools used for pathogen detection. They involve counting of bacteria, DNA analysis and antigen-antibody interactions, respectively. Despite drawbacks such as the time required for testing and the complexity of their use, they are still the recommended testing methods for water quality. Therefore, the standard IDEXX Colilert Quanti-Tray®/2000 method will be used to compare the data generated by the digital water quality test probe to validate the results.

Drone adaptation and configuration to sensor apparatus for on-site, real-time digitalised water quality test application.

## ACKNOWLEDGEMENTS

The project team wishes to thank the following people for their contributions to the project.

<b>Water Research Commission</b>	Yazeed van Wyk and Gerda Kruger
<b>Reference Group members</b>	
Dr W Stone	Stellenbosch University
Dr F Francois	University of the Free State
Mr K Majola	Department of Water and Sanitation
<b>Drobotics Drone Adapted Winch /Coms Build</b>	LS Telkom / LS Multicopter
Advisor and Data/Network Specialist	Koen Schutte
Team Leader Winch Prototype Build/ Drone Ops	Paul Schutte
Communications Integrations	Michael Mommsen
Electrical Engineer	Cedric Nshimba
CAD design program	Machiel Carstens
<b>Multiprobe Jig Design and Build</b>	Stingray Laser Lab
Design and Prototype build of high buoyancy Jig	Yunus Moola
<b>Winch Adapted Expanded Platform</b>	Bulugaya Engineering
Systems Engineering and Fabrications Advisor	Imraan Fahmay
Fabrication of Rail Cart Chassis and Rail Platform	Theo Silobi
Rail Cart Mock up Prototype Assembly and build	MZ Vahed (2 <sup>nd</sup> year UCT Mechatronics)
<b>SUN biosensor Housing</b>	
Design and 3D print of housing Prototype Mark 1	Ewert Snyman
<b>Other Support</b>	Admin, Technical & Logistics Resources
Armscor Mil Vet Incubation Program	Sitembiso Manyoni
WASAA ESD Program	Nokwanele Qonde
<b>Jig, sampling bag and biosensor housing unit design</b>	University of Johannesburg
Designers	Robin Robertson and Xylan de Jager
<b>Other support</b>	University of Johannesburg
Drone footage and YouTube link	Kyle van Heyde
Photographer and Videographer	Annette Ford
Site location	X-Factor Trout Farm – Daniel Factor, Kyle Odgers, (Edenvale)
	Khoisan Village – Johannes Ralph Goliath (Eikenhof)
	University of Johannesburg Island (Vereeniging)
<b>Postgraduate Students</b>	Stellenbosch University
	Nathanial Jiri
	Diron Hurn

# CONTENTS

---

<b>EXECUTIVE SUMMARY</b> .....	<b>iii</b>
<b>ACKNOWLEDGEMENTS</b> .....	<b>v</b>
<b>CONTENTS</b> .....	<b>vi</b>
<b>LIST OF FIGURES</b> .....	<b>x</b>
<b>LIST OF TABLES</b> .....	<b>xii</b>
<b>ACRONYMS &amp; ABBREVIATIONS</b> .....	<b>xiii</b>
<b>CHAPTER 1: BACKGROUND</b> .....	<b>1</b>
<b>1.1 INTRODUCTION</b> .....	<b>1</b>
<b>1.1.2 Technology application process</b> .....	<b>4</b>
<b>1.1.2.1 Pre-testing parameters and protocols</b> .....	<b>4</b>
<b>1.1.2.2 Testing processes</b> .....	<b>5</b>
<b>1.1.3 On-site test platform performance and benefits</b> .....	<b>5</b>
<b>1.2 PROJECT AIMS</b> .....	<b>6</b>
<b>1.3 SCOPE</b> .....	<b>6</b>
<b>1.3.1 Mobile Laboratory</b> .....	<b>6</b>
<b>1.3.2 Computing Capacity</b> .....	<b>7</b>
<b>1.3.3 Communication Capacity</b> .....	<b>7</b>
<b>1.3.4 Software processing of Binary Data</b> .....	<b>7</b>
<b>CHAPTER 2: STELLENBOSCH UNIVERSITY DIGITAL PROBE LITERATURE REVIEW</b> .....	<b>8</b>
<b>2.1 BACKGROUND</b> .....	<b>8</b>
<b>2.2 LITERATURE REVIEW AIMS, SCOPE AND LIMITATIONS</b> .....	<b>9</b>
<b>2.3 OVERVIEW OF WATER QUALITY TESTING</b> .....	<b>9</b>
<b>2.4 CURRENT MICROBIAL WATER QUALITY TESTING METHODS</b> .....	<b>10</b>
<b>2.4.1 Culture-based methods</b> .....	<b>11</b>
<b>2.4.2 Immunological methods</b> .....	<b>12</b>
<b>2.4.3 Molecular-based methods</b> .....	<b>13</b>
<b>2.4.4 Digital probes/biosensors</b> .....	<b>13</b>
<b>2.5 BIOSENSORS</b> .....	<b>14</b>
<b>2.5.1 Transduction mechanism</b> .....	<b>15</b>
<b>2.5.2 Biorecognition element</b> .....	<b>16</b>
<b>2.6 BACTERIOPHAGE-BASED BIOSENSORS</b> .....	<b>16</b>
<b>2.7 BACTERIOPHAGE IMMOBILISATION</b> .....	<b>17</b>
<b>2.7.1 Physical adsorption</b> .....	<b>17</b>
<b>2.7.2 Chemical functionalisation</b> .....	<b>18</b>
<b>2.7.2.1 Popular Covalent Linking Agents</b> .....	<b>18</b>
<b>2.7.3 Electric deposition</b> .....	<b>18</b>
<b>2.8 CONCLUSION</b> .....	<b>19</b>
<b>CHAPTER 3: SIMULATIONS AND MODELLING FOR THE DIGITAL PROBE</b> .....	<b>20</b>

<b>3.1</b>	<b>INTRODUCTION</b> .....	<b>20</b>
<b>3.2</b>	<b>SIMULATION ASSUMPTIONS</b> .....	<b>21</b>
<b>3.3</b>	<b>2D SIMULATION MODEL</b> .....	<b>21</b>
<b>3.3.1</b>	<b>EIS simulation of the model height</b> .....	<b>21</b>
<b>3.3.2</b>	<b>EIS simulation of the redox pair concentration</b> .....	<b>22</b>
<b>3.3.3</b>	<b>EIS simulation of the digit width and gaps between the digits</b> .....	<b>22</b>
<b>3.3.4</b>	<b>EIS simulation of bare and immobilised IDEs</b> .....	<b>22</b>
<b>3.3.5</b>	<b>Cyclic voltammetry of bare and immobilised IDEs</b> .....	<b>23</b>
<b>3.4</b>	<b>3D SIMULATION MODEL</b> .....	<b>24</b>
<b>3.4.1</b>	<b>EIS simulation of the redox pair concentration</b> .....	<b>24</b>
<b>3.4.2</b>	<b>EIS simulation of bare and immobilised IDEs</b> .....	<b>24</b>
<b>3.4.3</b>	<b>Implication of the 3D model</b> .....	<b>24</b>
<b>3.5</b>	<b>CONCLUSION</b> .....	<b>25</b>
<b>CHAPTER 4: METHODOLOGY FOR THE DIGITAL PROBE</b> .....		<b>26</b>
<b>4.1</b>	<b>INTRODUCTION</b> .....	<b>26</b>
<b>4.2</b>	<b>DESIGN DECISIONS AND GOALS</b> .....	<b>26</b>
<b>4.2.1</b>	<b>Selection of the transducer</b> .....	<b>26</b>
<b>4.2.2</b>	<b>Selection of the biorecognition element</b> .....	<b>26</b>
<b>4.2.3</b>	<b>Choosing the immobilisation method</b> .....	<b>27</b>
<b>4.2.4</b>	<b>The biosensor communication protocol and power supply</b> .....	<b>27</b>
<b>4.2.5</b>	<b>Potential for multiplexing</b> .....	<b>27</b>
<b>4.2.6</b>	<b>Laboratory equipment used to develop the biosensor</b> .....	<b>27</b>
<b>4.3</b>	<b>BACTERIOPHAGE CULTURING AND ENUMERATION</b> .....	<b>28</b>
<b>4.3.1</b>	<b>Determining an OD600 calibration curve for <i>E. coli BL21 (DE3)</i></b> .....	<b>28</b>
<b>4.3.2</b>	<b><i>E. coli BL21 (DE3)</i> phage stock preparation and concentration</b> .....	<b>28</b>
<b>4.3.3</b>	<b>Enumeration of <i>E. coli BL21 (DE3)</i> phage using plaque assays</b> .....	<b>29</b>
<b>4.3.4</b>	<b>Determining the lysis profile for <i>E. coli BL21 (DE3)</i> using the TECAN Spark</b> .....	<b>29</b>
<b>4.4</b>	<b>BACTERIOPHAGE IMMOBILISATION PROTOCOLS</b> .....	<b>30</b>
<b>4.4.1</b>	<b>The IDE cleaning protocol</b> .....	<b>30</b>
<b>4.4.2</b>	<b>Physical adsorption protocol</b> .....	<b>31</b>
<b>4.4.3</b>	<b>Covalent immobilisation using cysteamine and glutaraldehyde protocol</b> .....	<b>31</b>
<b>4.4.4</b>	<b>Immobilisation using the electric deposition protocol</b> .....	<b>32</b>
<b>4.5</b>	<b>CONFIRMATION OF THE IMMOBILISATION PROTOCOLS</b> .....	<b>33</b>
<b>4.5.1</b>	<b>The disk-diffusion technique</b> .....	<b>33</b>
<b>4.5.2</b>	<b>Scanning electron microscopy (SEM)</b> .....	<b>34</b>
<b>4.5.3</b>	<b>Confocal microscopy</b> .....	<b>35</b>
<b>4.5.4</b>	<b>Electrochemical Impedance Spectroscopy (EIS) measurements</b> .....	<b>35</b>
<b>4.6</b>	<b>IMPEDANCE ANALYSER</b> .....	<b>36</b>
<b>4.6.1</b>	<b>Design for small signal excitement voltage circuit</b> .....	<b>36</b>
<b>4.6.2</b>	<b>Design for small signal voltage measurement</b> .....	<b>37</b>
<b>4.6.3</b>	<b>Design for current measurement</b> .....	<b>39</b>
<b>CHAPTER 5: RESULTS AND DISCUSSIONS FOR THE DIGITAL PROBE</b> .....		<b>40</b>
<b>5.5</b>	<b>CONCLUSIONS</b> .....	<b>56</b>
<b>CHAPTER 6: DROBOTICS DEVELOPMENT OF WINCH/HOIST SYSTEM FOR THE DRONE-LITERATURE REVIEW</b> .....		<b>58</b>

Drone adaptation and configuration to sensor apparatus for on-site, real-time digitalised water quality test application.

---

<b>6.1</b>	<b>INTRODUCTION</b> .....	<b>58</b>
<b>6.2</b>	<b>SCOPE</b> .....	<b>58</b>
<b>6.2.1</b>	<b>Basic winch/hoist system</b> .....	<b>58</b>
<b>6.2.2</b>	<b>System design protocols</b> .....	<b>59</b>
<b>6.2.3</b>	<b>Winch/hoist system development</b> .....	<b>59</b>
<b>6.2.4</b>	<b>Drone adaptation</b> .....	<b>60</b>
<b>6.2.5</b>	<b>Drone adaptation protocols</b> .....	<b>60</b>
<b>6.2.6</b>	<b>Mobile laboratory installed winch/hoist and drone support system</b> .....	<b>60</b>
 <b>CHAPTER 7: FINAL ASSESSMENT OF WINCH/JIG/COMS SYSTEMS IN OPERATIONAL ENVIROMENT 61</b>		
<b>7.1</b>	<b>INTRODUCTION</b> .....	<b>61</b>
<b>7.2</b>	<b>SCOPE</b> .....	<b>61</b>
<b>7.3</b>	<b>METHODOLOGY</b> .....	<b>61</b>
<b>7.3.1</b>	<b>Drone Platform</b> .....	<b>62</b>
<b>7.3.1.1</b>	<b>DRONE FINAL DEMO</b> .....	<b>63</b>
<b>7.3.2</b>	<b>WINCH/HOIST SYSTEM</b> .....	<b>64</b>
<b>7.3.2.2</b>	<b>Winch/Hoist Final Demo</b> .....	<b>66</b>
<b>7.3.3</b>	<b>JIG DEVELOPMENT</b> .....	<b>Error! Bookmark not defined.</b>
<b>7.3.3.1</b>	<b>JIG Final Demo</b> .....	<b>68</b>
<b>7.3.4</b>	<b>COMMUNICATIONS</b> .....	<b>69</b>
<b>7.3.4.1</b>	<b>Final Communications Demo</b> .....	<b>71</b>
<b>7.3.5</b>	<b>EXPANDED PLATFORM</b> .....	<b>73</b>
<b>7.3.6</b>	<b>FINAL VALIDATION SYNOPSIS</b> .....	<b>74</b>
 <b>CHAPTER 8: UNIVERSITY OF JOHANNESBURG SAMPLING BAG AND BIOSENSOR SAMPLING CARTRIDGE UNIT DEVELOPMENT .....</b>		
<b>75</b>		
<b>8.1</b>	<b>BACKGROUND</b> .....	<b>75</b>
<b>8.2</b>	<b>BIOSENSOR SAMPLING CARTDRIDGE UNIT</b> .....	<b>76</b>
<b>8.2.1</b>	<b>Design Considerations / Goals</b> .....	<b>76</b>
<b>8.2.2</b>	<b>Design Methodology</b> .....	<b>76</b>
<b>8.2.3</b>	<b>System Operations</b> .....	<b>78</b>
<b>8.3</b>	<b>TESTING FLOW OF DRONE SAMPLING WATER COLLECTION BAG</b> .....	<b>79</b>
<b>8.4</b>	<b>METHOD FOR SAMPLING</b> .....	<b>79</b>
 <b>CHAPTER 9: WRC DEMO MICROBIOLOGY RESULTS DISCUSSION .....</b>		
<b>82</b>		
<b>9.1</b>	<b>INTRODUCTION</b> .....	<b>82</b>
<b>9.2</b>	<b>DIGITAL PROBE METHODOLOGY AND RESULTS DISCUSSION</b> .....	<b>82</b>
<b>9.3</b>	<b>CONVENTIONAL METHODS METHODOLOGY AND RESULTS DISCUSSION</b> .....	<b>83</b>
<b>9.4</b>	<b>COMPARISION BETWEEN THE DIGITAL PROBE AND CONVENTIONAL METHODS</b> .....	<b>84</b>
<b>9.5</b>	<b>CONCLUSION</b> .....	<b>85</b>
 <b>CHAPTER 10: CONCLUSIONS, RECOMMENDATIONS AND KNOWLEDGE DISSEMINATION.....</b>		
<b>87</b>		
<b>10.1</b>	<b>CONCLUSIONS</b> .....	<b>87</b>
<b>10.2</b>	<b>RECOMMENDATIONS</b> .....	<b>87</b>
<b>10.3</b>	<b>KNOWLEDGE DISSEMINATION</b> .....	<b>88</b>
<b>REFERENCES</b> .....		<b>89</b>

---

Drone adaptation and configuration to sensor apparatus for on-site, real-time digitalised water quality test application.

---

**APPENDIX A: SIMULATION PARAMETERS.....95**

## LIST OF FIGURES

---

Figure 1:	Illustration for current process matrix vis-e-vie proposed drone water sampling process matrix (Olsson, 2018). .....	3
Figure 2:	Typical Wayward Point Definition using Mission planning Software (Erena et al., 2019). .....	4
Figure 3:	LiDAR, Orthophotography, Bathymetric and 3D images developed using drones (Erena et al., 2019). .....	5
Figure 4:	UJ mobile water testing laboratory. ....	7
Figure 5:	Water quality testing procedure for water resources. ....	9
Figure 6:	The comparison of microbial water testing methods. ....	11
Figure 7:	A typical biosensor model (D. Li et al., 2021). .....	15
Figure 8:	The phage electrical deposition chamber model (Richter et al., 2016; Richter et al., 2017) .....	19
Figure 9:	2D representation of the IDE. ....	20
Figure 10:	Nyquist plot to compare digit widths ranging from 130um to 180um. ....	22
Figure 11:	The Nyquist plot for bare and immobilised electrodes for a 2D model. ....	23
Figure 12:	The cyclic voltammetry for bare and immobilised electrodes in a 2D model. ....	24
Figure 13:	An interdigitated electrode manufactured from TRAX (Cape Town, South Africa) .....	26
Figure 14:	Procedure to obtain the OD600 calibration curve. ....	28
Figure 15:	IDE cleaning procedure. ....	31
Figure 16:	The physical adsorption immobilisation protocol. ....	31
Figure 17:	Covalent immobilisation protocol. ....	32
Figure 18:	Electric deposition protocol. ....	33
Figure 19:	Voltage waveform for electrical deposition. ....	33
Figure 20:	The disk-diffusion technique. ....	34
Figure 21:	The EIS measurement equipment. ....	36
Figure 22:	Small signal excitement circuit. ....	37
Figure 23:	INA331 Instrumental amplifier circuit diagram. ....	38
Figure 24:	Voltage measurement circuit. ....	38
Figure 25:	Current measurement circuit. ....	39
Figure 26:	Excitement signal circuit testing. ....	40
Figure 27:	Small signal voltage measurement circuit testing. ....	41
Figure 28:	Current measurement dc gain testing a) instrumental amplifier output (above) b) overall circuit output (below). ....	42
Figure 29:	ac current measurement circuit testing. ....	42
Figure 30:	Electrical chamber signal generation testing. ....	43

Figure 31:	OD <sub>600</sub> calibration curve for <i>E. coli</i> BL21 (DE3).....	44
Figure 32:	TECAN Spark lysis profile in BHI medium. ....	45
Figure 33:	TECAN Spark lysis profile in PBS. ....	45
Figure 34:	TECAN Spark lysis profile in laboratory Milli-Q. ....	46
Figure 35:	Disk-diffusion test with a) <i>E. coli</i> and b) non-specific <i>S. epidermidis</i> . ....	47
Figure 36:	SEM images of treated IDE: a) Before exposure, and b) After exposure to <i>E. coli</i> BL21 ..... 48	
Figure 37:	Validation of bacteria capture efficacy using confocal microscopy - a) Blank (top), b).....	50
Figure 38:	Raw EIS measurements to confirm immobilisation: a) First day (above) and b) Second day (below). ....	51
Figure 39:	EIS measurements to confirm bacteria capture. ....	53
Figure 40:	Illustration of the winch conceptual (Winch conceptual sketch, 2022).....	58
Figure 41:	Cross section of the motor structural diagram (Structure of stepper motors, 2022). ....	59
Figure 42:	Figure of a) camera, b) laser range finder, c) remote control, d) universal recorder .....	59
Figure 43:	a) Matrice 600 Pro Drone; b) 5 kg Weighted Hover Test using RTK at 5 m height .....	62
Figure 44:	LS Multicopter Matrice 600 Pro Drone Fully Winch/Jig loaded on take-off and Water .....	63
Figure 45:	Control panel screen shot of Geo located sampling and insitu test operations at X- .....	63
Figure 46:	a) Drobotics winch design concept; b) Illustration of the motor structural diagram: cross section parallel to shaft (Anon, 2022). ....	64
Figure 47:	CAD Drawings for the development of the winch/hoist system .....	65
Figure 48:	Winch 3D Printed Housing .....	65
Figure 49:	On-board Winch Computing	65
Figure 50:	Winch Battery Unit	65
Figure 51:	Telemetry Board	65
Figure 52:	Installed Winch Lift Components.	66
Figure 53:	Prototype 2 (aluminium).....	66
Figure 54:	LS Multicopter Multiple Platform Adapted Winch/Hoist System and Remote-Control Unit... 66	
Figure 55:	Schematic of Jig. ....	67
Figure 56:	Prototype Multi Probe holding Jig.....	67
Figure 57:	(A) UJ's Multi Probe holding Jig (B) New Design Protocols (C) Probe Specific Jig (D) SUN biosensor housing (E) SUN biosensor attachment to Jig.....	68
Figure 58:	(A) Drobotics multi probe Jig with onboard aggregate sensor microprocessor (B) Air tag locator (C) Air tag track on iPhone (D) Buoyancy Test. ....	69
Figure 59:	Drobotics Communication Protocols and Architecture.....	69
Figure 60:	Com's assessment, LS Multicopter winch remote, on-board computer.....	70
Figure 61:	LS Multicopter ORP and pH coms integration design architecture.....	70
Figure 62:	Pictures of live stream data captured via YouTube link in Johannesburg, Venda and New Zealand.....	72
Figure 63:	Picture of live stream data from chemical sensors and video footage from.....	72

Figure 64:	Real time communications received from ORP and pH sensors simultaneously on contact with water. ....	72
Figure 65:	ORP, pH integrated coms hardware and improved winch remote control. ....	73
Figure 66:	A) Printed winch housing attached to alternate platform (left). B) Winch system .....	73
Figure 67:	Demonstration at UJ Vaal Dam Island, Vereeniging .....	75
Figure 68:	Exploded Axonometric of all the sample and logic cartridge components creating the Biosensor Sampling Cartridge .....	76
Figure 69:	Rendering of the assembled Biosensor Sampling Cartridge .....	77
Figure 70:	Rendering of the proposed assembly of multiple Biosensor Sampling Cartridges .....	77
Figure 71:	Rendering of the 16 Pin quick connect detail used for hot swapping of the assembly and logic cartridges in the Biosensor Sampling Cartridge .....	78
Figure 72:	Rendering of the internal mechanism of the complete Biosensor Sampling Cartridge .....	79
Figure 73:	Process of sampling to validate the methods .....	80
Figure 74:	Demonstration of sampling methods at X-Factor Trout farm and Khoisan Village. ....	80
Figure 75:	Group picture of members from Water Research Commission, UJ Water and Health .....	81

## LIST OF TABLES

---

Table 1:	Work completed to date .....	<b>Error! Bookmark not defined.</b>
Table 2:	Deliverable due dates and deliverables submitted to date .....	<b>Error! Bookmark not defined.</b>
Table 3:	Examples of microbial water testing methods .....	10
Table 4:	Ideal biosensor properties .....	14
Table 5:	Comparison of bacteriophage immobilisation techniques .....	17
Table 6:	Plaque Assay results .....	44
Table 7:	EIS measurements analysis to confirm immobilisation .....	52
Table 8:	EIS measurements to confirm bacteria capture .....	54
Table 9:	EIS measurement to confirm bacteria capture using a non-specific binding blocking agent .....	54
Table 10:	EIS measurements to confirm biosensor functionality .....	55
Table 11:	Defining the non-linear limit of detections of the biosensor .....	56
Table 12:	Digital chemical testing via Drone platform versus conventional testing. ....	71
Table 13:	Comparison between the conventional methods and digital probe .....	85
Table 14:	Simulation parameters .....	95

## ACRONYMS & ABBREVIATIONS

DWS	Department of Water and Sanitation
BHI	Brain heart infusion
BSSC	Biosensor sampling cartridge
BSL	Biosafety Lab Level
BVLOS	Beyond visual line of sight
CCA	Chromocult Coliforms Agar
CFU	Colony forming units
CHO	Aldehyde group
CNTS	Carbon nanotubes
DNA	Deoxyribonucleic Acid
DST®	Defined Substrate Technology®
DTSP	Dithiobis (succinimidyl propionate)
<i>E. coli</i>	<i>Escherichia coli</i>
ELISA	Enzyme-Linked Immunosorbent Assay
EIS	Electrochemical Impedance Spectroscopy
FISH	Fluorescence in-situ hybridisation
GFP	Green fluorescent protein
GIS	Geographic information system
IDE	Interdigitated electrode
IMS	Immunomagnetic separation
IPTG	Isopropyl Thiogalactopyranoside
lacZ	Gene encoding $\beta$ -galactosidase
Lin	Input current
LiNbO3	Lithium niobate
LFA	Lateral flow assays
LOD	Limit of detection
MHz	Megahertz (Resonant frequency)
m-LGA	Membrane Lactose Glucuronide Agar
MOI	Multiplicity of infection
MPN	Most probable number
MUG	4-methylumbelliferyl- $\beta$ -D-glucuronide
NASBA	Nucleic Acid Sequence-based Amplification
NIWIS	National Integrated Water Information Systems
ONPG	O-nitrophenyl- $\beta$ -D-galactopyranoside
PBS	Phosphate-buffered saline
Phages	Bacteriophages
PCR	Polymerase chain reaction
PEG	Polyethylene glycol

PFU	Plaque forming units
PTFE	Polytetrafluoroethylene
RNA	Ribonucleic Acid
RQIS	Resource Quality Information Systems
RTK	Real-time kinematic positioning
RT-qPCR	Real-time quantitative PCR
SACAA	South African Civil Aviation Authority
SAM	Self-assembled monolayer
SANS	South African National Standards
<i>S. epidermidis</i>	<i>Staphylococcus epidermidis</i>
SEM	Scanning Electron Microscopy
SiO <sub>2</sub>	Silicon dioxide (Quartz)
SPEs	Screen Printed Electrodes
SPR	Surface Plasmon Resonance
SPREETA	Electro Optical Device
SUN	Stellenbosch University
TC	Total Coliform
TIA	Technology Innovation Agency
UAV	Unmanned aerial vehicle
uidA	β-D-galactosidase
UJ	University of Johannesburg
UV	Ultraviolet
VLOS	Visual line of sight
WHO	World Health Organisation
WMS	Water Management Systems
ZnO	Zinc Oxide

## CHAPTER 1: BACKGROUND

---

### 1.1 INTRODUCTION

The need to pursue onsite real-time water quality testing is largely prompted and informed to resolve challenges related to an effective dashboard system that is critical to the management, monitoring and oversight of our water resources.

In 2013/14, the Department of Water and Sanitation (DWS) developed the National Integrated Water Information System (NIWIS) platform whose objective and technology is laudable but whose effectiveness is contingent on data received. A major drawback is the fact that responsibility for populating data into the NIWIS platform is delegated to a responsible human interface and, in the event that such data population should not occur, for whatever reason, the effectiveness of the dashboard is compromised to negatively impact the management and oversight of our water resource. Based on extensive research, we can arguably determine that 75% of binary data aggregated to the NIWIS platform originates directly from the water source, be they dams, lakes, rivers, reservoir, treatment plants, etc.

Staff within the DWS informed the project team that, currently, Resource Quality Information Systems (RQIS) and regional staff collect water samples at prescribed intervals and submit them for quality analysis at RQIS or other appointed laboratories. The water quality results are validated before being captured in the Water Management System (WMS) database. The uploading, storage and validation of such information in the WMS database is time consuming, as the stored procedure for monthly values uses the monthly mean value for each variable while annual information requires the use of the yearly median values of each variable, prior to comparison against the drinking water guidelines.

Thus, currently most water quality and water resource compliance situations deteriorate substantially before government is alerted, mainly by media often in the face of impending or resultant disasters associated with excess waste effluent, industrial pollution, or environmental changes in response to drought.

In contrast, our initiative is designed to support a radically new approach to testing, monitoring and oversight of water quality protocols to improve current water quality testing by involving more real-time testing and analytical assessments to ensure a rapid response that includes interventions designed to improve situational awareness in the management of critical water resources.

The establishment of onsite water quality testing and delivery of results at, or near, real time is a paradigm shift in water testing and oversight protocols and offers a salient solution in the sustained capture of 75% of source binary data needed for effective implementation of dashboard communication strategies. Such effective implementation is central to optimal planning, management and oversight of water resources, as well as infrastructure management, security, and oversight processes.

The University of Johannesburg (UJ) mobile laboratory expansion program, including this project with embedded drone is geared to strengthening and supporting conventional and digitized onsite testing. As indicated previously, all water quality tests are carried out at laboratories mostly located at centers away from the water source. This requires a process whereby accredited personnel visit water locations and physically acquire samples which are then transported to laboratories where tests are carried out and evaluated. In contrast, the proposed implementation of digital test probes and expanded scope in the use of drone water sampler technology and subsequent onsite tests using the mobile laboratory system provides for almost

Drone adaptation and configuration to sensor apparatus for on-site, real-time digitalised water quality test application.

---

instantaneous analysis and evaluation resulting from binary data being uploaded in real time or near real time, subject only to specific test incubation protocol constraints.

The implementation of this digital testing technology shall be established and implemented in all districts and metros nationally and the protocols supported by water sampler technology will enhance the mobile laboratory system in carrying out water quality tests at remote locations is a novel testing and analytical paradigm in relation to:

- Conducting all tests and sourcing all imagery at remote locations.
- Securing 75% of binary data contingent for effective dashboard communication.
- Acquiring near real time critical data from remote locations.
- Obtaining national cover through deployment of mobile units aligned to districts.
- Managing district modular water resources and oversight.
- Optimizing, reinvigorating, and resuscitating the NIWIS Dashboard Platform.
- Removing the human interface in processing and uploading of data to the NIWIS platform.
- Obviating the use of boats or putting personnel into the water.

The principal outcome in the development of such technology is to ensure maximum consistency in periodic scheduled water quality testing to Blue and Green Drop and other regulatory standards.

The technology improves on previous and current modus operandi in the following ways:

- The mobile suite of testing equipment and consumables meets all requirements for:
  - Bacterial detection analysis.
  - Physical chemical analysis.
  - Metal detection analysis.
  - All aerial imagery-related applications.
- Improves planning and coordination of testing activity.
- Improves test efficacy through onsite testing.
- Aligns testing within districts according to national scope objectives.
- Improves monitoring and oversight of the statutory testing mandate.
- The real time results promote instant intervention.

The binary data received from all districts aligned test will provide critical source data to reinvigorate the NIWIS system. It will re-establish the NIWIS dashboard platform as originally intended, allow for substantial saving in finances that are required to recreate an alternate platform, the proposed technologies are unambiguous with clearly defined tangible and the measurable outcomes related to application expectations and budgetary costs (CAPEX and OPEX) are all factors critical for long term planning in water quality analysis.

Mobile laboratories offer an improved and faster option for a multitude of required tests. Remote onsite testing in the mobile laboratory is more efficient because results can be obtained quickly by a single analyst using representative samples. Results may be saved on an instrument data log for upload to the Cloud and may also be saved manually in an analyst notebook.

Unmanned aerial vehicles (UAVs), or drones, that are used as platforms to launch digital probes and are also capable of collecting and retrieving water samples will revolutionize water quality test processes. Costs related to current processes will significantly be reduced. Such costs typically include a boat and associated equipment, boat transportation, access road maintenance, water safety devices, water safety training, and additional staff. Hazards include the potential for drowning, unstable pit walls, and unconsolidated sediment surrounding tailing ponds (Olsson, 2018). Robotics use a novel device for aerial drones which currently enables the collection of water samples from depths up to 10 m. This system only requires a remote-controlled pilot, a sample technician, and a safe operations point overlooking the water body. We anticipate that this will

improve safety, reduce staffing requirements, and accelerating data acquisition. The diagram below illustrates the current process matrix vis-e-vie the proposed drone water sampling process matrix (Figure 1).

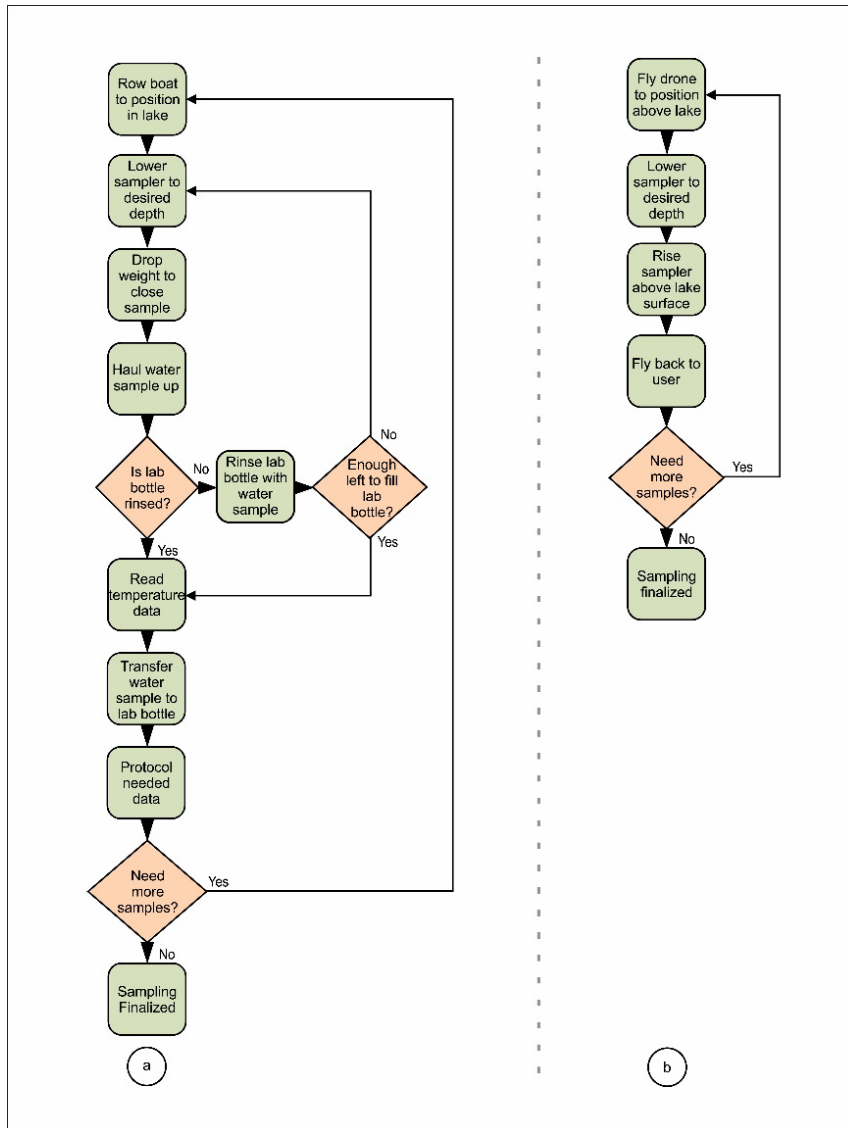


**Figure 1:** Comparison of (a) standard and (b) proposed drone water sampling processes (Olsson, 2018).

In South Africa there is a scarcity of fresh water that is decreasing in quality due to increased pollution and destruction of river basins, caused by urbanization, deforestation, damming of rivers, destruction of wetlands, illegal uses in industry, mining and agriculture (Mclure, 2021). The situation is further aggravated by drought and floods attributed to the impact of global warming, climate change, and unfortunately poor planning and water management systems (Kusangaya et al., 2021).

The technology proposed in this study is geared to respond proactively to all challenges, as the mobile laboratory system, when fully resourced and equipped, is designed to test and detect microbiological and chemical pollutants in water systems within defined scheduled periodic timetables to serve as an early detection system in our water management and oversight processes and protocols.

The current failure and weakness in South African water resource management can be directly attributed to the lack of binary information and data on water quality and security and adopting our technology provides a holistic and sustainable approach to the water quality test in a methodical framework.

Drone adaptation and configuration to sensor apparatus for on-site, real-time digitalised water quality test application.

---

The impact of this technology within our embedded drone mobile laboratory system will correlate directly with its renewed and sustained ability to acquire and process critical information and data in the management of water resources. The solution provided by this technology is to provide a platform and process to primarily conduct remote onsite scheduled and ad hoc test and evaluations related to microbiological, physiochemical, and heavy metals analysis, before uploading results in real time to a department cloud engine feeding into the NIWIS. Drone operations shall also be expanded to carry out aerial type operations to deliver geographic information systems (GIS) mapping, Lidar, and infra-thermal, multi-spectral and photographic imagery (Figure 2). The direct access to the water resource and infrastructure allows the embedded drone mobile laboratory system to provide 75% of all binary data.

The impact on the water sector will be to establish a mandatory scheduled water test system at all district levels that provides a critical service in the monitoring and oversight of water quality and water security.

### 1.1.1 Proposed application of onsite platform

The UJ has developed a mobile water testing laboratory that was funded by the Technology Innovation Agency (TIA) in 2016-2018. This mobile laboratory can travel off-road and stay off the grid for a week without an external electricity supply. The laboratory is equipped to test for water, sanitation and hygiene, faecal analysis, and physical chemistry (pH, EC, turbidity, free and total chlorine). The methods used in the mobile laboratory for microbiology analysis and enumeration of *E. coli*, Total coliforms, *Vibrio*, *Salmonella*, *Shigella* and *Enterococci* are standard manual methods such as membrane filtration and IDEXX Colilert® Quanti-Tray methods.

Stellenbosch University (SUN) has developed a bacterial biosensor that will target *E. coli* directly from the water source. Biosensors measure biological or chemical reactants by generating signals proportional to the concentrations of an analyte in the reaction.

### 1.1.2 Technology application process

#### 1.1.2.1 Pre-testing parameters and protocols

In the implementation of an on-site test platform, certain preliminary groundwork must be conducted to generate capacity-defining grid coordinates of test parameters for all water quality holding areas against which future digitalized testing may be compared. This is important for monitoring and oversight in the evaluation of the consistency of the data from specific points (Figure 2).

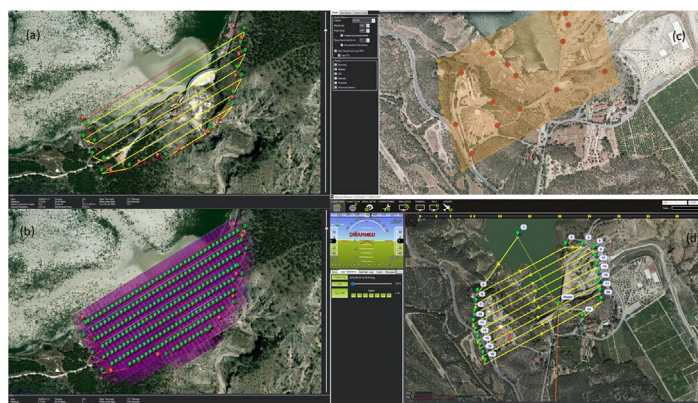


**Figure 2:** Typical wayward point definition using mission planning software (Erena et al., 2019).

Drone adaptation and configuration to sensor apparatus for on-site, real-time digitalised water quality test application.

### 1.1.2.2 Testing processes

The drone-adapted water sampler can be used to collect samples at multiple depths from lakes, dams, reservoirs and other water catchment areas within defined GPS grid identified locations. Sufficient water will be collected from each point for microbiological, physio-chemical and heavy metal analysis. These tests will be conducted onsite, and the resulting evaluation and analysis binary data will be uploaded in real time to a cloud-based management system.

The expanded scope of the drone will provide the GIS mapping, Lidar, infra-thermal, multi-spectral and photographic imagery that will also be uploaded and fed into the cloud-based management system (Figure 3).

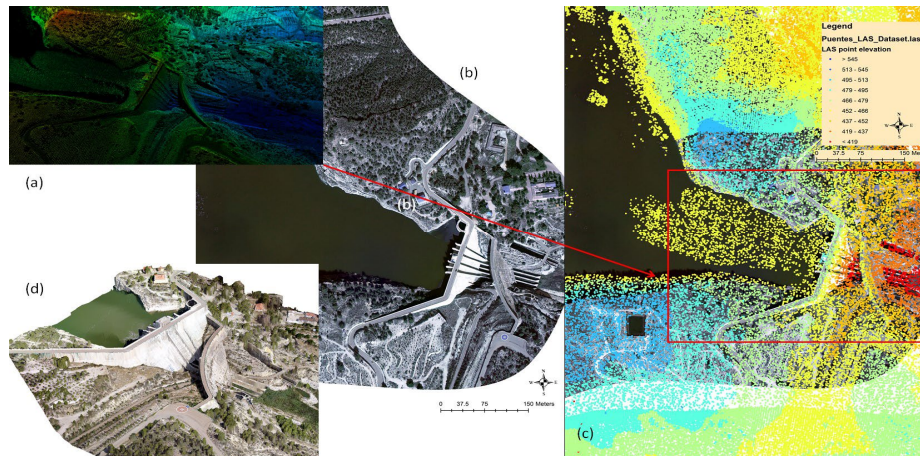


**Figure 3:** LiDAR, orthophotography, bathymetric and 3D images developed using drones (Erena et al., 2019).

The expanded scope of drone operations supported by an onsite mobile laboratory and real-time communication link provides a salient solution in securing comprehensive data, critical for water resource management.

### 1.1.3 On-site test platform performance and benefits

The core focus of this concept is to provide a sustainable solution to the testing, monitoring and oversight of water quality from point-of-source to consumer. This requires that all testing activities be conducted directly at water source and/or water storage and/or water treatment locations. The expanded scope consists of conducting periodic aerial monitoring and supervision of water availability and infrastructure.

The mobile platform, drone-supported digitised testing, and water sampling apparatus technology is an integral part of the basket of technologies operating as a system designed to support water resource management in critical monitoring and oversight functions related to water quality, water security, and water infrastructure. Such technologies were introduced in the creation of systems and have all been proven in their independent and individual scopes of operations. As cited by Olsson (2018), documented studies conducted by Auckland and Sydney local authorities indicated that the water samplers all worked adequately in their various applications. The mobile laboratory has proven successful in all testing protocols as required in water quality test operating in Congo, Gabon, Vietnam and Uganda (Wagtech Projects, 2022).

A recent technological development that is vastly simplifying bacterial detection is the new category of integrated systems collectively known as biosensors/digital probes. Biosensors use biological recognition elements specific to the target bacteria and integrate them with optical, electrochemical, or piezoelectric

sensors for signal detection. Portable biosensors are capable of accurately detecting and identifying bacteria in less than ten minutes (Nikkhoo et al., 2016). These can be embedded within a drone such as the Drobotics drone that is locally manufactured and has successfully carried out surveillance operations for crime intelligence. This drone will initially adapt the Van Dorn Sampler for its operations (Olsson, 2018). The cloud-based system will be designed to accommodate all envisaged water monitoring dashboard objectives and is geared and configured to receive binary data provided as outcome deliverables for the water sampler and digitised technology as they are fed into the expanded drone-embedded mobile laboratory system.

The implementation of our technology will directly benefit the regular scheduled binary data on the following:

1. Drinking water quality.
2. Wastewater quality.
3. Raw water quality.
4. Surface water status.
5. Surface water storage.
6. Groundwater status.
7. River flows.
8. Monitoring of dams.
9. Eutrophication hot spots.
10. Water reservoir monitoring.
11. Government water schemes monitoring.

## **1.2 PROJECT AIMS**

The following are the aims of the project:

1. To develop a drone winch lift system to transport digital probes and collected water samples
2. To develop a remote test platform for on-site, real-time digitalised water quality test applications

## **1.3 SCOPE**

Our fundamental scope is to expand the UJ mobile laboratory to ensure real-time, onsite water quality test processes with integrated capacity for instantaneous and real-time transmission of data aggregated and posted to the dashboard.

### **1.3.1 Mobile Laboratory**

The UJ mobile laboratory is currently installed in a trailer type vehicle, which is equipped and can be transported to any remote area and perform microbiology analysis outside the grid (Figure 4). The mobile laboratory is currently capacitated to carry out on-site tests for conventional analysis. The objective in embedding a drone port system enhances and supports current scope in that through using a drone that is installed with a winch/hoist system, this provides the ability to both collect samples and conduct digitalized testing of bacteria, as well as physiochemical and chemical parameters.

Drone adaptation and configuration to sensor apparatus for on-site, real-time digitalised water quality test application.

---



**Figure 4: UJ mobile water testing laboratory.**

The success of the proposed system depends on the mobile laboratory being installed with the following additional capacity:

- a) 1x mobile laboratory (UJ)
- b) Vehicle embedded with DronePort (Drobotics)
- c) Vehicle installed with communication system (Drobotics)
- d) Vehicle installed with auxiliary power capacity (Drobotics)
- e) 1x Electric Drone (Drobotics)
- f) Combined manual test kits for bacteriological analysis (UJ)
- g) 1x digital bacterial probe (SUN)
- h) Winch/Hoist adapted water Sampler (Drobotics)
- i) Access to all photogrammetry and other aerial imagery capture equipment (Drobotics)

### **1.3.2 Computing Capacity**

Computing capacity will be installed to mobile laboratory to receive test binary data from the winch-installed universal recorder for aggregation and transmission to Cloud in real and/or near real-time.

### **1.3.3 Communication Capacity**

We have access to multiple off-the-shelf technologies that meet our requirements. The ability to upload and download to and from drone using radio frequency for up to 1 km and up/download from Cloud as well as video data transmission and receive using satellite.

### **1.3.4 Software processing of Binary Data**

Software development to process the binary data must meet expectations regarding information and communication stakeholder-designed format in their dashboard. This process is a critical outcome deliverable to ensure intervention and, more importantly, oversight and monitoring of the water management system. The paradigm shift presented in testing protocols to elicit real-time results shall not be met if back-end conversion of binary data to dashboard communicator is not integrated. The conversion of binary data is a deliverable of the proposed total integrated test system.

## CHAPTER 2: STELLENBOSCH UNIVERSITY DIGITAL PROBE LITERATURE REVIEW

---

### 2.1 BACKGROUND

Clean water has become a global issue that affects many countries, with 2.2 billion people worldwide lacking access to safe drinking water (Boretti & Rosa, 2019). Freshwater resources provide more than 70% of the world's water supply, making them a critical resource (Ahuja, 2017; Albert, 2000). It is predicted that if we do not start to manage and maintain the current water resources well, almost 6 billion people will lack access to clean water by 2050 (Boretti & Rosa, 2019). And, as indicated by the rising occurrences of water-related disease outbreaks and demand for water treatment, ensuring water quality is critical to managing water resources, and water quality monitoring serves as the first step towards achieving this.

Water quality monitoring alerts authorities as to when water is contaminated with, for example, pathogenic bacteria such as *E. coli* or pollutants such as heavy metals. A rapid test can aid governments and communities in expanding water resource monitoring. This will provide more information on water quality, to allow its treatment, to identify areas for improvement, and to track progress towards Sustainable Development Goal 6. Additionally, data collected on water quality would also enable governments to develop evidence-based policies and implement early, preventative measures on a national scale. According to UNICEF, which supports approximately 100 national-scale household water quality surveys to track progress towards access to safe water, these household surveys alone require at least 1 million tests per year for this purpose, demonstrating the enormous potential demand for a rapid test (UNICEF, 2023).

The current field-testing methods for water quality are time-consuming, taking 18-24 hours to return a result. The required equipment is bulky to carry, is complex to use, requiring trained technicians. In addition, in remote settings, there is limited access to laboratories, electricity, and cold-chain transport (Offenbaume et al., 2020; Sartory & Watkins, 1999). Due to the long processing time, communities often do not get to see the water quality results and this limits their ability to understand and communicate risks. As a result of these issues, there is a need for the development of an easy-to-use, rapid-detection method or portable kit capable of accurately identifying contaminants in drinking water. According to the UNICEF Office of Innovation, early water testing prototypes have reduced testing time from 24 hours to less than 10 hours (UNICEF, 2023).

Stellenbosch University's Sensor Application and Nano-devices research group, in collaboration with various departments from the university, has been actively developing biosensors for diverse applications ranging from environmental monitoring to medical diagnostics. While most of these research projects have yet to transition into real-life adoption to replace traditional systems, the collaboration with the University of Johannesburg and Drobotics presents Stellenbosch University with a unique opportunity and platform to extend their activities. This partnership aims to develop and demonstrate an entire system capable of replacing and enhancing traditional water resource testing capabilities in South Africa. Stellenbosch University's immediate mandate and deliverable outcome involves designing and developing digital probes for testing *Escherichia coli* (*E. coli*), to achieve near real-time uploading of analysis results. This chapter provides a summary of the literature considered in the development of digital probes, offering an overview of current microbial water quality testing methods and biosensing.

## 2.2 LITERATURE REVIEW AIMS, SCOPE AND LIMITATIONS

The aim of the literature review was to provide an overview so as to understand water quality testing of water resources from the following perspectives

1. Current trends in microbial water quality testing
2. Current biosensors for water quality testing
3. Bacteriophages and their immobilisation protocols for use in biosensing.

## 2.3 OVERVIEW OF WATER QUALITY TESTING

Figure 5 summarises the water quality testing procedure for water resources, from sampling to the analysis and presentation of the water quality results. To ensure that the water resource results are representative, proper sampling techniques must be used, which include selecting representative sampling points and water sample collection in sterile bottles or containers to avoid contamination. Furthermore, optimal preservation and transportation of water samples prior to testing is critical to ensuring proper water source representation. Physical, chemical, and biological parameters are tested to establish the quality of water. Physical parameters indicate sense-detectable properties, whereas chemical tests quantify the amounts of mineral and organic substances that influence water quality, and biological tests reveal the presence of microorganisms in water.

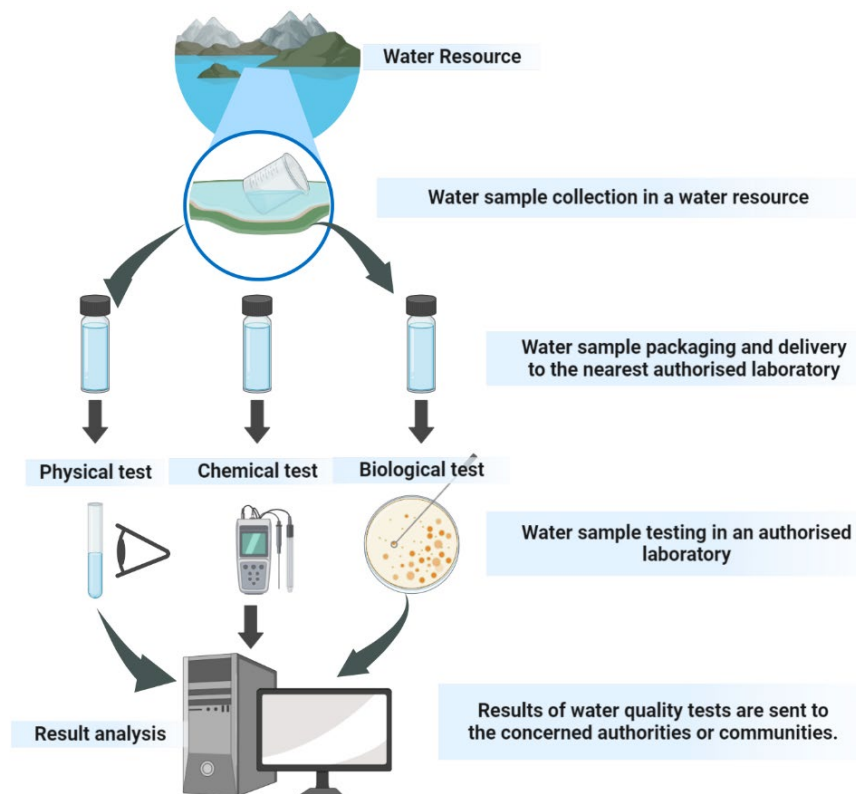


**Figure 5:** Water quality testing procedure for water resources.

Physical parameters are evaluated to properly understand the appearance and clarity of the water. These parameters provide early warning signs of water quality problems. Temperature, turbidity (cloudiness), colour, odour, and taste are many of the potential measurements. Temperature has the potential to influence biological processes in bodies of water, and abnormal readings may indicate pollution (Patil, 2012). Turbidity is a measure of suspended particles that can impact light penetration and thus aquatic ecosystems. The presence

of contaminants or pollutants may be indicated by unusual colour, odour, or taste. There are numerous commercially available sensors for these various physical parameters.

Chemical testing has long been used to evaluate the quality of water (Patil, 2012). Common parameters measured include pH, dissolved oxygen, turbidity, and concentrations of various chemical compounds such as nitrates, phosphates, heavy metals, and organic pollutants. These tests provide valuable information about the composition of the water, levels of contamination, and potential health risks. However, chemical testing alone may not reveal the full extent of water quality issues, as it does not account for biological factors (Patil, 2012). Many commercially available sensors are extremely reliable for performing these chemical tests.

Biological parameters provide insights into the presence of microorganisms, including bacteria, viruses, and parasites. Of these parameters, indicator bacteria are routinely tested, indicating the risk of faecal contamination, while other microorganisms may be examined in cases of water-related emergencies. Bacterial indicators such as *E. coli* and coliform bacteria are commonly used to monitor water quality because they are cost-effective and provide rapid results, making them valuable tools for assessing water quality (Basili et al., 2023; Hoefel et al., 2003; Rompré et al., 2002). Coliforms including *E. coli* are commonly found in a variety of natural habitats but their presence in drinking water should be regarded as a potential indicator of a decline in microbiological water quality (Guidelines for Drinking-Water Quality, 2017). Scientists have been debating for many years whether the coliform group can be used to detect the presence of enteric pathogens in water, with many authors reporting outbreaks of waterborne diseases in water that met the coliform regulation standards (Leclerc et al., 2001). However, the goal of this review is not to debate the indicator concept, but rather to identify methods for monitoring these coliforms in water. Biological parameters are frequently tested using microbial laboratory methods, and currently, there are limited reliable biosensors, with the majority still in the research phase (Ahovan et al., 2020; Cesewski & Johnson, 2020; Kaya et al., 2021; Lazcka et al., 2007; Maas et al., 2017; Thévenot et al., 2001).

## 2.4 CURRENT MICROBIAL WATER QUALITY TESTING METHODS

As summarised in Table 3, microbial water quality testing methods can be classified into three types: qualitative, quantitative, and identification. Qualitative test methods provide presence/absence results that describe the presence or absence of microbial contamination in a water sample. Quantitative testing methods yield a numerical result that represents the total number of contaminants/bacteria in the water sample. Identification techniques provide particular strain information on bacteria found in a water sample.

**Table 1:** Examples of microbial water testing methods

Classification	Example
Qualitative	Using selective culture media; most probable number (MPN) test
Quantitative	Using plate count on a solid agar medium; membrane filtration
Strain identification	Using polymerase chain reaction (PCR); next-generation sequencing

These methods can be categorised into culture-based, molecular-based, and biosensor-based methods. Figure 6 illustrates a comparison of these method categories, emphasising the advantages of culture-based methods compared to emerging molecular and biosensor-based methods. The current methods are relatively simple and require basic laboratory equipment. However, they are labour-intensive and necessitate at least an overnight incubation. Depending on the available laboratory technicians, a relatively large number of samples can be analysed daily in a basic laboratory.

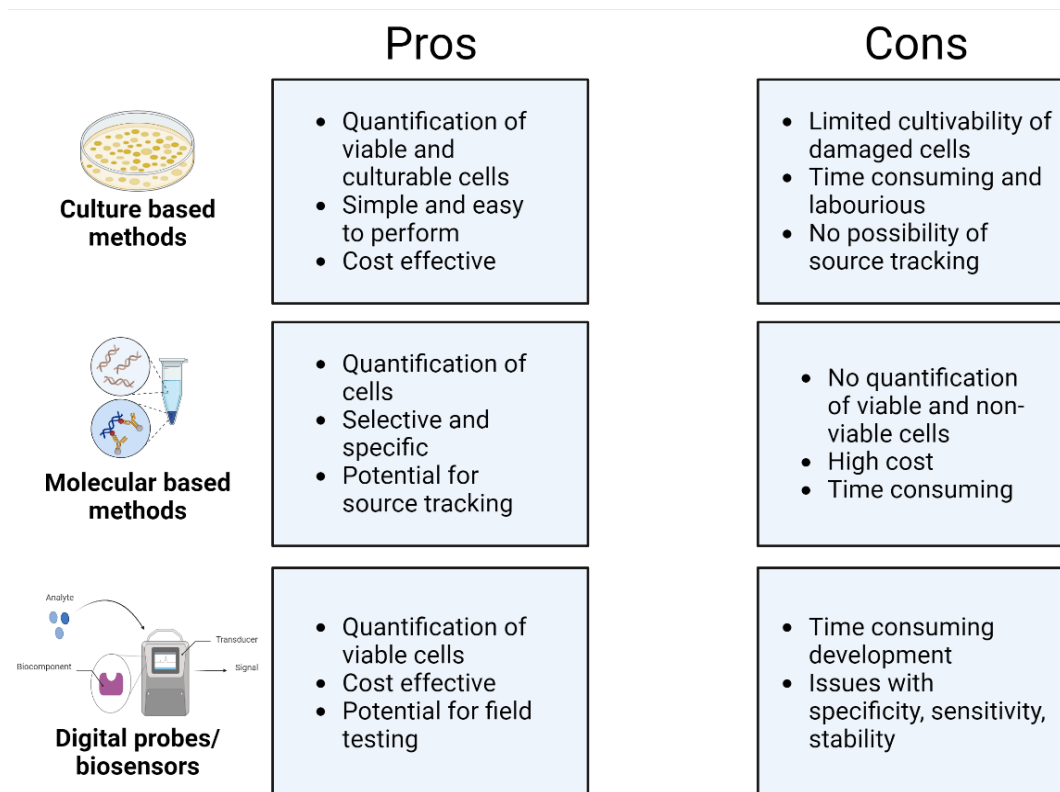


**Figure 6:** Comparison of microbial water testing methods.

### 2.4.1 Culture-based methods

The culture-based techniques are considered the gold standard because they provide a model for *in vivo* and *in vitro* analysis of microbial water quality, enhancing the understanding of microbial diversity (Lagier et al., 2015). Among these culture-based methods, the membrane filtration and plate count method are commonly used; they assess the number of bacteria in water samples that can form visible colonies under specified test conditions, such as medium nutrients, incubation time, incubation temperature, etc. (Eccles et al., 2004; Lagier et al., 2015; Sartory & Watkins, 1999). However, these culture-based techniques have limitations. For example, the methods are time-consuming as they require 18-48 hours for bacterial growth, and necessitate a laboratory with trained professionals, making them inadequate when rapid results are required (Eccles et al., 2004; Lagier et al., 2015; Niemela et al., 2003; Sartory & Watkins, 1999).

The 3M™ Petrifilm™ *E. coli*/coliform count plates are examples of commercially available media plates that offer a cost-effective, convenient, and reliable method for testing various samples, including water (Murcott et al., 2015). These count plates constitute a sample-ready culture medium system containing a beta-glucuronidase-specific indicator dye, that results in a permanent blue halo around *E. coli* colonies, and contain the coliform selective agents found in violet-red bile (VRB) nutrients. By eliminating subsequent confirmation steps required by most traditional reference methods, this method can contribute to increased productivity and reduced overall laboratory costs by providing confirmed results within 24-48 hours.

The Aquagenx Compartment Bag Test (CBT) is another commercial test that detects the presence or absence of *E. coli* in a series of five differentially sized compartments of a WhirlPak-type bag and allows scoring of results in 20-48 hours (Aquagenx, n.d.). The most probable number of *E. coli* bacteria is estimated from the combination of positive and negative compartments.

The Easygel® Card (now renamed as R-Card®) is another commercial card-based media plate that can be used to count for both *E. coli* and total coliforms. Similar to Petrifilm™, the test contains a colour-linked sugar for easy counting of bacterial colonies providing results in 20-24 hours (Roth Bioscience, 2022).

The Colilert-18 defined-substrate technology system (IDEXX Laboratories, Inc., Westbrook, Maine) for the enumeration of *E. coli* and total coliforms is approved by many environmental water bodies worldwide as a standard for water quality testing, and this system provides rapid results in 18 hours (DeSarno et al., 2018; Pisciotta et al., 2002). A most probable number (MPN) estimate of total coliform and *E. coli* numbers is achieved through the use of a Quanti-tray partitioned into 48 small (120- $\mu$ l) and 49 large (1.6 ml) wells. Various versions of the Colilert system have been shown to yield results that are statistically consistent with the standard methods of membrane filtration and multiple-tube fermentation methods used for the detection of coliforms and *E. coli* in water (Covert et al., 1989; Covert et al., 1992; Eckner, 1998; Edberg et al., 1988). The IDEXX Quanti-Tray® is both reliable and accurate, producing results for 100 ml samples with 95% confidence limits. While standardly approved for wide use, the high cost per test limits its suitability for resource-constrained settings. Moreover, the Quanti-Tray® requires a laboratory setting (Pisciotta et al., 2002).

The biochemical test is one of the most useful conventional culture-based method for identifying bacteria and is usually performed after bacterial culture. The fundamental idea of biochemical tests is based on differences in the biochemical activities of bacteria, such as the ability to hydrolyse starch. However, several drawbacks of this approach have been identified (Hameed et al., 2018; Atiq et al., 2020; Ramees et al., 2017). Some assays, for example, are not specific and must rely on a series of other biochemical tests to identify bacteria that match the results. This technique has limited accuracy as evidenced by false positive/negative results (Atiq et al., 2020; Ramees et al., 2017). One example of a biochemical test is the hydrogen sulphide ( $H_2S$ ) strip/powder technique, where the water sample is placed in a bottle with a  $H_2S$  strip/powder and allowed to react. The positive reaction produces hydrogen sulphide gas, which can be detected by the appearance of a black colour (Gunda & Mitra, 2016). This method is a qualitative test that provides a presence/absence assessment for coliform bacteria and can be carried out at the source or point-of-use.

## 2.4.2 Immunological methods

The immunological identification techniques are based on the principle of specific binding between antibodies and antigens. The availability of known and appropriate antisera containing monoclonal or polyclonal antibodies capable of detecting the presence of an unknown antigen or microbial pathogen is the fundamental requirement for the immunological technique (Chang et al., 2016; Välimaa et al., 2015). Generally, the limit of detection of immunological assay techniques is between  $10^4$  and  $10^5$  CFU/ml, giving it a higher sensitivity than the culture-based techniques (Liu et al., 2022). Although immunological techniques can be used to analyse water samples more rapidly, culture enrichment is still required for the assay, and this enrichment step is its major limitation. The enzyme-linked immunosorbent assay (ELISA) and immunomagnetic separation are such examples discussed in this literature review.

The ELISA is an extensively used assay for quantitative detection of antibodies against pathogens in biological fluids and has high specificity and sensitivity (Popli, 2023; Nnachi et al., 2022; Dixon, 1987). It is performed in 96-well microtiter plates and employs the antigen-antibody interaction and enzyme-dependent development reaction (colourimetric, fluorescent or chemiluminescent) The intensity of the signal measured by a spectrophotometer as the optical density (OD) of a well can be directly or inversely proportional to the concentration/number of antibodies detected (Nnachi et al., 2022; González et al., 1993). The ELISA requires a shorter detection time than culture-based methods. However, producing suitable antibodies for the target bacteria envisioned is difficult and time-consuming due to the requirement of living organisms as hosts. Several studies have reported the detection of pathogenic bacteria in water samples, primarily focusing on *E. coli* O157:H7, one of the most dangerous pathogens worldwide (Pang et al., 2018; Shan et al., 2016). An

innovative, fast, and low-cost paper-based enzyme-linked immunosorbent assay (p-ELISA) has been developed, demonstrating high sensitivity and specificity for on-site detection of *E. coli* (Li et al., 2019; Pang et al., 2018; Gonzalez et al., 2018).

Immunomagnetic separation (IMS) detects pathogens in samples by using immunomagnetic beads. Similar to ELISA, this technique however selectively concentrates the target pathogen by allowing it to grow while suppressing the growth of other non-target pathogens. The target pathogens are concentrated using magnetic beads that have been conjugated with antibodies against the pathogens of interest (Hussain et al., 2017; Jones, 2015). The IMS technique gained popularity due to its ability to (1) selectively separate and concentrate the target pathogen from various samples within a short time and (2) produce the same accuracy across multiple detections. This method is easy to use because the user can observe a present/absent result. Currently, the IMS technique is used in conjunction with other techniques such as PCR to increase the sensitivity of the assay. Combining IMS with other assay techniques is necessary because it reduces the time required to detect bacterial pathogens (Dąbrowiecki et al., 2019).

### 2.4.3 Molecular-based methods

Water quality testing using molecular methods is recommended, as these techniques enable highly specific and rapid detection without the need for lengthy cultivation and additional confirmation steps. Examples of such techniques include polymerase chain reaction (PCR) and fluorescence *in situ* hybridisation (FISH). The PCR utilises signal amplification to detect coliform bacteria, with DNA sequences encoding the *lacZ* gene ( $\beta$ -galactosidase gene) and the *uidA* gene ( $\beta$ -d-glucuronidase gene) being employed to detect total coliforms and *E. coli*, respectively (Kuo et al., 2021). However, PCR still suffers from limited precision and requires significant laboratory work. The FISH technique employs oligonucleotide probes to detect complementary sequences within specific cells (Batani et al., 2019; Kuo et al., 2021) and offers advantages such as high sensitivity, stability, cell visualisation capability, safety, short detection times, and the ability for multiple colour labelling. Nevertheless, further research is still necessary.

### 2.4.4 Digital probes/biosensors

Standard microbiological methods for water bacteria identification are time-consuming; besides, molecular methods such as quantitative PCR or DNA hybridisation require high-purity specimens. Likewise, enzymatic assays such as ELISA are very sensitive but are not suitable for high-throughput screenings. Upcoming biosensor technologies are considered as better alternatives to these standard methods for water quality testing because:

- Long-term, continuous environmental water monitoring is possible with biosensors.
- They can provide data over long periods, which is useful for establishing trends and changes to water quality. By incorporating biosensors into automated systems, the testing process can be streamlined and require less manual intervention. This can improve the efficiency and accuracy of water quality monitoring.
- The ability of certain biosensors to achieve incredibly low detection limits is essential for detecting and quantifying pollutants that may be hazardous to human health or the environment even at low concentrations.
- Once developed, biosensors can have relatively low operating costs, especially if they require minimal reagents and use renewable biological components (e.g., enzymes or bacteriophages).
- Many biosensors provide results within minutes, making them suitable for rapid testing in situations such as emergency response to water-related disease outbreaks.
- Biosensors can be customized to meet the specific requirements of different applications, allowing for flexibility in design and adaptation to varying environmental needs.

Drone adaptation and configuration to sensor apparatus for on-site, real-time digitalised water quality test application.

An ideal biosensor should have the properties in Table 4, and the remainder of this section will delve into the research and development of biosensors.

**Table 2:** Ideal biosensor properties

<b>Properties</b>	<b>Desired behaviour</b>
Assay time	Near real-time responses are desired (< 1 hour desirable)
Assay protocol and monitoring	No reagent addition is needed and should be direct without pre-enrichment
Species selectivity	Able to distinguish individual bacterial species in the presence of other microorganisms or cells
Strain selectivity	Able to distinguish an individual bacterial strain from other strains of the same species
Low limit of detection	Able to detect single bacteria in a reasonably small sample volume (from 1 to 100 mL)
Compatible interface	Should be compatible with the transduction principle and resist non-specific binding
Viable cell count	Should discriminate between live and dead cells
Operator	Should be automated and require minimal operator skills
Robustness	Mechanical and chemical stability are required

## 2.5 BIOSENSORS

A biosensor measures biological or chemical reactions by generating observable changes or signals proportional to the concentrations of an analyte in the reaction (Bhalla et al., 2016). A biosensor can also be defined as an “integrated receptor-transducer device, which is capable of providing specific quantitative or semi-quantitative analytical information” (Thévenot et al., 2001, p. 123). A typical biosensor model is represented in Figure 7; and consists of the following components:

- An analyte is a biological substance of interest that needs detection in a sample. For instance, *E. coli* is an analyte in a biosensor designed to detect water pathogens (Thévenot et al., 2001; Bhalla et al., 2016).
- Bioreceptors commonly known as biorecognition elements are biological substances immobilised (attached) to transducer surfaces. Biorecognition elements use the specificity of biological conjugates to create sensors that only recognise the desired analyte. An appropriate biorecognition element must be chosen that only reacts with a specific pathogen or analyte, forms a relatively stable complex with the target and binds to the surface of the transducer (Maas et al., 2017).
- A transducer is an element that converts one form of energy into another. In a biosensor, the role of the transducer is to convert the bio-recognition event into a measurable signal. Most transducers produce either optical or electrical signals that are usually proportional to the number of analyte-bioreceptor interactions (Bhalla et al., 2016).
- A signal readout is responsible for processing the transduced signal and displaying the result. It consists of complex electronic circuitry that performs signal conditioning such as amplification and conversion of signals from analogue to digital (Bhalla et al., 2016).

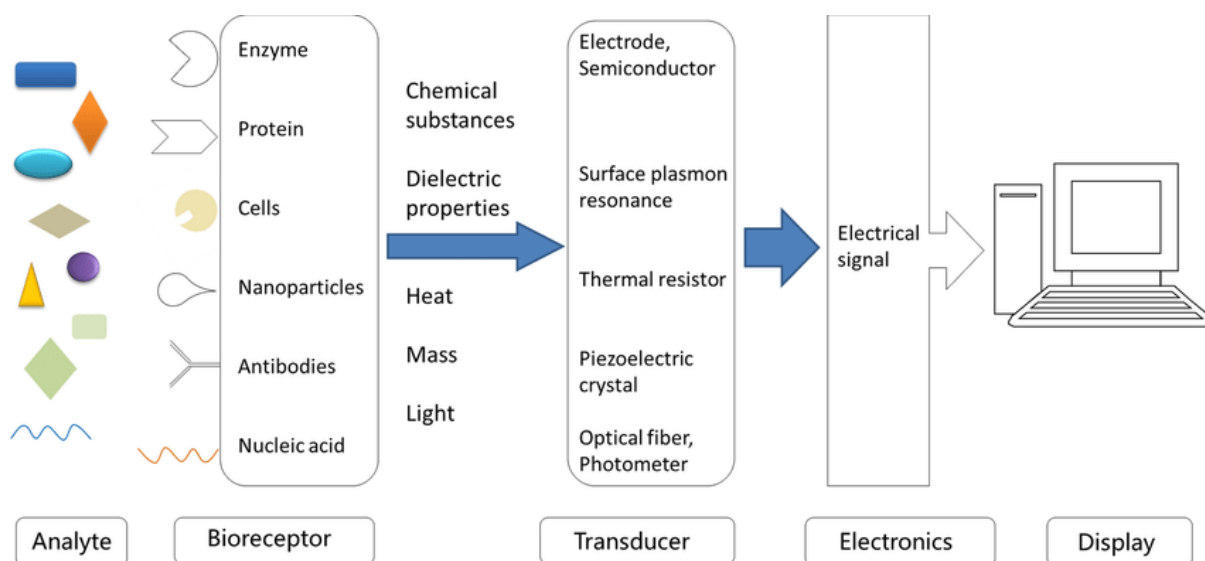


**Figure 7:** A typical biosensor model (Li et al., 2021).

### 2.5.1 Transduction mechanism

A transducer is defined as a device that converts physical or chemical changes into electronic signals. Transduction types are classified as mechanical, magnetic, thermal, piezoelectric, optical, or electrochemical (Thévenot et al., 2001). Of these, the piezoelectric, electrochemical, and optical transduction types are popular, mainly due to low manufacturing cost, simple design, high sensitivity, robust sensing mechanisms and simple signal analyses (Kadadou et al., 2022).

Piezoelectric biosensors are mass-sensitive detectors consisting of a crystal surface layered with the biorecognition element (Pilevar et al., 2021). After being exposed to the analyte, a change happens in the resonant frequency (MHz) of the crystal which relates to the mass change at the crystal surface. Piezoelectric transducers are widely used in acoustic wave biosensors since they generate acoustic waves in a frequency-dependent manner. Quartz ( $\text{SiO}_2$ ) and lithium niobate ( $\text{LiNbO}_3$ ) are the most popular materials used in piezoelectric transducers (Babacan et al., 2000; Halánek et al., 2005; Skládal, 2016; Tombelli & Mascini, 2000).

Optical biosensors detect changes in absorbance, reflectance, fluorescence, chemiluminescence, evanescent wave, or bioluminescence caused by the interaction between the biorecognition element and the target analyte (Maas et al., 2018). More sophisticated biosensors make use of fibre optics, lateral flow assays (LFAs), surface plasmon resonance (SPR), and enzyme-linked immunosorbent assays (ELISAs) (Maas et al., 2017; Maas et al., 2018). A colourimetric biosensor is also referred to as an optical biosensor which uses the lateral flow assay transduction type (Pilevar et al., 2021).

Electrochemical biosensors operate by measuring the biological changes (at the biosensor surface) that occur because of the interaction between the biorecognition element and the analyte. The biological changes could be in conductance (S/m), current (A), resistance ( $\Omega$ ), or capacitance (F) at the sensing surface (Pilevar et al., 2021). An electrode is immobilized with a biorecognition element that interacts with the target analyte and generates signals that could be amplified for analyte detection (Thévenot et al., 2001; Maas et al., 2018a; Cesewski & Johnson, 2020; Offenbaume et al., 2020; Viviers et al., 2020; Kaya et al., 2021; Pilevar et al., 2021).

### 2.5.2 Biorecognition element

Biorecognition elements can be used in labelled and label-free biosensors. External techniques of tagging the analyte with secondary or fluorescently labelled antibodies, or antibody-nanomaterial conjugates, are used in labelled biosensors (Luo & Davis, 2013). This is normally done as part of the pre-processing step. This could make the system more complicated, making it more expensive and time-consuming (Luo & Davis, 2013). As a result, label-free sensors are of special importance. Label-free sensors are widely researched since they do not require auxiliary pathogen labelling through other means. Catalytic biosensors refer to electrodes that are chemically catalytic and immobilised with enzymes, whereas affinity biosensors refer to the binding of a target to immobilised biorecognition elements on transducer surfaces (Luo & Davis, 2013).

Enzymes, cells, tissues, and microorganisms are used as biorecognition elements in catalytic biosensors (Maas et al., 2017). Due to the catalytic activity provided by enzymes, biosensors containing enzymes can reach high sensitivities and allow for a lower limit of detection (LOD) (Vo-Dinh & Cullum, 2000). Nanostructures, carbon nanotubes (CNTs) and semiconductive materials such as zinc oxide (ZnO) have been immobilised with enzymes in biosensors to improve sensitivity (Neveling et al., 2014; Yun et al., 2009).

Antibodies, nucleic acids, and polymer antibodies are used as biorecognition elements in affinity biosensors (Maas et al., 2017). Biosensors based on deoxyribonucleic acid (DNA) and ribonucleic acid (RNA) are chemically more stable than antibody-based sensors (Luo & Davis, 2013), although they can be more complicated due to the need for DNA amplification in the pre-conditioning step. Antibody-based biosensors are very sensitive to temperature and humidity during immobilisation (Mairal et al., 2008). Aptamers are suitable substitutes for antibodies in biosensing systems, and they can address the heat stability problem (Mairal et al., 2008). Bacteriophages are a great alternative to antibodies and aptamers because they have high specificity for host bacteria, resulting in efficient bacteria screening, are easy to generate large quantities of progeny bacteriophages due to their short replication time, and can tolerate a wide range of pH and temperature (Ahovan et al., 2020).

## 2.6 BACTERIOPHAGE-BASED BIOSENSORS

Bacteriophages are specialised viruses that interact with specific receptors on the surface of bacteria, injecting their genetic material into the host cell resulting in the production of new bacteriophages and death of the bacteria. They are commonly employed and immobilised as bio-receptors on sensor surfaces to capture target analytes and develop functional phage-based biosensors.

Researchers from Auburn University in Auburn, USA, developed biosensors using bacteriophage (Balasubramanian et al., 2007; Nanduri et al., 2007; Olsen et al., 2006). In one study, they designed a biosensor by physically adsorbing bacteriophages onto a quartz crystal microbalance surface to detect  $\beta$ -galactosidase from *E. coli*. The bacteriophages exhibited high selectivity for  $\beta$ -galactosidase over BSA, even when the BSA concentration was 2000 times higher. Analysis using ELISA showed that bacteriophages display comparable specificity to monoclonal antibodies. Moreover, the binding ability of bacteriophages remained detectable for over six weeks at 63°C and three days at 76°C (Nanduri et al., 2007). In another study, researchers developed a biosensor for rapid detection of *Salmonella typhimurium* using physically adsorbed filamentous bacteriophages as probes on piezoelectric transducers. Evaluation through fluorescent microscopy, scanning electron microscopy, and changes in resonance frequency confirmed specific bacterial binding and the efficacy of these prepared biosensors (Olsen et al., 2006). The team also reported a label-free detection of *Staphylococcus aureus* in a third study, utilising a lytic bacteriophage and a surface plasmon resonance-based SPREETA sensor (SPREETA is an electro-optical device that detects minute changes in the refractive index of liquids using surface plasmon resonance) as the detection platform. This biosensor achieved a limit of detection of  $10^4$  CFU/ml (Balasubramanian et al., 2007).

Researchers from the University of Alberta, Canada developed techniques for chemically attaching wild-type bacteriophages to biosensor surfaces and subsequently capturing their host bacteria (Arya et al., 2011; Singh et al., 2009). In the study by Singh et al. (2009), the surfaces were modified with sugars (dextrose and sucrose) and amino acids (histidine and cysteine) to facilitate attachment. Bacterial capture was confirmed using fluorescence microscopy, and a bacterial capture density of  $11.9 \pm 0.2$  CFU/100  $\mu\text{m}^2$  was achieved, a 9-fold improvement over physically adsorbed bacteriophages. In the study conducted by Arya et al. (2011), these researchers demonstrated successful regeneration and reuse of chemically anchored bacteriophage-based surfaces by treating them with 20 mM NaOH. The specificity of recognition was further demonstrated by exposing similar surfaces to three strains of non-host bacteria, which showed no evidence of bacterial capture. Moreover, in the absence of phage, no host capture was observed.

Researchers from the Polish Academy of Sciences, Warsaw, Poland developed methods for immobilising bacteriophage using electric fields. They initially demonstrated the effectiveness of this approach which enabled subsequent measurements of impedance spectroscopy, allowing further analysis and characterisation (Richter et al., 2016). They then focused on enhancing the sensitivity of a model sensing element for *E. coli* bacteria detection (Richter et al., 2017) and investigated different surface activation methods using a combination of cysteamine and glutaraldehyde or dithiobis (succinimidyl propionate) (DTSP) before electrical deposition, and found great improvement in sensitivity due to the improved arrangement of bacteriophage obtained by orienting them in an alternating electric field.

## 2.7 BACTERIOPHAGE IMMOBILISATION

It is essential that immobilised phage particles retain their infectivity and binding affinity to host bacteria cells. Moreover, ensuring uniform and repeatable surface modification is of paramount importance to ensure the stability, reliability, and high sensitivity of biosensors. Phage immobilisation techniques include physical adsorption, chemical functionalisation, and the utilisation of special interactions such as biotin-avidin coupling. Additionally, the use of electric deposition, capitalising on their inherent electric properties has gained recent popularity as a promising immobilisation method.

### 2.7.1 Physical adsorption

Physical adsorption is a straightforward method commonly employed for immobilising bacteriophages on solid substrate surfaces. The binding of bacteriophages to gold surfaces can occur through hydrophobic interactions, weak hydrogen bonding, van der Waals forces, and potential covalent bonding between the surface and the amine and thiol groups present on bacteriophage's surfaces (Balasubramanian et al., 2007; Nanduri et al., 2007; Olsen et al., 2006). While physical adsorption is a practical and cost-effective immobilisation technique, it has limitations such as possible desorption during analyte detection and low surface coverage of bacteriophages. These drawbacks arise from weak and nonspecific bonding influenced by surface properties like charge, hydrophobicity, and hydrophilicity, resulting in poor stability of the biosensor. Nevertheless, physical adsorption is frequently used as a control when evaluating other immobilisation strategies. The comparison of this method with other methods is summarised in Table 5, illustrating why other methods are still utilised despite its simplicity and straightforwardness.

**Table 3: Comparison of bacteriophage immobilisation techniques**

Physical adsorption	Covalent attachment	Electric deposition
It is relatively straightforward and requires minimal steps	More complex and requires multiple steps	Requires specialised equipment and expertise
Adsorbed bacteriophages have lower stability and are more susceptible to detachment	Provide increased stability and less susceptible to detachment	Can be coupled with covalent attachment to increase stability

Drone adaptation and configuration to sensor apparatus for on-site, real-time digitalised water quality test application.

Physical adsorption	Covalent attachment	Electric deposition
Low specificity for target bacteria, leading to potential non-specific binding	Improved specificity and minimise non-specific binding, enhancing selectivity	Improved specificity and capture efficiency.
Results in non-uniform immobilisation since the attachment is random	Harsher conditions during covalent bonding may lead to decreased phage activity.	Facilitating uniform phage immobilisation

## 2.7.2 Chemical functionalisation

Covalent immobilisation is a highly stable and irreversible method of attaching bacteriophages to substrates, as demonstrated by the ability of covalently immobilised bacteriophages to remain bound even under harsh conditions such as sonication forces (Arya et al., 2011; Ionescu, 2022; Singh et al., 2009). This immobilisation technique involves crosslinking the bacteriophages to sensor surfaces, utilising amino acid residues on the viral capsids such as glutamine, aspartic acid, lysine, cysteine, and tyrosine. However, covalent immobilisation has some drawbacks, including the potential disruption of phage activity after bond formation, particularly if the bonding site interferes with the phage's adsorption ability. Additionally, the process is relatively complex and may pose challenges when scaling up.

Protein-ligand interactions can be utilised for immobilising bacteriophages by taking advantage of the natural tendency of proteins to bind to specific ligands (Gervais et al., 2007). This method involves coupling a binding protein to the surface and its corresponding ligand to the absorbate, resulting in immobilisation upon their encounter. However, this approach is intricate, time-consuming, and may lead to phage inactivation.

### 2.7.2.1 Popular Covalent Linking Agents

Cysteamine is used as a linking agent in the functionalisation of sensor surfaces for self-assembly monolayers (SAM) due to its thiol (-SH) and amine (-NH<sub>2</sub>) moieties (Ionescu, 2022; PubChem Compound Summary for CID 6058, Cysteamine, 2023). For example, when a gold-coated substrate is incubated with cysteamine, the unique thiol group facilitates SAM formation at room temperature through the Au-SH bond. Thus, cysteamine has been frequently used in the construction of sensitive immunosensors for screening the content of specific biomarkers and drugs in both saline buffers and body fluids (Ionescu, 2022).

Glutaraldehyde is a highly reactive aldehyde reagent, used as a crosslinking agent in several biological tests (Ionescu, 2022; PubChem Compound Summary for CID 3485, Glutaraldehyde, 2023). Each dialdehyde molecule has a terminal aldehyde group (-CHO) that facilitate the covalent immobilisation of either larger biological species (e.g., cells, proteins) or small chemical species (e.g., cysteamine) on various solid supports. For example, if the amino- and sulphur-containing molecules are adsorbed on gold support and activated by glutaraldehyde, the -CHO groups can bind to the -NH<sub>2</sub> groups of the proteins (e.g., enzymes, antibodies) to form Schiff bases (Ionescu, 2022).

## 2.7.3 Electric deposition

Bacteriophages have a negatively charged capsid, or head, filled with DNA or RNA molecules and positively charged tails (Ahovan et al., 2020; Paczesny et al., 2020; Richter et al., 2016; Richter et al., 2017; Rosner & Clark, 2021; Singh et al., 2009; Viazis et al., 2011). This bacteriophage electric dipole property could align them in a "head-down and tail-up" orientation due to the polarisation induced by the external electric field, according to the Lorentz force in electromagnetics theory (Richter et al., 2016; Richter et al., 2017); as a result, for the electric deposition chamber shown in Figure 8, a positive voltage is applied to the gold surface of the

biosensor to obtain the desired orientation. The negative voltage (ground) is connected to the copper electrode, with a separation distance of approximately 1 mm between the two electrodes. A thick polytetrafluoroethylene (PTFE) separator is placed between the copper electrode and the phage suspension to prevent bacteriophage inactivation due to faradaic current flow (Richter et al., 2016; Richter et al., 2017).

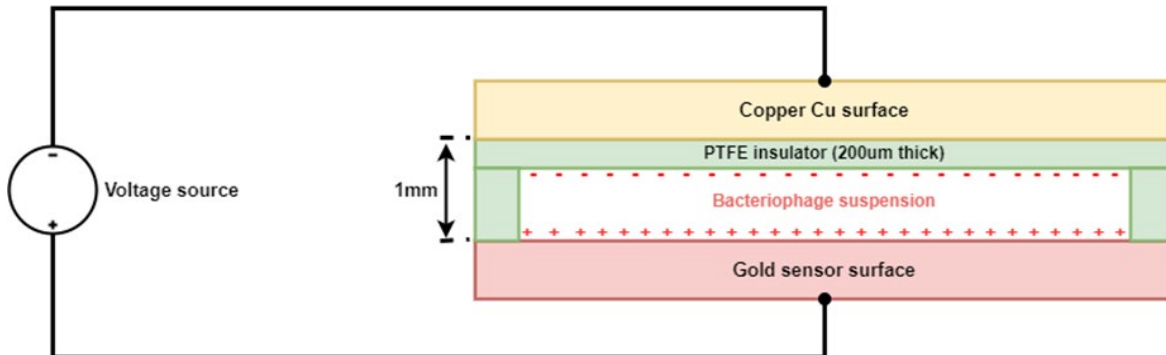


**Figure 8:** The phage electrical deposition chamber model (Richter et al., 2016; Richter et al., 2017)

## 2.8 CONCLUSION

We propose the use of a bacteriophage-based electrochemical biosensor with electrochemical impedance spectroscopy acting as a transduction method. In phage-based biosensors, bacteriophages are attached to the sensor surface to detect pathogens. Bacteriophages have excellent host specificity and selectivity, as well as ease of amplification, and a wide pH and temperature tolerance range resulting in a biosensor with high sensitivity, precision, and reliability. The EIS biosensors are based on detecting the transducer's impedance over a frequency range. The key advantages of this approach are it is rapid, simple and straightforward to use while still being quite sensitive.

## CHAPTER 3: SIMULATIONS AND MODELLING FOR THE DIGITAL PROBE

---

### 3.1 INTRODUCTION

Electrochemical transduction is a simple, label-free transduction method. Even though it is a well-established method, there is little theory about how it works and thus it is worth investigating. Simulations are an important step in the design and fabrication of biosensors for the following reasons:

- Without simulations, it may be difficult to understand how the biosensor works and why it may not perform effectively. This is easily resolved in a simulation environment by considering effects such as how electrochemical analysis is performed, the environment in which the biosensor will be tested, as well as the biosensor's geometry and material. The simulations can then be used to compare with the prototypes.
- Certain parameters of the biosensor prototype must be changed for the biosensor to perform properly; without simulations, this can take a long time and need repetitive testing.

COMSOL Multiphysics is simulation software used to solve simulation models in environments that contain multiple physics modules or studies. It uses a finite element model to generate the required geometry, which is then defined by mathematical equations that can be implemented as boundary conditions, domains, and initial conditions. This software was chosen for the simulation because of the amount of modelling control it provides, as well as the extensive library of resources and electrochemistry support.

It is crucial to include all simulation considerations as well as how the theory is implemented in the model, as even minor modifications might have a significant impact on the simulation outcome. It is also critical to specify any reductions made to the simulation model to minimise the computing time. The simulation in this chapter assumes an interdigitated electrode (IDE) with gold active digits, as shown in Figure 9.

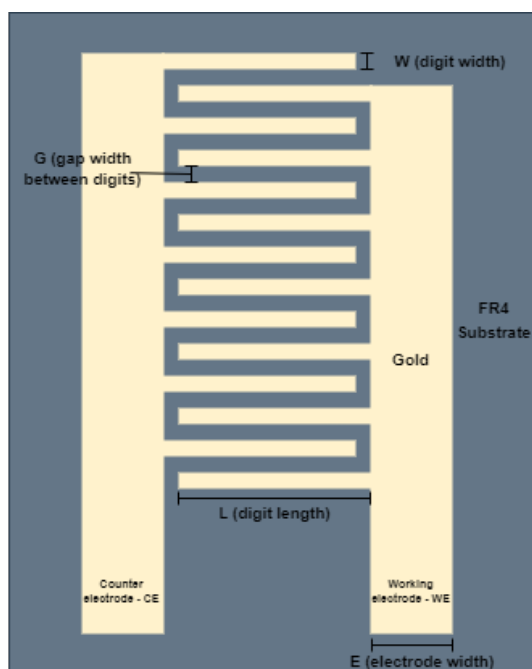


Figure 9: 2D representation of the IDE.

## 3.2 SIMULATION ASSUMPTIONS

The goal of the simulation was to understand and perform the following on IDEs as to their application in biosensors:

- Model the geometry and material of the IDEs.
- Perform and understand how the electrochemical impedance spectroscopy (EIS) of the IDEs work, and finally compare EIS with cyclic voltammetry of the IDEs.
- Understand the electrochemical reactions on the surface of the IDEs and how they affect EIS measurements.

Repetitive unit cells with a high aspect ratio are used in many electrochemical systems; the combined effect of edge phenomena in these systems are negligible. For instance, it is viable to use a two-dimensional geometry with no loss of detail when considering surface reactions of IDEs. Because IDEs have symmetrical geometry and materials, a model can be made even simpler by simulating one IDE digit, which will reduce the simulation's meshing and solving time. Since an electrode is a good conductor, the voltage over its surface is normally constant. This implies that either the electrolyte's intrinsic resistance or the rate of the electrochemical reaction at the electrode-electrolyte interface controls the current drawn at the electrode surface.

The electrode domain does not need to be modelled under the assumption of this constant surface voltage; instead, an electrode surface node handles the coupling of charge and mass transport at its surface. The kinetics of the counter electrode were not studied but instead represented by a constant potential boundary condition. This is only done when the counter electrode can draw arbitrarily large amounts of current compared to the working electrode, so that it never limits the current flow in the electrochemical cell.

## 3.3 2D SIMULATION MODEL

A cross-section of the IDE was examined to simplify the simulation model and reduce computation time. Only six finger of the working electrode and five adjacent counter electrodes were used. The different parameters of the IDE were varied to observe and optimise the design. All the default parameters for the simulation are shown in Table 14 including geometry and reaction parameters.

### 3.3.1 EIS simulation of the model height

The model height was estimated from the mean theoretical diffusion layer thickness ( $x_{diff}$ ) which is given by

$$x_{diff} = \sqrt{\frac{D}{2 \times \pi \times freq}}$$

where D is the diffusion coefficient of the redox pair and freq is the frequency of the applied EIS voltage.

The model height was varied to determine whether the simulation can accommodate the entire diffusion layer across all frequency ranges. The concentration profiles clearly showed that the model includes the entire diffusion layer, and that increasing the height excessively had no effect on the EIS, so a model height of 1.0555 mm was used for the remainder of the simulations.

### 3.3.2 EIS simulation of the redox pair concentration

The concentration of the redox pairs was varied to see how they affect the EIS simulation results. The increase in reductant  $C_{red}$  concentration had the expected effect of decreasing impedance across the entire frequency range. In addition, the oxidant  $C_{ox}$  concentration was also varied and shown to reduce impedance.

### 3.3.3 EIS simulation of the digit width and gaps between the digits

To study the effect of the digit width, the IDE digit widths were varied, and the impedance Nyquist plots were observed, as shown in Figure 10. The Nyquist plots clearly show that decreasing the digit width results in lower impedance and, consequently, improved performance. The digit width is limited by its manufacturability and smaller digit width IDEs are currently expensive. The gap between the digits was also varied to see how it affected the impedance. It was observed that the gap between the digits has minimum effect on the impedance, therefore a digit width of 130  $\mu\text{m}$  was chosen.

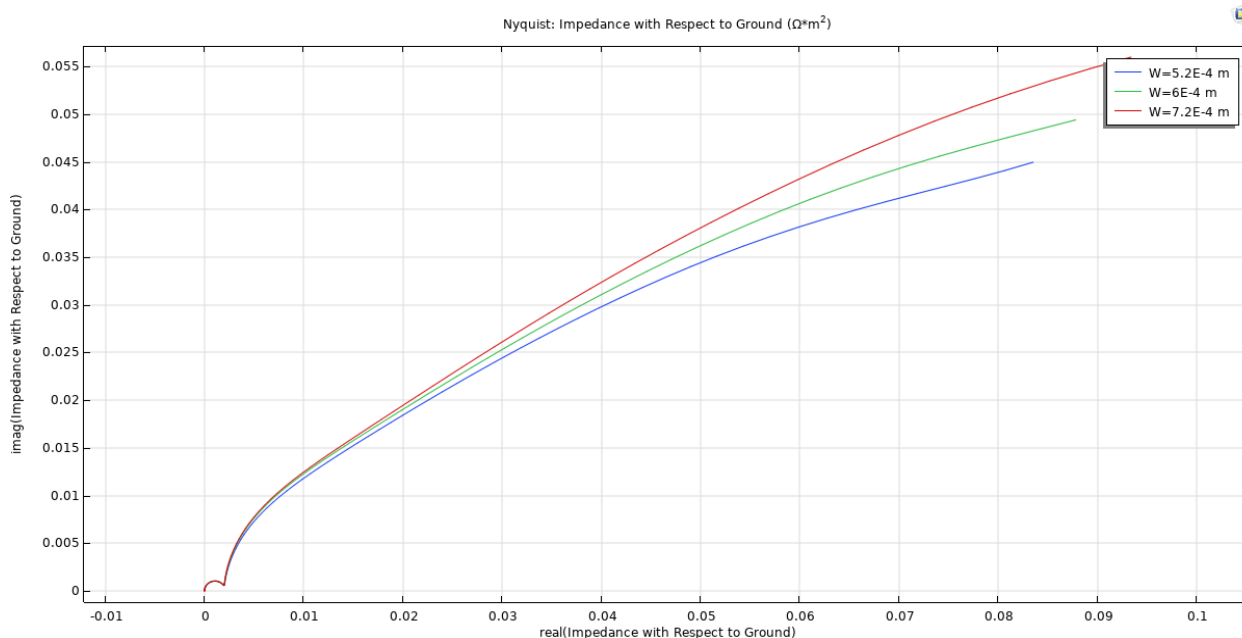
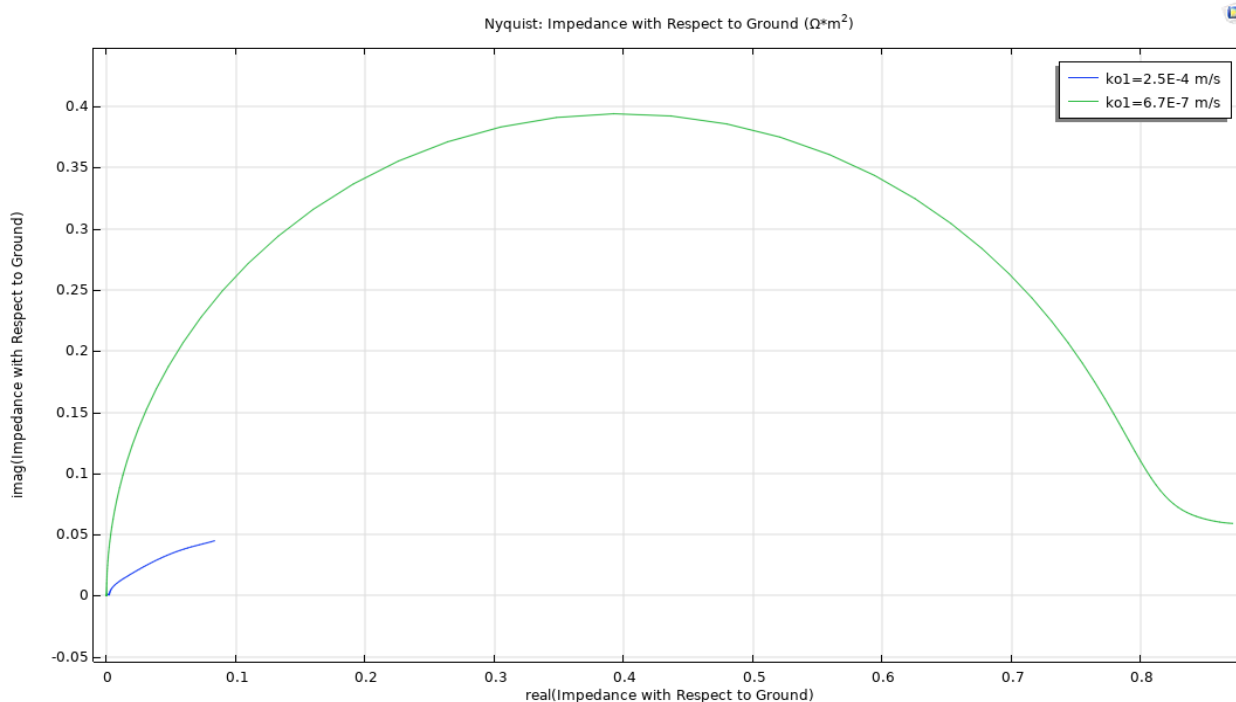


Figure 10: Nyquist plot to compare digit widths ranging from 130  $\mu\text{m}$  to 180  $\mu\text{m}$ .

### 3.3.4 EIS simulation of bare and immobilised IDEs

All the previous simulations were carried out on a bare IDE using a standard heterogeneous reaction rate ( $ko_1$ ) of  $2.5 \times 10^{-4} \text{ [m/s]}$ . To simulate an immobilised IDE, the  $ko_1$  was reduced to  $6.7 \times 10^{-7} \text{ [m/s]}$ . An immobilised IDE had higher impedance than a bare IDE, as demonstrated by the Nyquist plot shown in Figure 11. As a result, using appropriate impedance identification software, it is possible to detect an increase in impedance if bacteriophages are bound to the IDE surface, and the model can be used to conduct other studies such as to quantify how much bacteriophages are immobilised on the electrode surface.



**Figure 11:** The Nyquist plot for bare and immobilised electrodes for a 2D model.

### 3.3.5 Cyclic voltammetry of bare and immobilised IDEs

The model system setup for EIS was changed to perform cyclic voltammetry at a scan rate of 500 mV/s and vertex voltages of 500 mV and -500 mV, respectively. The obtained voltammetry is shown in Figure 12, where the bare electrode has a standard heterogeneous reaction rate ( $ko1$ ) of  $2.5e-4$  m/s while the immobilised electrode has  $ko1 = 6.7e-7$  m/s and is as expected from the literature. The results clearly showed that the immobilised current peak is lower and has moved further away from 0 V.

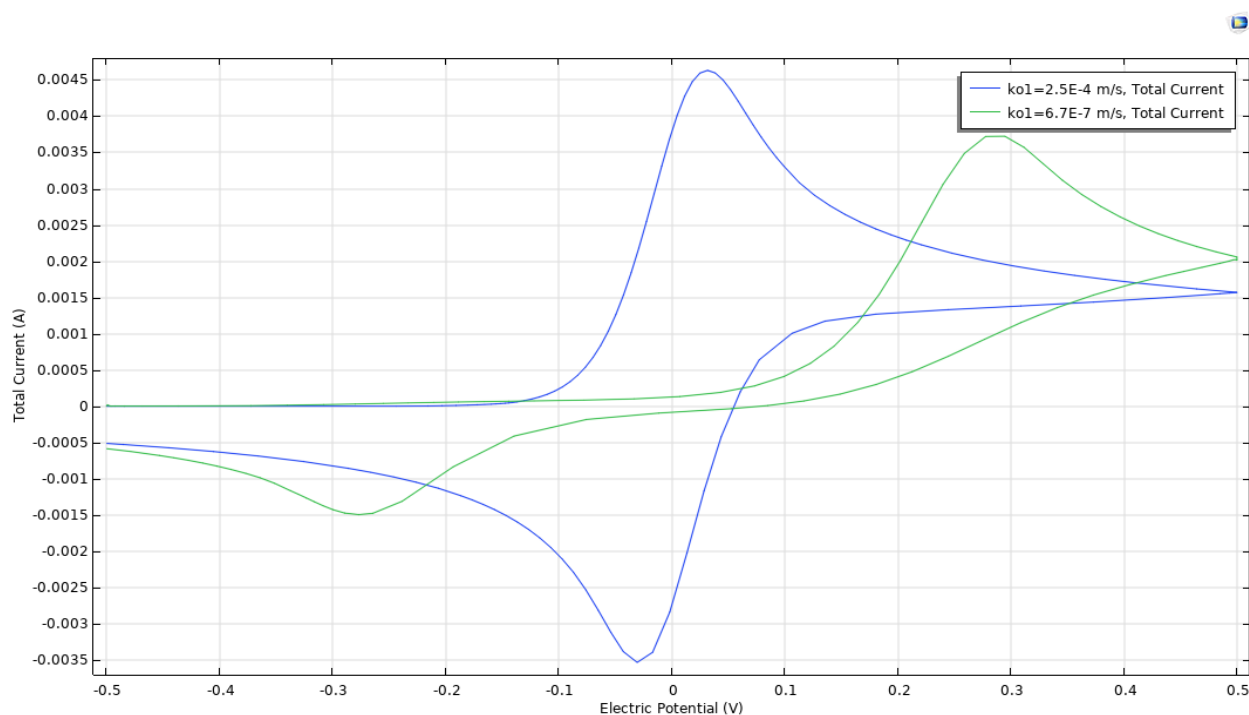


Figure 12: The cyclic voltammery for bare and immobilised electrodes in a 2D model.

### 3.4 3D SIMULATION MODEL

The previously simulated model was expanded to 3D and the used parameters are the same as in the 2D model.

#### 3.4.1 EIS simulation of the redox pair concentration

The concentration of the redox pairs was varied to see how they affect the EIS simulation results. The increase in reductant  $C_{red}$  concentration had the expected effect of decreasing impedance across the entire frequency range. In addition, the oxidant  $C_{ox}$  concentration was also varied and shown to reduce impedance. The results are the same as observed in the 2D model.

#### 3.4.2 EIS simulation of bare and immobilised IDEs

All the previous simulations were carried out on a bare IDE using a standard heterogeneous reaction rate of  $2.5E-4$  m/s. To simulate an immobilised IDE, the standard heterogeneous reaction rate was reduced to  $6.7E-7$  m/s. An immobilised IDE has a higher impedance than a bare IDE (Figure 12). The observed results are the same as the 2D model.

#### 3.4.3 Implication of the 3D model

Simulating the IDEs in 3D makes the model more realistic, so it is naturally more accurate (even though it takes more simulation time and is difficult to vary the model's different geometry parameters) and can be used as a control to confirm if the 2D model is valid for modelling the IDEs. Because the 3D model produces the

Drone adaptation and configuration to sensor apparatus for on-site, real-time digitalised water quality test application.

---

same results as the 2D model, the 2D model is an accurate representation of the IDEs. As a result, we decided to stick with the 2D model of the IDEs, and the geometry of the IDEs was decided in 2D.

### **3.5 CONCLUSION**

Comparing the simulation results to the literature showed that the model behaved as expected. As a result, we moved on to select the IDEs to use as the transducer for this project. According to the simulations, digit width and gap should be as small as possible to have a very sensitive biosensor. Interdigitated electrodes are typically manufactured and bought from Europe, particularly Germany, and are highly priced depending on performance. Our research group has been testing cheap (less than R2.50 each) printed circuit board IDEs. As a result, we will be experimenting with these low-cost interdigitated electrodes for a bacteriophage-based biosensor.

## CHAPTER 4: METHODOLOGY FOR THE DIGITAL PROBE

---

### 4.1 INTRODUCTION

In this chapter all decisions and steps that were followed to design the biosensor are discussed. An overview is provided of the specific goals that need to be achieved, design decisions that create a framework to achieve the goals in a realistic way, and greater detail regarding protocols that need to be followed for laboratory tests is included. In addition, details are provided as to ensuring that protocol steps are successfully followed.

### 4.2 DESIGN DECISIONS AND GOALS

#### 4.2.1 Selection of the transducer

The commercially available interdigitated electrodes (IDEs) from MicruX (Asturias, Spain) were considered as well as the screen-printed electrodes (SPEs) from the same manufacturer. We opted for the IDEs because of their precise control of the electrode geometry, high sensitivity, and reduced electrode polarisation effects compared to SPEs. After reading and advice from literature and fellow students about their inconsistency they experienced with the IDEs from MicruX, we decided to choose the relatively inexpensive printed circuit board (PCB) IDEs from TRAX (Cape Town, South Africa) which were successfully utilised by some students in our research group. These IDEs from TRAX shown in Figure 13, are manufactured at an average price of less than R2.50 per IDE which is significantly cheaper than the price of IDEs from MicruX.

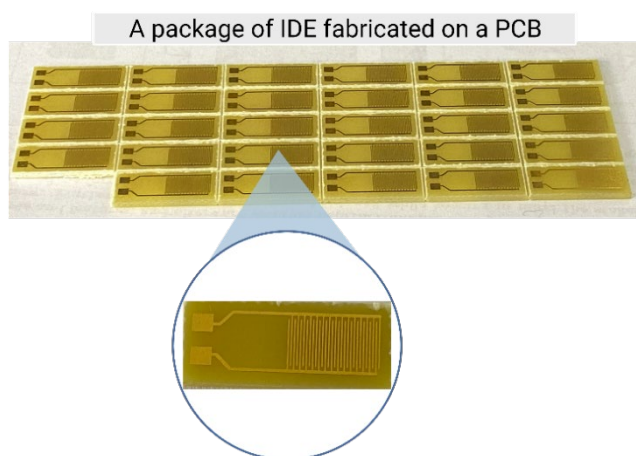


**Figure 13:** An interdigitated electrode manufactured from TRAX (Cape Town, South Africa).

#### 4.2.2 Selection of the biorecognition element

A bacteriophage-based electrochemical biosensor with electrochemical impedance spectroscopy was chosen. In this phage-based biosensor, the phage is attached to the IDE's active surface to detect water pathogenic bacteria of interest. Bacteriophages have excellent host specificity and selectivity, as well as ease of amplification, and a wide pH and temperature tolerance range resulting in a biosensor with high sensitivity, precision, and reliability. In addition, we selected the EIS transduction mechanism over other techniques due to its simplicity and accuracy, as well as its ease of compatibility with IDEs. The EIS biosensors can use redox

reactions - faradaic EIS - or without using redox reactions - non-faradaic EIS - and we chose the latter since it is simple and straightforward to use while still being very sensitive.

#### 4.2.3 Choosing the immobilisation method

The immobilisation of bacteriophages is an essential element in the design of a biosensor since it influences its specificity and sensitivity. We chose to follow all three methods discussed in the literature earlier i.e., physical adsorption, covalent attachment, and electrical deposition. This will allow us to build up from the simple methods to the more complex ones that are more accurate. The exact protocols followed for each method are discussed later in this chapter.

#### 4.2.4 The biosensor communication protocol and power supply

Because the biosensors are designed to be carried by a drone to conduct water quality monitoring, the design goal is to have as little wiring as possible to facilitate mobility and easy integration with the rest of the system. Therefore, we decided to allow Wi-Fi communication of the functional biosensor as well as a battery power source to allow the biosensor to be readily fitted to a drone or other platforms.

#### 4.2.5 Potential for multiplexing

This multiplexing of biosensors to test for different water pathogens is not part of this current project but rather developing a single biosensor to test for *E. coli* BL21 (DE3) as a proof-of-concept for on-site and remote water quality testing. To prove the concept, biosafety level (BSL) 1 organisms were used to determine the feasibility of the biosensor. Once the concept was proved, bacteriophages were collected from environmental samples and screened for their host specificity toward *E. coli* strains (ATCC, environmental and pathogenic). These newly isolated bacteriophages can easily be incorporated into the system and further validated.

#### 4.2.6 Laboratory equipment used to develop the biosensor

The following equipment besides the used reagents, solutions and other basic laboratory equipment were required for the successful development of the biosensor:

1. *Calibrated pipettes* of various sizes were used to measure specific volumes of solutions, phage, bacteria, and other liquid reagents used.
2. Any reagents that were in powder or crystal form were weighed on a *calibrated microscale* and stored in 1.5 ml, 2 ml, or 5 ml *Eppendorf tubes*, to avoid contamination.
3. During bacteriophage immobilisation stage, the IDEs were incubated in Eppendorf tubes to avoid dirt from settling on the IDEs surface.
4. Different *incubations rooms* with set temperatures were also used to incubate the different bacteria and used during the immobilisation steps when specific temperatures were required.
5. *The Zeiss LSM 780* and *Zeiss Gemini 2* (Carl Zeiss, Germany) for confocal microscopy and scanning electron microscopy, respectively, were used to assess the success of the bacteriophage immobilisation methods. To ensure that the images were comparable during the analyses, they were all obtained at the same magnification.

Drone adaptation and configuration to sensor apparatus for on-site, real-time digitalised water quality test application.

6. *PalmSens 4* (PalmSens, Netherlands) was used to conduct EIS experiments, which were set to an AC amplitude of 10 mV and a frequency range of 1 Hz to 100 kHz using the PStace 5.8 software.

### 4.3 BACTERIOPHAGE CULTURING AND ENUMERATION

#### 4.3.1 Determining an OD<sub>600</sub> calibration curve for *E. coli BL21 (DE3)*

The following procedure was used to obtain the OD<sub>600</sub> calibration curve, which would allow the bacteria cell concentration to be estimated for future experiments using OD<sub>600</sub> measurements:

1. Inoculate a culture of *E. coli BL21 (DE3)* in Brain Heart Infusion (BHI) medium, and incubate overnight at 37°C.
2. Dilute the overnight culture to the desired OD<sub>600</sub> (i.e., 0.1, 0.3, 0.5) using a spectrophotometer.
3. Perform serial dilutions of the diluted culture at the correct OD<sub>600</sub> to obtain a range of concentrations (i.e., 10<sup>0</sup> – 10<sup>-10</sup>).
4. Plate the serial dilution samples in triplicate using BHI agar overlay plates (0.8% w/v) and incubate overnight at 37°C.
5. Enumerate colony-forming units per milliliter (CFU/ml) from the plate count assays and average the CFU/ml at each OD<sub>600</sub>.
6. Plot a calibration curve with OD<sub>600</sub> values on the x-axis and log<sub>10</sub> (CFU/ml) on the y-axis using the obtained CFU/ml data.

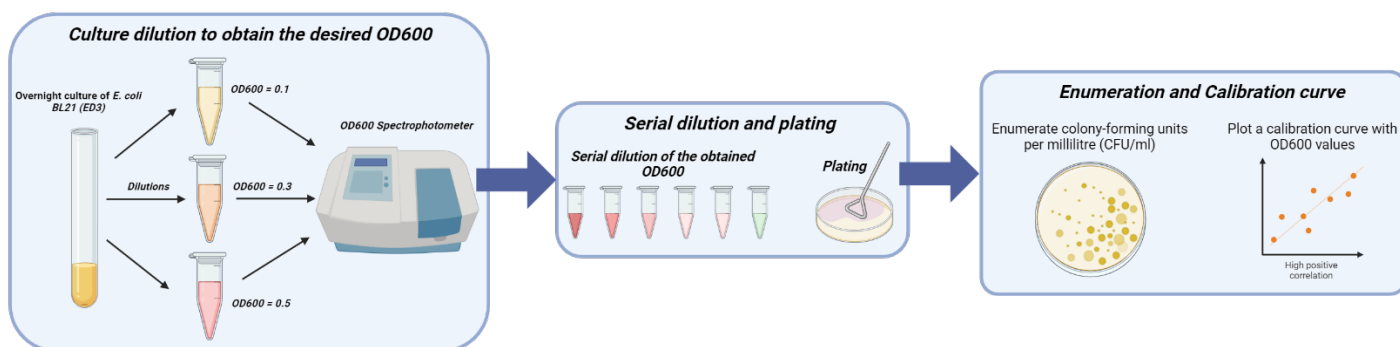


**Figure 14:** Procedure to obtain the OD<sub>600</sub> calibration curve.

#### 4.3.2 *E. coli BL21 (DE3)* phage stock preparation and concentration

The following procedure described by Aaron et al. (2022) was used to prepare bacteriophages specific for *E. coli BL21 (DE3)*:

1. Inoculate a culture of *E. coli BL21 (DE3)* in Brain Heart Infusion (BHI) medium, and incubate overnight at 37°C.
2. Prepare 50 ml of BHI in a flask and autoclave to sterilise. Add 1% of the overnight culture and incubate at 37°C until it reaches the exponential growth phase.

3. From the phage stock stored in the -80°C fridge, inoculate the phage to a BHI solution and vortex. Add 1 ml of this to the above flask and incubate for 16 hours at 37°C.
4. After 16 hours of incubation, harvest cells (10,000 g, 20 min, 4°C) and filter the cell-free supernatant through a sterile nitrocellulose filter (0.45 µm and 0.22 µm pore size).
5. Concentrate the phage solution using polyethylene glycol (PEG) precipitation
  - a. Suspend the phage filtrate in 20% PEG6000 for 16 hours at 4°C.
  - b. After this incubation, harvest cells (20,000× g, 1 hour, 4°C).
  - c. Finally, the pellet is suspended and stored in a phage buffer (10 mM Tris, pH 7.5, 10 mM MgSO<sub>4</sub>, 60 mM NaCl).
6. This finally phage stock was ready for use, but bacteriophage enumeration was done to confirm the efficiency of the phage concentration step and quantify the amount of the phage for downstream applications on the biosensor.

#### 4.3.3 Enumeration of *E. coli* BL21 (DE3) phage using plaque assays

The following procedure was used to enumerate bacteriophages specific for *E. coli* BL21 (DE3):

1. Inoculate a culture of *E. coli* BL21 (DE3) in Brain Heart Infusion (BHI) medium, and incubate overnight at 37°C.
2. Prepare 10 ml sloppy tubes with BHI and 0.8% w/v agar. Autoclave the sloppy tubes.
3. In the biosafety cabinet, quickly add 0.1% of the overnight *E. coli* BL21 (DE3) bacterial culture to the sloppy tubes and vortex the tubes.
4. Immediately after vortexing, add 100 µl of the prepared phage solution (after serial dilution) to each sloppy tube and vortex the tubes again to mix well.
5. Pour the sloppy tubes onto the respective agar plates, swirl the plates gently to evenly distribute the bacterial culture and phage solution, and allow the agar to solidify. Incubate the plates at 26°C overnight.
6. Count the plaques formed on the plates and calculate plaque forming units per millilitre (PFU/ml) using the dilution factor and plated phage volume.
7. Perform the assay in triplicate for each dilution to ensure accuracy.

#### 4.3.4 Determining the lysis profile for *E. coli* BL21 (DE3) using the TECAN Spark

The lysis profile was estimated by measuring the change in OD<sub>600</sub> using the TECAN system over a specified time period. This benchtop instrument dispenses picolitre to microlitre volumes directly to the assay plate with exceptional flexibility, saving time, minimizing waste of valuable reagents and accelerating experimental set-up. Using the previous experiments, we were able to calculate and setup the experiment at different multiplicity of infection (MOI):

1. The first set of experiments was carried out in HBI media for two hours at 37°C with starting OD<sub>600</sub> values of 0.3 and 0.5.
2. The second experiment was conducted in PBS solution for three hours at 37°C with starting OD<sub>600</sub> of 0.3 and 0.5.
3. The last set of experiments was conducted in Milli-Q at 37°C for four hours at starting OD<sub>600</sub> of 0.3 and 0.5.

#### 4.4 BACTERIOPHAGE IMMOBILISATION PROTOCOLS

This section describes the various immobilisation techniques used to develop the biosensor, beginning with physical adsorption, and progressing to electric deposition. And, because electrochemical impedance spectroscopy (EIS) is a very sensitive technique in biosensing, the cleaning procedure for the IDEs was critical before immobilising the phage.

The following calculations were performed to estimate the maximum surface densities of phage and *E. coli BL21 (DE3)* cells that can be accommodated on the IDE surface without them overlapping, and these calculated values were used for the biosensor's first preliminary design:

1. The surface area of the IDEs was approximated by  $9 \text{ mm} \times 5 \text{ mm} = 45 \text{ mm}^2$ .
2. A typical tailed phage has a length of 20 – 200 nm and width of 50 nm. Assuming this phage size, the maximum number of phages that can be accommodated on the IDE surface without overlapping is approximated by.

$$N_{\text{phage}} = \frac{\text{nanochip surface area}}{\text{approx size of one phage}} = \frac{(9 \times 5) \times 10^{12} \text{ nm}^2}{(100 \times 50) \text{ nm}^2} = 9 \times 10^9 \text{ PFU}$$

3. Typical *E. coli BL21 (DE3)* has a rod length of 1 – 2 μm and width of 0.5 μm. Assuming this bacterial size, the maximum number of *BL21 cells* that can be accommodated on the IDE surface without overlapping is estimated by.

$$N_{\text{BL21}} = \frac{\text{nanochip surface area}}{\text{approx size of one BL21 cell}} = \frac{(9 \times 5) \times 10^6 \text{ μm}^2}{(1 \times 0.5) \text{ μm}^2} = 9 \times 10^6 \text{ CFU}$$

##### 4.4.1 The IDE cleaning protocol

We adapted various gold surfacing cleaning procedures from the literature and ended up using the following procedure, as shown in Figure 15, every time before using the IDEs:

1. The IDEs were gently wiped and thoroughly washed with filtered 70% ethanol, isopropanol, and acetone.
2. The IDEs were then sonicated for 10 minutes in Milli-Q before being washed with 70% ethanol, isopropanol, and finally acetone again.
3. Thereafter, the IDEs were UVO ozone-cleaned for 10 minutes, and washed with filtered 70% ethanol, isopropanol, acetone, and finally Milli-Q before use.

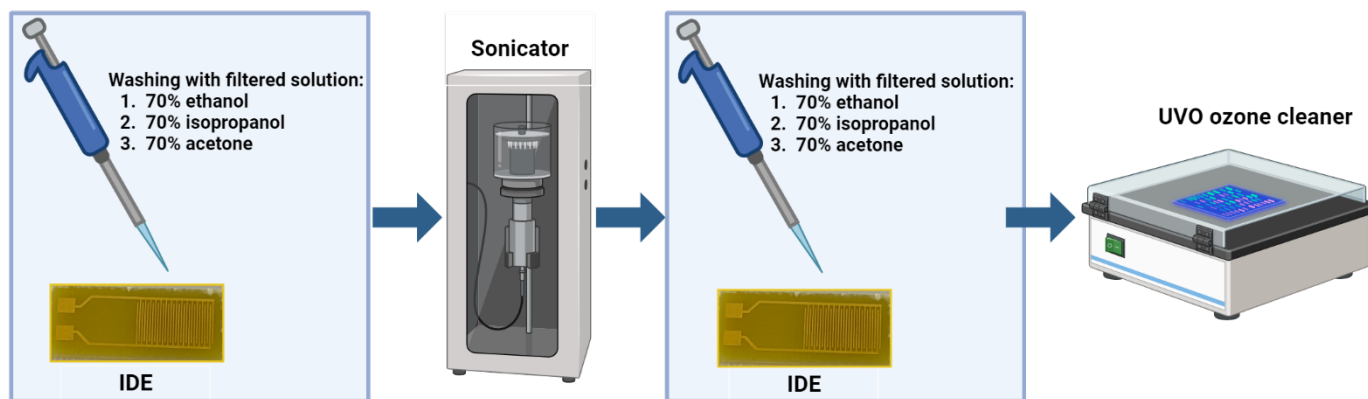


Figure 15: IDE cleaning procedure.

#### 4.4.2 Physical adsorption protocol

To physically immobilise the phage on the IDE, the following steps were taken, and all solutions used were autoclaved and filtered before use:

1. The cleaned IDEs were initially incubated overnight in the refrigerator with a 200  $\mu$ l phage/PBS solution; this method was later improved by incubating overnight in the refrigerator and in 1.5 ml Eppendorf tubes for better IDE exposure to the solution.
2. The unbound phages were then washed away with a PBS solution and stored for testing.

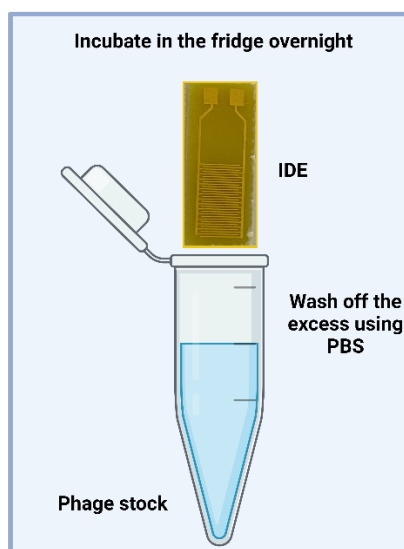


Figure 16: The physical adsorption immobilisation protocol.

#### 4.4.3 Covalent immobilisation using cysteamine and glutaraldehyde protocol

To covalently immobilise the phage on the IDE, the following steps were taken:

1. The IDEs were rinsed with PBS solution before being incubated for 20 hours at 37°C in a 100 mM cysteamine/PBS solution. Following this incubation period, the IDEs were rinsed with PBS solution.

2. The IDEs were then incubated for 1 hour at room temperature in the dark in a 1.5% glutaraldehyde/MilliQ solution.
3. The IDE samples were rinsed with a PBS solution after incubation.
4. Finally, the IDEs were incubated overnight in phage/PBS stock solution placed in the fridge.
5. Thereafter, the IDE samples were rinsed and placed in a PBS buffer to be tested.

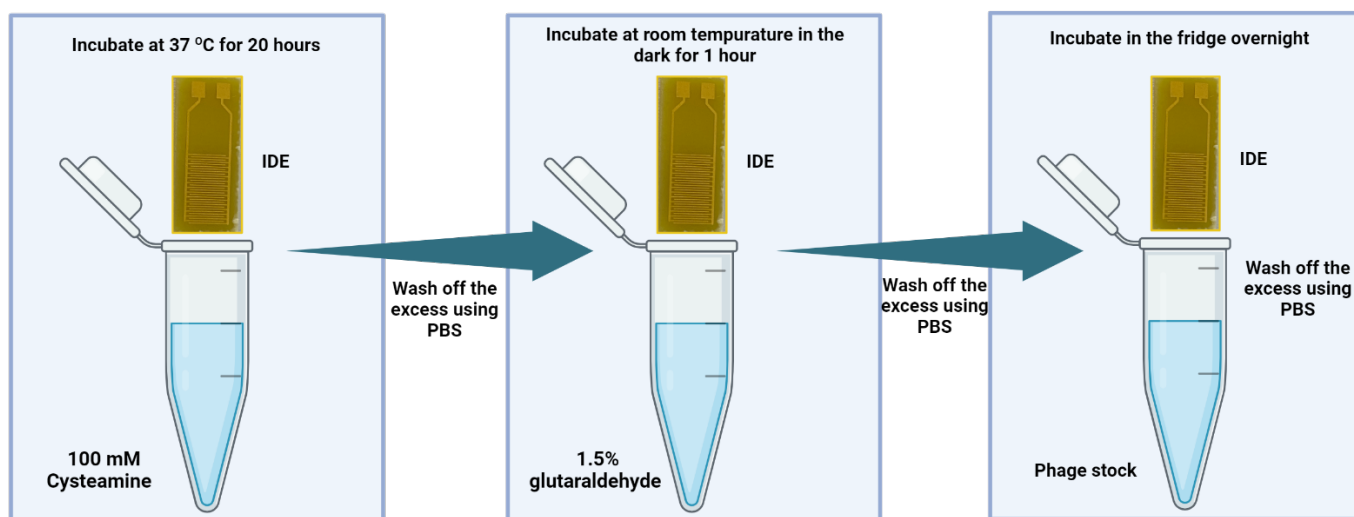


**Figure 17:** Covalent immobilisation protocol.

#### 4.4.4 Immobilisation using the electric deposition protocol

A procedure similar to the covalent immobilisation method was followed with the only difference being the addition of phage where bacteriophages were deposited by running a voltage-defined waveform. This waveform generates an electric field in one direction, causing the phage to experience a force that orients them in the correct order.

1. The IDEs were rinsed with PBS solution before being incubated for 20 hours at 37°C in a 100 mM cysteamine/PBS solution. Following this incubation period, the IDEs were rinsed with PBS solution.
2. The IDEs were then incubated for 1 hour at room temperature in the dark in a 1.5% glutaraldehyde/Milli-Q solution.
3. The IDE samples were rinsed with a PBS solution after incubation.
4. Thereafter, the IDEs were ready for electrical deposition, which was performed using a deposition chamber to ensure that a uniform and strong electrical field existed in the wells with the phage solution. The used deposition chamber is described elsewhere in this chapter. The IDE wells were filled with phage solution and the defined waveform runs for 30 minutes to electrically orient the phage.
5. Thereafter this, the IDE samples were stored in PBS solution and incubated in the refrigerator overnight to allow more binding before washing.

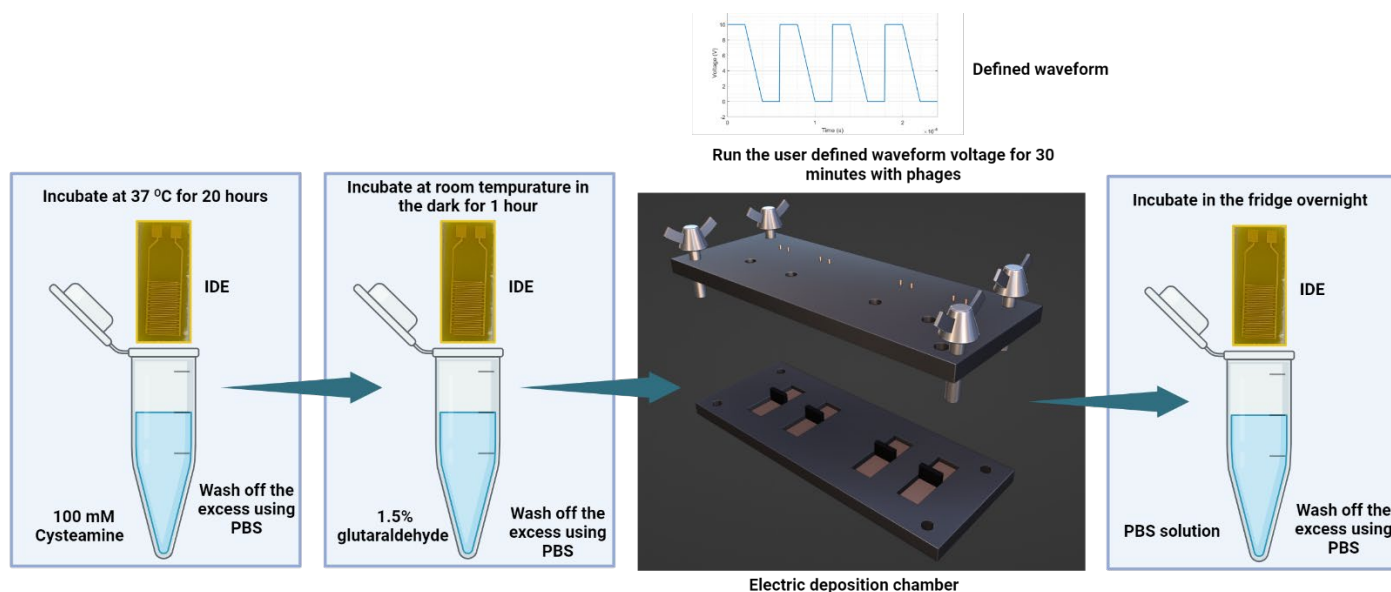


Figure 18: Electric deposition protocol.

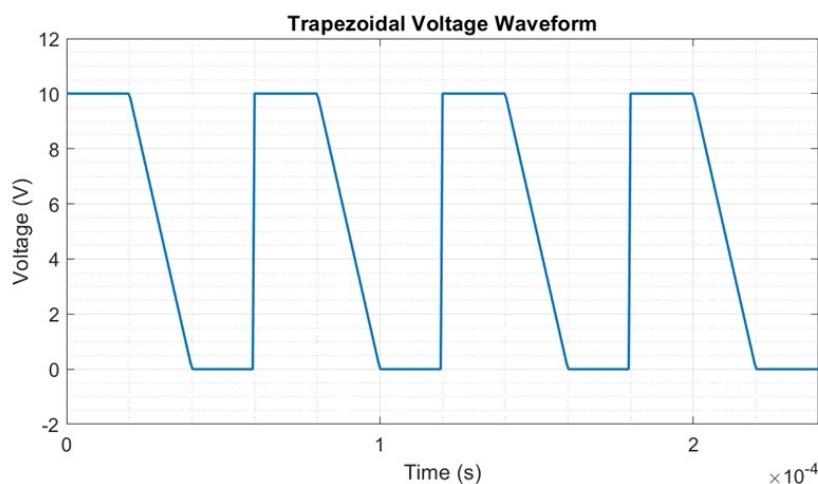


Figure 19: Voltage waveform for electrical deposition.

## 4.5 CONFIRMATION OF THE IMMOBILISATION PROTOCOLS

The disk-diffusion technique was initially used to confirm the effectivity of the immobilised phage, and initial electrochemical impedance spectroscopy measurements were performed to confirm the potential of this biosensor concept without the use of expensive microscopy methods.

### 4.5.1 The disk-diffusion technique

To test the viability of chemically immobilized bacteriophages, IDEs were placed on Brain Heart Infusion (BHI) agar overlay plates (0.8% w/v) containing either *E. coli* BL21 (DE3) or *S. epidermidis*, a commensal bacterial strain:

1. Two agar overlay plates were prepared using BHI agar. For one plate, an overnight culture of 0.1% *E. coli* BL21 was added before pouring, and for the other plate, an overnight culture of 0.1% *S. epidermidis* was added before pouring.

2. After the agar overlay plates had solidified, they were divided into four sections to assess the effectiveness of the immobilisation methods. These sections are depicted in Figure 20 and are designated as follows:
  - a. Positive control: Represents the phage solution directly applied to the plate.
  - b. Physical adsorption: Indicates the IDE treated using the physical adsorption method.
  - c. C&G + no phage: Represents the IDE treated with cysteamine and glutaraldehyde without the overnight phage incubation step.
  - d. C&G + phage: Indicates the IDE that underwent the complete covalent immobilisation method, involving cysteamine, glutaraldehyde, and phage.
3. Following the labelling of the plates and the addition of their respective IDEs, the plates were incubated overnight at 37°C.

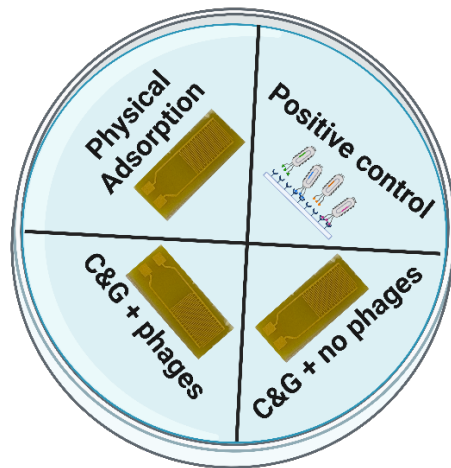


**Figure 20:** The disk-diffusion technique.

#### 4.5.2 Scanning electron microscopy (SEM)

The immobilised IDEs were examined using SEM imaging to confirm the success of the immobilisation protocol. Prior to SEM imaging, it is critical to ensure that the proper controls are in place for the correct comparison of the IDEs. The same IDEs as above were prepared but sets with and without *E. coli BL21* were prepared for SEM imaging. It is also critical that the samples be completely dry for perfect SEM imaging, so the samples need pre-drying to preserve the morphology and structure of the immobilised phage as well as the bound bacteria. In order to prepare the IDE samples for SEM imaging, the following procedure was followed:

1. After the immobilised IDEs were prepared, one set of IDEs was allowed to bind with *E. coli BL21* for 10 minutes before washing off the unbound and excess cells on the IDE, and this set was labelled "with *E. coli BL21*".
2. Both sets with and without *E. coli BL21* were pre-dried before SEM imaging:
  - a. Allow to air-dry for about an hour in the safety cabinet.

- b. Fix the phage and cells on the IDEs by incubating with 2.5% glutaraldehyde/PBS solution for an hour in the refrigerator. And after incubation, rinse with PBS to remove any excess glutaraldehyde/PBS solution.
- c. Dehydrate the phage and cells through an ethanol series from 30%, 50%, 70%, 90%, and 100%.
- d. Finally, place the IDE samples overnight in the oven to dry completely.

#### 4.5.3 Confocal microscopy

After the initial testing of the immobilisation methods with SEM, we could not accurately distinguish the differently treated IDEs. Thus, we decided to go with a different test to confirm immobilisation, and we decided to use confocal microscopy. This method required the *E. coli* cells to be induced with a green fluorescent protein:

1. In 5 ml BHI medium, inoculate an *E. coli BL21 (DE3)* culture with 2.5  $\mu$ l kanamycin (KAN100) and promote GFP expression by adding 1  $\mu$ l isopropyl-D-1-thiogalactopyranoside (IPTG) and incubate overnight at 26°C.
2. Centrifuge the induced cells and wash them with PBS to remove residual media and avoid autofluorescence. Then resuspend the cells in PBS, which is also tested to see if the phage is still active against these *E. coli BL21* cells.
3. The IDEs are prepared as from the last section with and without GFP-expressing *E. coli BL21* ready for confocal microscopy.

#### 4.5.4 Electrochemical Impedance Spectroscopy (EIS) measurements

The PalmSens 4 is used to perform the electrochemical impedance spectroscopy (EIS) measurements of the IDEs across a frequency range, and the equivalent capacitance  $C_s$  across the IDE's digits was derived. The EIS measurement setup is shown in Figure 21, with the red and blue cables connecting to the PalmSens 4 working and counter electrodes, respectively. It is also worth noting that the measurements were performed using the IDE wells with PBS solution. The capacitance  $C_s$  was plotted against frequency for each measurement of the IDE and used later for analysis:

1. Figure 21 depicts the IDEs meter, in which the PalmSens is connected to the PC via a USB cable to send and receive data about the current measurement. The PalmSens is connected to the IDEs via external cables to perform the measurement, where a special holder for the IDEs should be built to facilitate connections. The IDEs also have a well on their active surface to keep the measuring liquid, in this case PBS, in place.
2. The IDEs were prepared as described in the last section with and without *E. coli BL21* but instead EIS measurements were done soon after the cell-binding step. The impedance of the IDEs was measured using the PalmSens over a frequency range from 1 kHz to 100 kHz with an AC amplitude of 10 mV and no DC offset, and this is configured in the PStace software for the PalmSens.
3. After the measurements were completed using the PalmSens, the resulting data were stored on the PC for analysis using Microsoft Excel to pick trends associated with the variously treated IDEs.

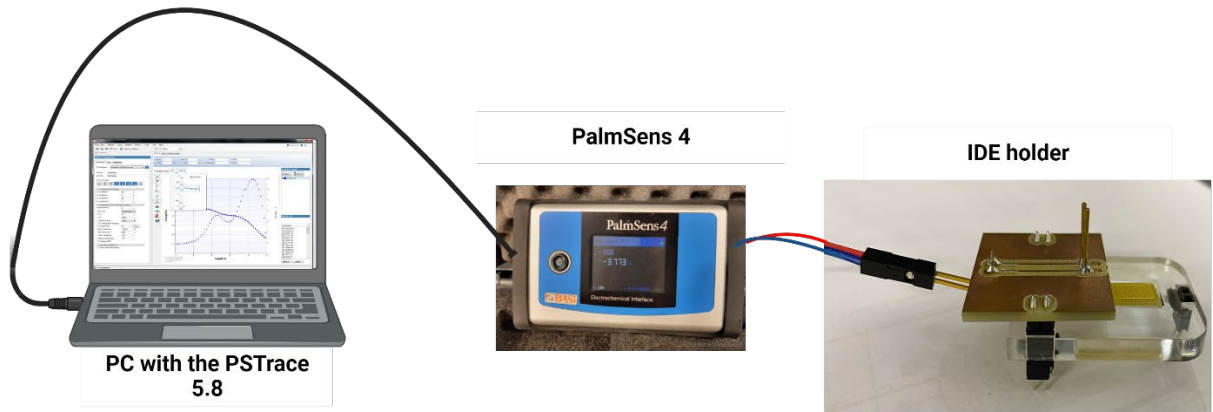


**Figure 21:** The EIS measurement equipment.

## 4.6 IMPEDANCE ANALYSER

In order to develop a functional biosensor, the biosensor should have an electrochemical impedance analyser and microcontroller with communication capabilities to perform impedance measurements at a predetermined frequency while also communicating with external systems or the user. This section is concerned with the development of the impedance analyser which was adapted from Ebrahim (2023). The electronic design goals provide an excitement voltage for impedance measurement as well as to measure this voltage and the IDE's response current. Then this electronic circuit interacts with the STM32 microcontroller which uses the standard GPIO voltage of 0 - 3.3 V. Thus, the design goals are broken down as follows:

1. **Provide an excitement voltage** to the IDE with an amplitude of 10 mV and a frequency of 100 kHz. Using EIS measurements, this excitement voltage frequency is derived from the IDE characterisation. As a result, the design goal is to condition a 100 kHz sinusoid voltage in the 0 to 2.5 V range to a small excitement sinusoid signal with an amplitude of 10 mV biased at 0 V.
2. **Measure a small signal voltage** with an amplitude of 10 mV and 100 kHz frequency biased at 0 V. This small signal voltage is the supplied excitement voltage but now measured at the IDE terminals. Therefor the design goal is to condition a 10-mV voltage signal biased at 0V to a voltage in the range 0 – 2.5 V range biased at 1.25 V.
3. **Measure the IDE current** in the  $\mu\text{A}$  range and this current has a frequency of 100 kHz. This current range is estimated from the excitement voltage and the IDE impedance since this is the resulting current flow when the small signal voltage is applied. As a result, the design goal is to convert a small signal current in the  $\mu\text{A}$  range to a voltage in the 0 - 2.5 V range biased at 1.25 V.

### 4.6.1 Design for small signal excitement voltage circuit

This excitement circuit's design goals are to amplify down a 0 - 2.5 V voltage signal at a frequency of 100 kHz (referred to as input) to a small voltage signal with an amplitude of 10 mV biased at 0 V (referred to as output).

In the first stage of this excitement circuit, the input was conditioned to be biased at 0 V by subtracting the offset voltage. This is modelled by the following equations and referring to the circuit shown in Figure 22:

$$V_{out1} = V_{bias} \times \left(1 + \frac{R2}{R1}\right) - V_{in} \left(\frac{R2}{R1}\right)$$

And assuming that  $R1 = R2$ , this equation simplifies to

$$V_{out1} = 2 \times V_{bias} - V_{in}$$

And, assuming that the offset voltage of the input is 1.25 V, as justified by the design goals outlined above, then  $V_{bias} = 0.625 \text{ V}$  ( $1.25/2 \text{ V}$ ) is required to condition this input at 0 V. Assuming we have a 2.5 V supply, and using voltage division to provide this  $V_{bias}$  voltage.

$$V_{bias} = 2.5 \text{ V} \times \left( \frac{R4}{R3 + R4} \right)$$

And assuming that  $R3 = 30 \text{ k}\Omega$  then we can calculate  $R4 = 10 \text{ k}\Omega$

In the second stage of this excitement circuit, assuming an input voltage amplitude of 1.25 V as justified by the design goals, and an output voltage amplitude of 10 mV. This stage should have a gain of 1/125 V/V (10/1 250 mV/mV) and the voltage output is given by the equation below.

$$V_{out} = -V_{out1} \times \left( \frac{R6}{R5} \right)$$

Assuming, that  $R5 = 22 \text{ k}\Omega$  and then by calculating  $R6 = 176 \Omega$  and picking a standard resistor  $R6 = 180 \Omega$

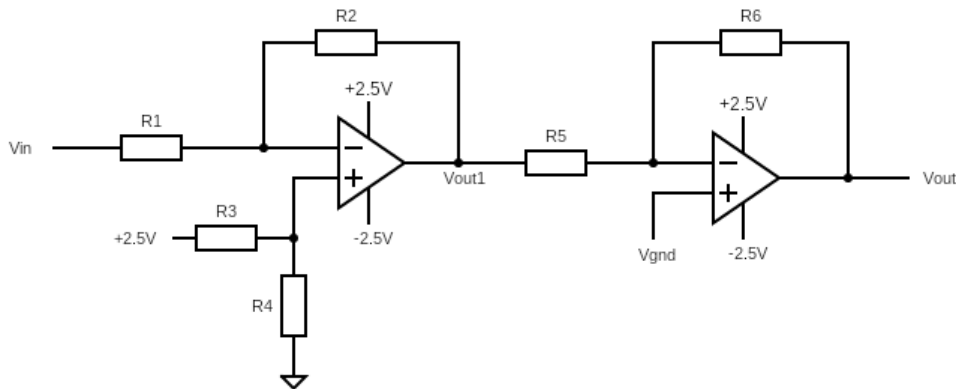


**Figure 22:** Small signal excitement circuit.

#### 4.6.2 Design for small signal voltage measurement

After the voltage excitement circuit, the next stage was to design the voltage measurement circuit using the design requirements of measuring a small signal voltage with an amplitude of 10 mV and a frequency of 100 kHz biased at 0 V to a voltage in the 0 - 2.5 V range. The first stage of this circuit is to amplify the measured small signal voltage to a voltage that can easily be used by the less expensive op-amps. And an instrumental amplifier was chosen for this purpose since it can amplify extremely small signals with a high gain even in the presence of high noise, and the chosen amplifier was the INA331 instrumental amplifier (Texas Instruments, USA).

The design requirement for the instrumental amplifier was based on the INA331 datasheet, which was modified by Ebrahim (2023) but we choose to use the recommended datasheet configuration. According to the INA331 datasheet, the amplifier has a gain of 5 V/V without using any external resistors, resulting in a small signal voltage with an amplitude of 100 mV assuming a 20 mV input, which is sufficient for the next stage with the cheaper op-amps. As a result, the design depicted in Figure 23 was chosen to employ this instrumental

amplifier without the addition of external resistors. The resistor  $R8$  shown in Figure 21, is a short-circuit which supports the claim that used the INA331 instrumental amplifier without any external resistors.

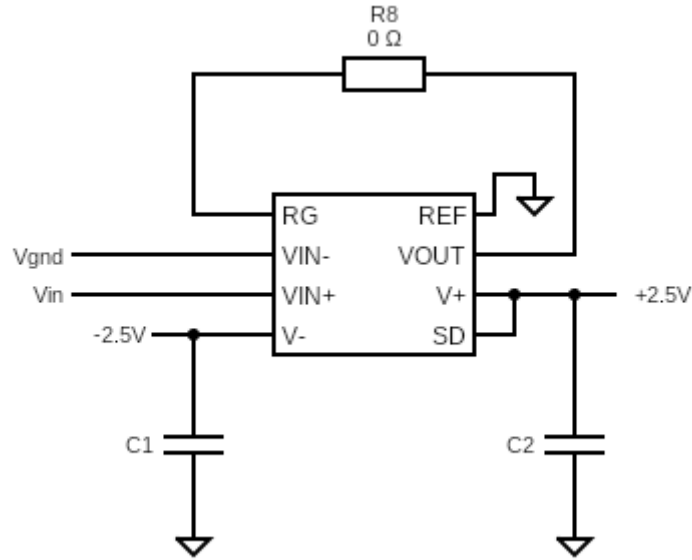


**Figure 23:** INA331 Instrumental amplifier circuit diagram.

The second stage of this design was to amplify and condition the instrumental amplifier output voltage to the 0 – 2.5 V range. In the first step of this stage, the signal is amplified to a 2.5 V signal, and using the configuration shown in Figure 24, and assuming the instrumental amplifier outputs a 100-mV signal i.e., ( $V_{out1} = 100\text{ mV}$ ) before designing for a gain of 18 V/V. In the second step of this stage, the output is biased at 1.25 V and only conditioning the signal without amplification, based on the configuration shown in Figure 24,  $V_{bias} = 0.625\text{ V}$ .

And this second stage uses that same circuit equations as from the previous section i.e.,

$$V_{out2} = -V_{out1} \times \left(\frac{R2}{R1}\right)$$

$$V_{out} = V_{bias} \times \left(1 + \frac{R6}{R5}\right) - V_{out2} \times \left(\frac{R6}{R5}\right)$$

$$V_{bias} = 2.5V \times \left(\frac{R4}{R3 + R4}\right)$$

Now assuming  $R1 = 430\ \Omega$  then  $R2 = 7\ 740\ \Omega$  and picking a standard resistor  $R2 = 7.5\ \text{k}\Omega$ . Assuming no amplification in the second step, conditioning the signal only  $R5 = R6 = 10\ \text{k}\Omega$ . And the bias voltage is set as previous discussed i.e.,  $R3 = 30\ \text{k}\Omega$  and  $R4 = 10\ \text{k}\Omega$ .

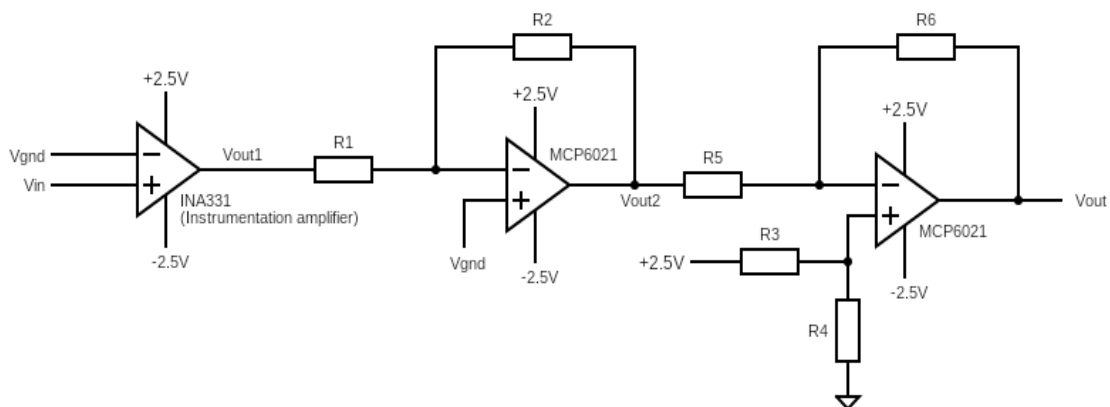


**Figure 24:** Voltage measurement circuit.

### 4.6.3 Design for current measurement

Finally, the design goals for current measurement were established above, where small signal current flowing through the IDE when a small signal voltage is applied was measured. This current was in the  $\pm 10 \mu\text{A}$  range, which was established using measured data from the PalmSens over more than 100 IDEs in prior experiments, so this circuitry was able to measure it and convert it to an equivalent voltage in the 0 - 2.5 V range biased at 1.25 V. A transimpedance op-amp circuit configuration with feedback resistance was used to convert the small signal current into an equivalent output voltage. The transimpedance step, which converted the measured current to an equivalent voltage was the first step in this circuitry, that was later amplified and conditioned to the 0 - 2.5 V range.

Since the measured current was designed for a maximum amplitude of  $1 \mu\text{A}$  and a minimum of  $0.01 \mu\text{A}$  with the feedback resistor for the transimpedance step chosen as  $R1 = 100 \text{ k}\Omega$  which resulted in an output range of 1 – 100 mV for  $0.01 - 1 \mu\text{A}$  from the circuitry shown in Figure 25 and modelled by the following equation:

$$V_{out1} = I_{in} \times (R1)$$

The capacitor C1 was chosen as 78.5 pF estimated from the following formula where  $R1$  is the feedback resistor and  $f_b$  is the required bandwidth frequency (200 kHz) for the transimpedance (investigate the feedback capacitor):

$$C1 \leq \frac{1}{2\pi \times R1 \times f_b}$$

After this step, the equivalent output voltage was amplified and conditioned to the 0 – 2.5 V range. The amplifying circuit was designed for a gain of 10 V/V and the conditioning circuit for a bias of 1.25 V. This step was completed in the same manner as in the previous section for the amplifying and conditioning circuit where the following standard resistors were used:  $R1 = 100 \text{ k}\Omega$ ,  $R2 = 1 \text{ k}\Omega$ ,  $R5 = 10 \text{ k}\Omega$ ,  $R6 = 10 \text{ k}\Omega$ ,  $R7 = 10 \text{ k}\Omega$ ,  $R3 = 30 \text{ k}\Omega$  and  $R4 = 10 \text{ k}\Omega$

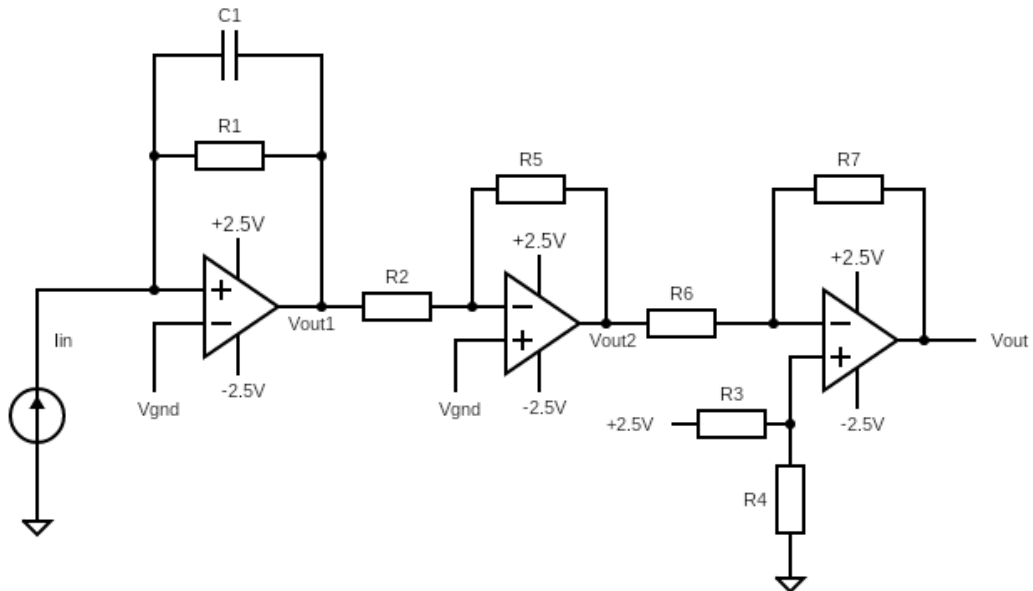


**Figure 25:** Current measurement circuit.

## CHAPTER 5: RESULTS AND DISCUSSIONS FOR THE DIGITAL PROBE

---

### 5.1 IMPEDANCE ANALYSER CIRCUIT TESTING

The following electronic engineering techniques were used to answer the above questions:

- Circuit simulations using LTSpice
- PCB design using KiCAD
- Circuit testing using electrical laboratory equipment.

The design for the impedance analyser was first done in LTSpice and soon after the PCB was prepared, and the components soldered to the test the circuit with real components. And decided to include the simulation results in this preliminary report where all the circuits were simulated at 1 kHz since I could not find the exact LTSpice model for the MCP6021 op-amps used for the design and circuit building.

#### 5.1.1 Design for small signal excitement voltage

The circuit designed in the previous chapter for the small signal excitement voltage was built and tested to confirm that they met the designed requirements. Figure 26 shows the obtained results in LTSpice with the circuit simulated at 1 kHz. The input signal is named  $V_{in}$  which was first conditioned to be biased at 0 V and this signal is named  $V_{out1}$ , and soon after this signal was amplified down to an amplitude of 10 mV. The designed signal worked as expected with the signed gain of  $1/125$  V/V and soon after proceeding with the circuit building.

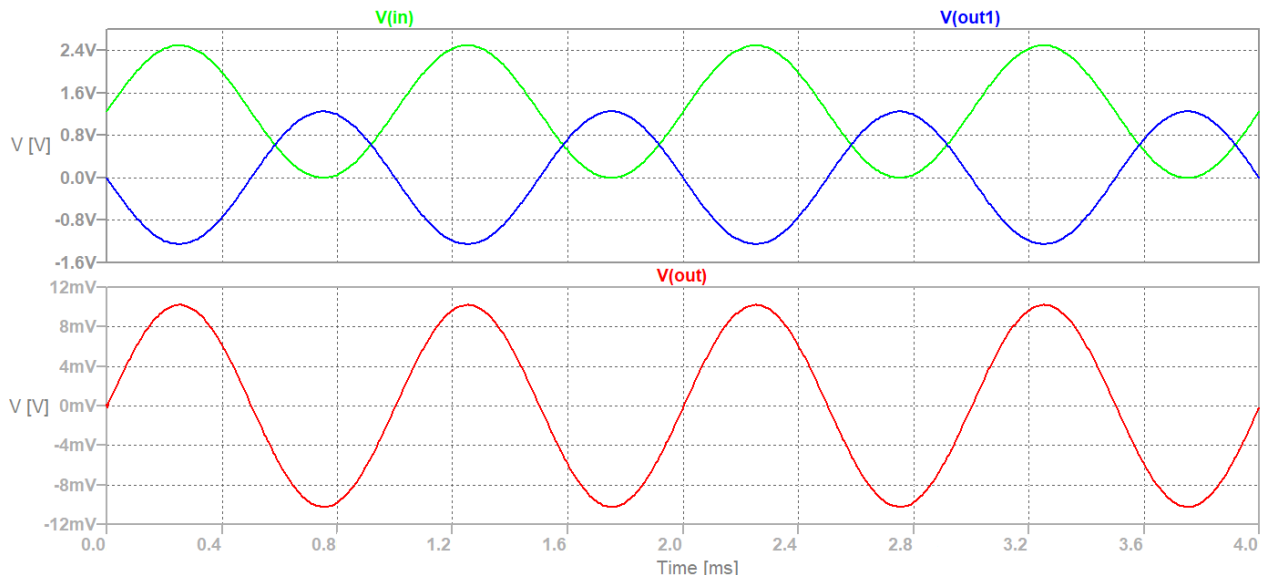
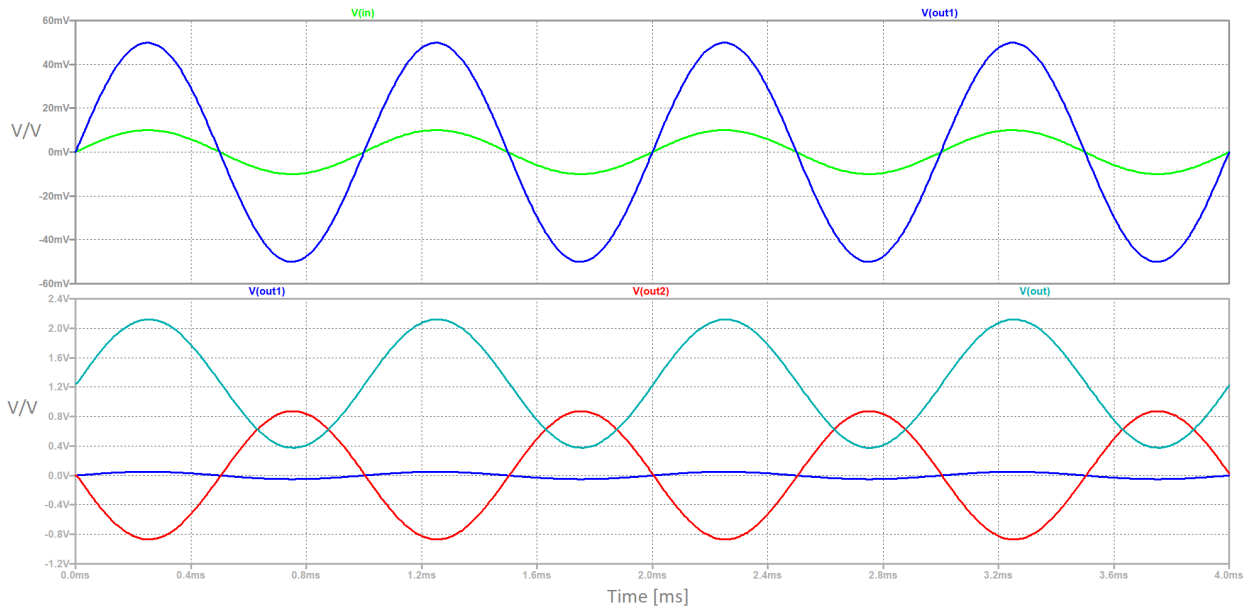


Figure 26: Excitement signal circuit testing.

#### 5.1.2 Design for small signal voltage measurement

The small signal voltage measurement circuit was also tested at 1 kHz, and the results are shown in Figure 27, where the input signal  $V_{in}$  is amplified first by the instrumental amplifier to a signal  $V_{out1}$  with an amplitude

of 50 mV, which is then amplified and conditioned to an amplitude of 1.25 V and biased at 1.25 V, which is shown as Vout2 and Vout respectively. This circuit worked as intended resulting in the expected outcomes based on the design specifications.



**Figure 27: Small signal voltage measurement circuit testing.**

### 5.1.3 Design for current measurement

The current measurement circuit was tested at 1 kHz with a 1  $\mu$ A small current signal. Figure 28 shows the measured DC results, starting with the input current (*I<sub>in</sub>*) of 1  $\mu$ A which is first converted by the transimpedance circuit to an equivalent voltage Vout1 which was measured at 10 mV and then amplified to a 250 mV signal biased at 1.25 V as specified. This circuit also worked as expected as shown by Figure 29 with the measured ac current and voltage.

Drone adaptation and configuration to sensor apparatus for on-site, real-time digitalised water quality test application.

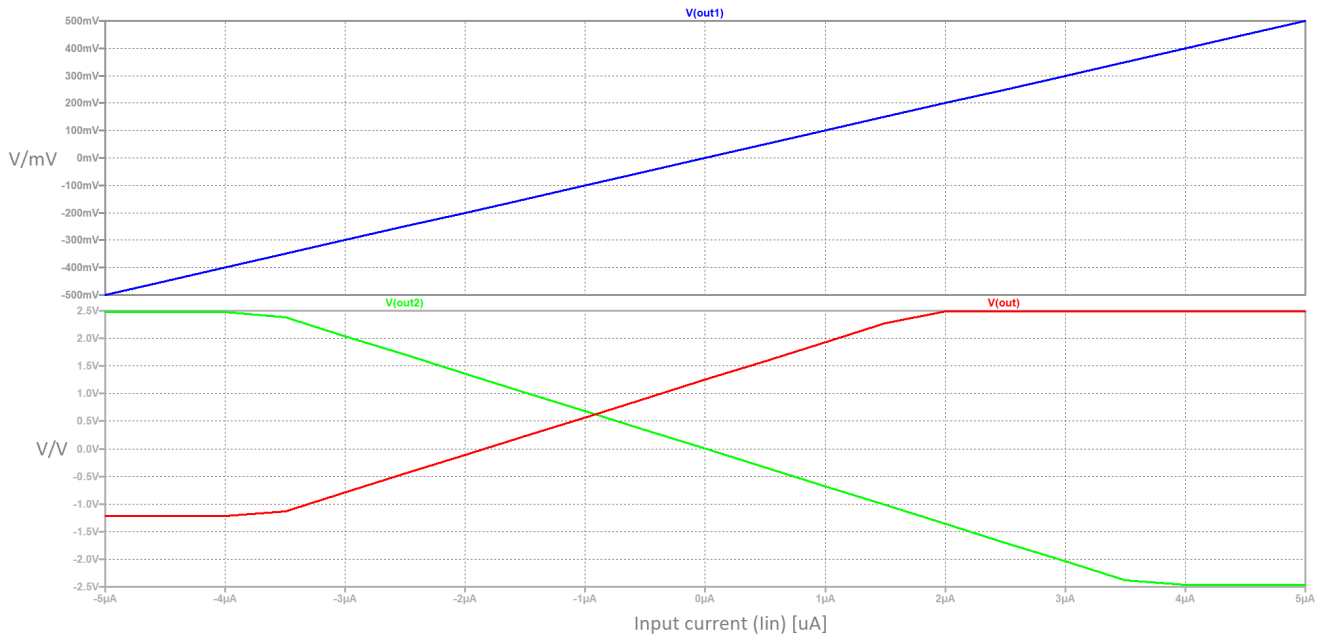


**Figure 28:** Current measurement DC gain testing. a) instrumental amplifier output (above) b) overall circuit output (below).

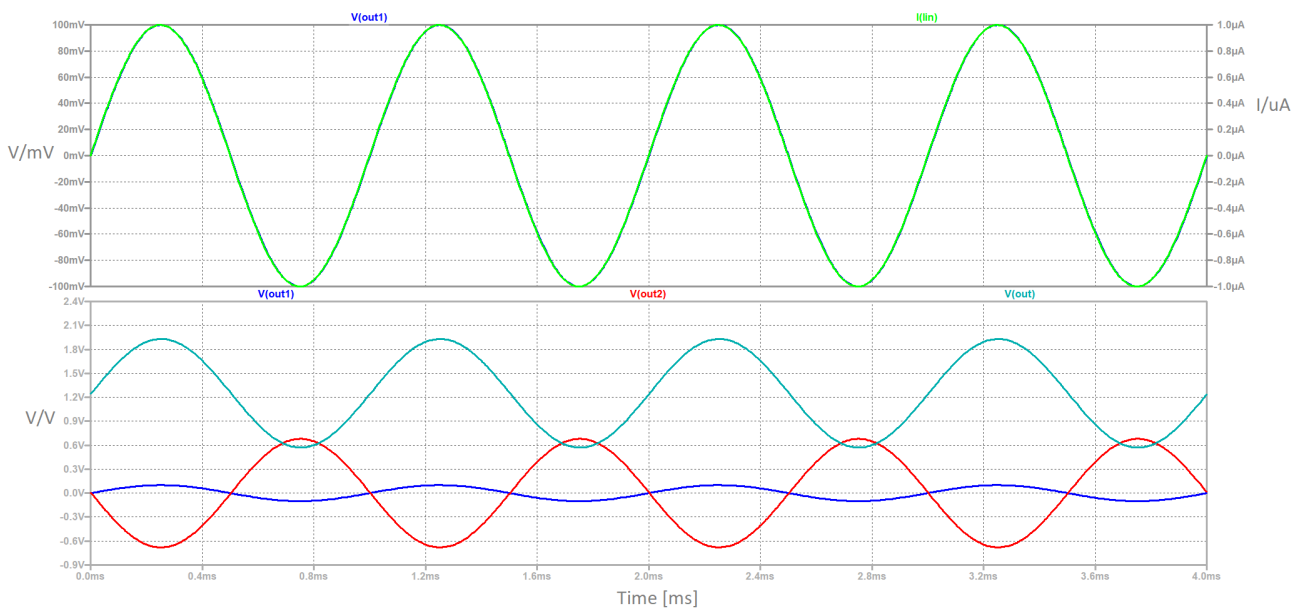


**Figure 29:** AC current measurement circuit testing.

#### 5.1.4 Design for the deposition chamber signal generation

The design for the electrical chamber signal generation could not be tested in LTSpice due to difficulty in generating the input waveform in this simulation software. Instead, a microcontroller was used to test this circuit using a breadboard. The waveform shown on the left in Figure 30 was outputted from the microcontroller at the required frequency, ON time, OFF time, and fall time as intended, then amplified by a simple non-inverting circuit to a signal with a 10 Vp-p value, which was required by the deposition chamber. The gain of this non-inverting op-circuit circuit was tuned by a potentiometer to the required level. The waveform shown in Figure 30 (right) represents the intended voltage range after tuning the potentiometer.

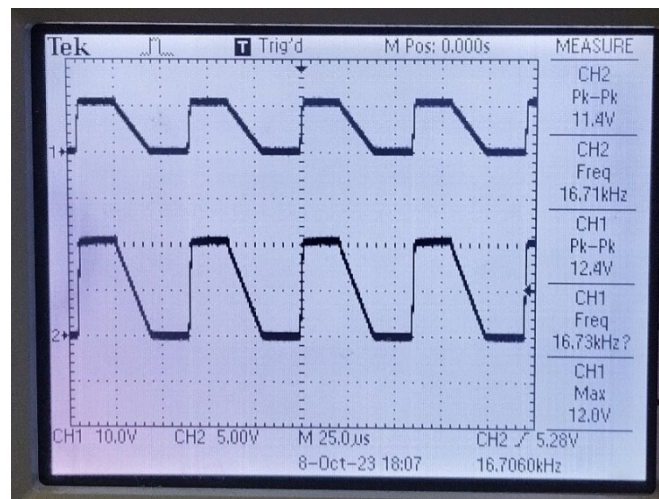
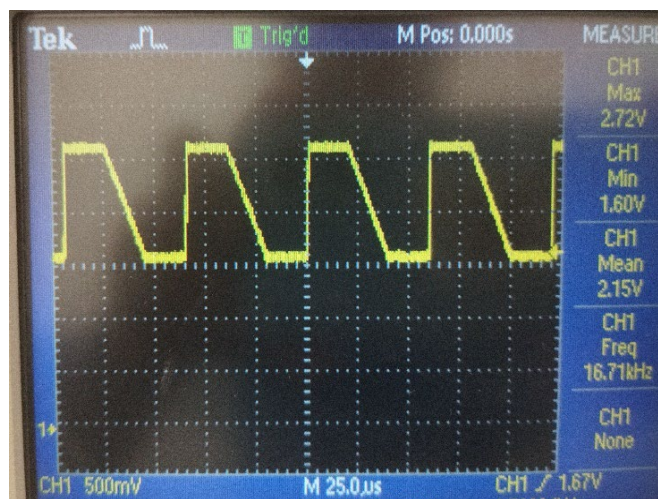


Figure 30: Electrical chamber signal generation testing.

## 5.2 BACTERIOPHAGE CULTURING AND ENUMERATION

The experiments discussed were performed in preparation for electrochemical impedance spectroscopy (EIS) measurements to confirm the precise functioning of the bacteriophage, which serve as the biorecognition element of the biosensor. The following questions were answered concerning bacteriophages and *E. coli BL21 (DE3)* cells:

1. The number of bacteria cells used in the binding assay and OD<sub>600</sub> calibration curve.
2. The number of phage viral particles used in the binding assay and concentration of the phage stock.
3. One step growth curve and lysis profile of the phage.

### 5.2.1 Determining an OD<sub>600</sub> calibration curve for *E. coli BL21 (DE3)*

The plate count assays were run in triplicate to determine the number of colony forming units per ml (CFU/ml) at specific OD<sub>600</sub> values. After these experiments, we plotted the OD<sub>600</sub> calibration curve to help estimate the number of CFU/ml at different OD<sub>600</sub> values. The calibration curve was found to be linear, as expected, as shown in Figure 31 with the linear equation displayed below.

$$Conce [CFU/ml] = (OD600\_val \times 2E8) + 1E6$$

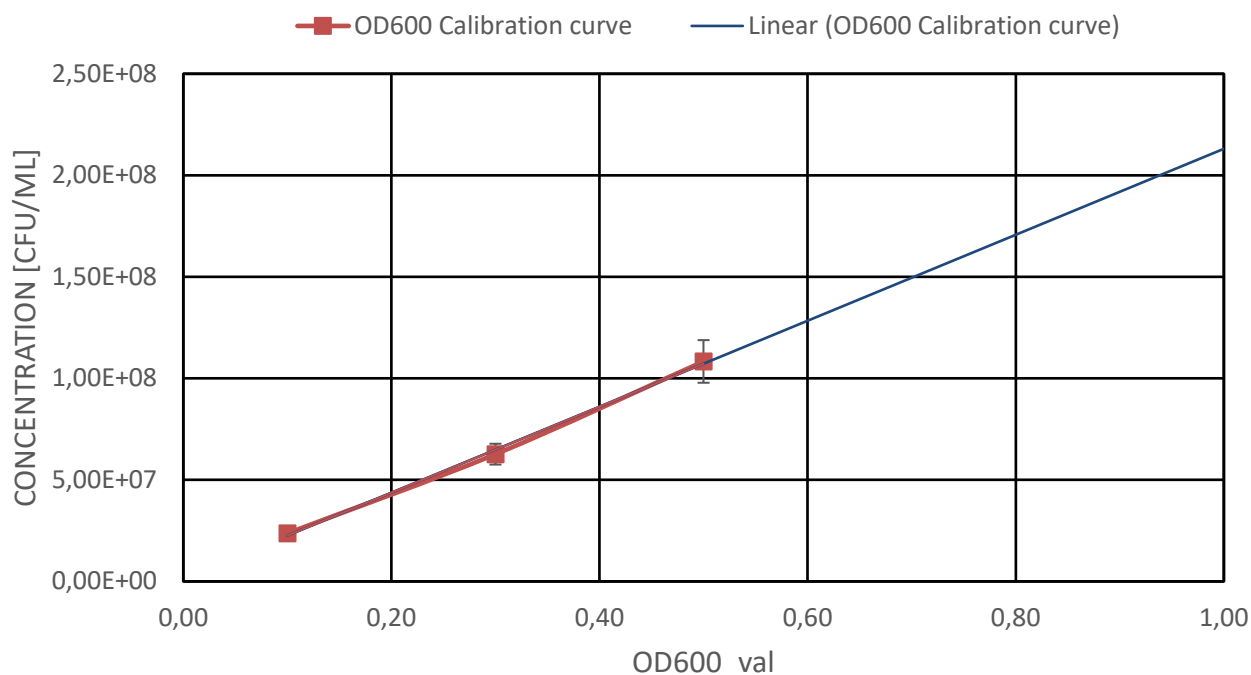


**Figure 31:** OD<sub>600</sub> calibration curve for *E. coli BL21 (DE3)*.

### 5.2.2 Enumeration of *E. coli BL21 (DE3)* bacteriophages

The bacteriophage stock was prepared and concentrated as described. The concentration and efficacy of the prepared bacteriophage stock was evaluated and confirmed using plaque assays. This experiment validated the high effectiveness of the prepared bacteriophage stock against *E. coli BL21 (DE3)*, confirming the success of the bacteriophage concentration procedure. The concentration of the bacteriophage stock was estimated at  $7.2 \times 10^{10}$  PFU/ml, as detailed in Table 6, which includes triplicate plaque assay counts.

**Table 4: Plaque Assay results**

	<b>Experiment 1 (Intra)</b>	<b>Experiment 2 (Inter)</b>	<b>Experiment 3 (Inter)</b>	<b>Average (All Experiment)</b>
<i>Plaque count (PFU)</i>	81 PFU (at $10^{-9}$ dilution)	62 PFU (at $10^{-9}$ dilution)	72 PFU (at $10^{-9}$ dilution)	72 PFU (at $10^{-9}$ dilution)
<i>Phage concentration (PFU/ml)</i>	$8.1 \times 10^{10}$ PFU/ml	$6.2 \times 10^{10}$ PFU/ml	$7.2 \times 10^{10}$ PFU/ml	$7.2 \times 10^{10}$ PFU/ml

### 5.2.3 Determining the lysis profile for *E. coli BL21 (DE3)*

The lysis profile of the bacteriophages was analysed in three different media: Brain Heart Infusion (BHI) growth medium, PBS buffer solution at a pH of 7.4, and Milli-Q water, to confirm their ability to induce lysis in these environments. The experiment encompassed various multiplicity of infection (MOI) values ranging from 1 to 0.001. Additionally, a negative control was included, where bacteriophages were omitted, and bacterial growth was monitored over time. This analysis was conducted using the automated TECAN Spark equipment system, which monitored the OD<sub>600</sub> of the medium and solution over time to observe changes in cell growth, which could be related to the presence of bacteriophages.

In BHI medium, the lysis profile was determined using the TECAN Spark to show that approximately 40 minutes was required to completely lyse all the *E. coli* cells, and it took less time to completely lyse the bacterial cells at a higher MOI, as shown in Figure 32. In the second experiment, the lysis profile was obtained in PBS; the cells did not multiply, nor did the bacteriophage lyse the cells, as shown in Figure 33. However, this does not mean that the bacteriophage does not bind to the cells in PBS. In the third experiment, the lysis profile was estimated in Milli-Q water. Figure 34 shows that the cells had very limited growth, and the bacteriophage did not lyse the cells. This same behaviour was observed at higher starting OD<sub>600</sub> densities.

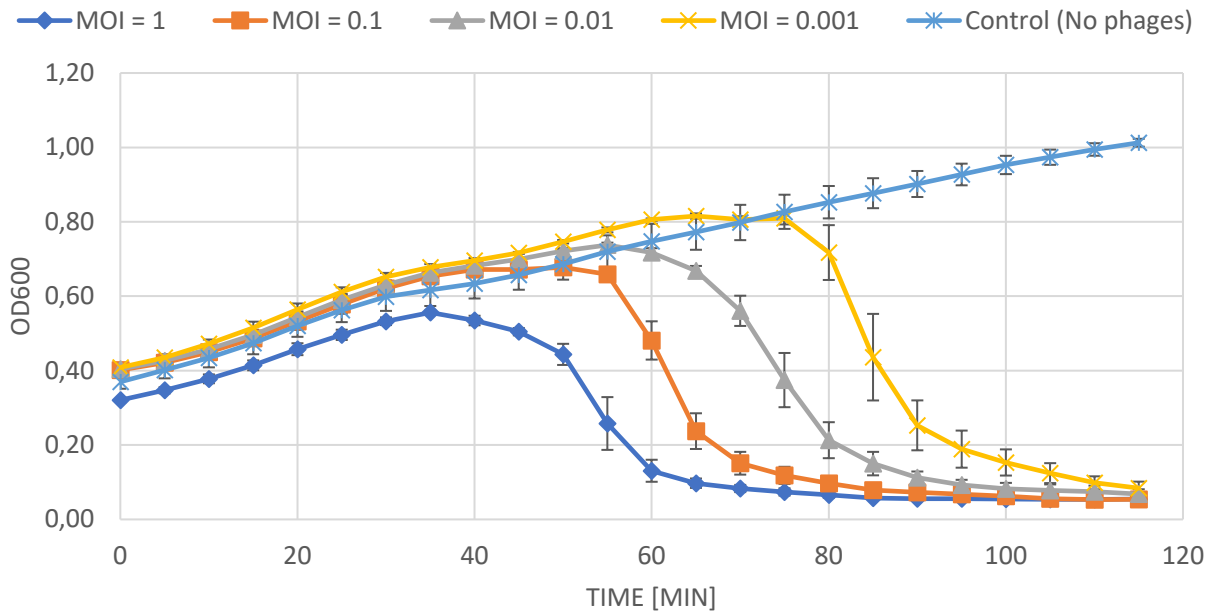


Figure 32: TECAN Spark lysis profile in BHI medium.

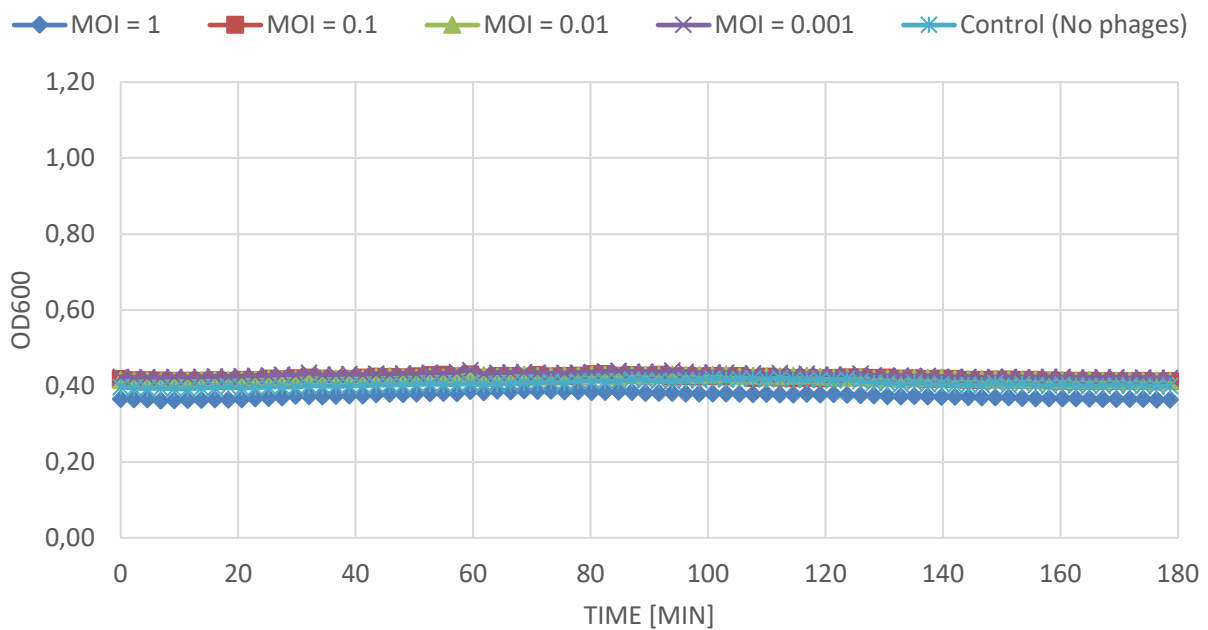
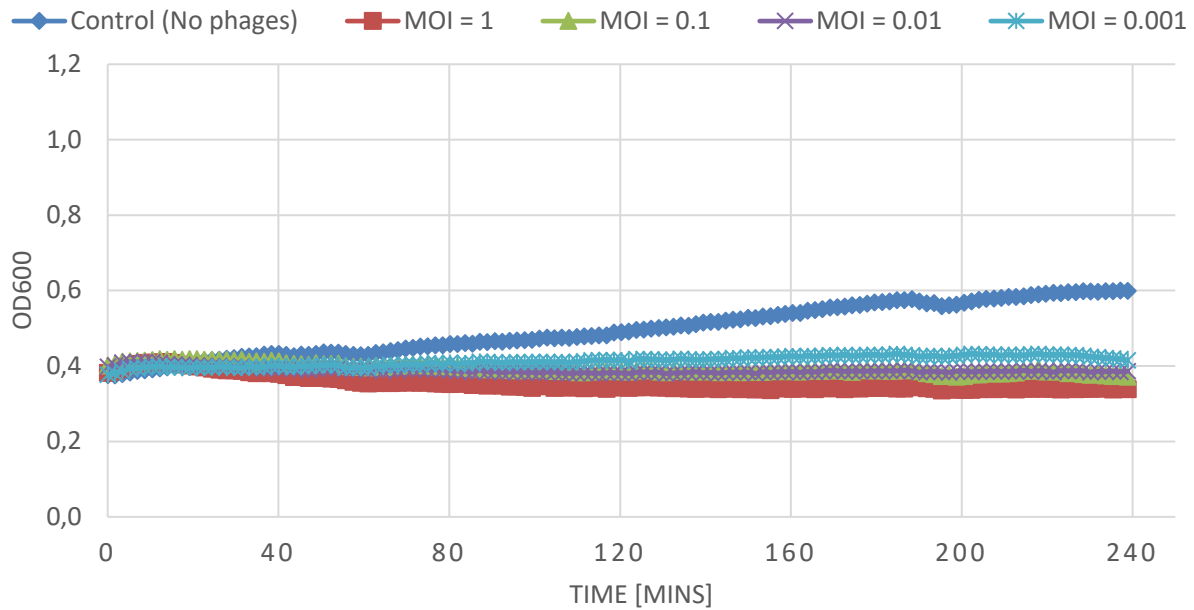


Figure 33: TECAN Spark lysis profile in PBS.



**Figure 34:** TECAN Spark lysis profile in laboratory Milli-Q.

#### 5.2.4 Conclusion

In summary, the experiments in this section yielded promising results in the preparation and characterisation of the bacteriophage stock. The effectiveness of the prepared bacteriophage stock against *E. coli BL21 (DE3)* cells was conclusively demonstrated, with a concentration estimated at  $7.2 \times 10^{10}$  PFU/ml. Furthermore, the establishment of the OD600 calibration curve for the *E. coli BL21 (DE3)*, exhibiting the expected linear behaviour based on existing literature, strengthens the reliability of the experimental setup.

The use of the TECAN Spark laboratory machine enabled us to estimate bacteriophage lysis profiles across various mediums. Interestingly, the lack of observed lysis in PBS and Milli-Q water could potentially benefit the biosensor development, as it suggests that bacterial lysis would not occur during the detection process using these mediums resulting in a dependable biosensor that does not interfere with the sample. Despite the absence of observable lysis in these media, the focus remains on developing a biosensor capable of capturing bacteriophage-binding events.

### 5.3 CONFIRMATION OF BACTERIOPHAGE IMMOBILISATION

The experiments detailed in this section were conducted to validate the successful immobilisation of bacteriophages onto the gold surfaces of the IDE chip. To assess the efficacy of the phage immobilisation technique, we utilised the plaque counting method, which involved quantifying the number of bacteriophages present in the suspension before and after immobilisation. By carefully recovering the excess bacteriophage suspension and employing plaque counting, we could determine the number of bacteriophages that remained unbound. However, this method was not conclusive, prompting us to continue with additional methods.

The disk-diffusion technique was employed to confirm the infectivity of the immobilised bacteriophages. This technique involved placing the immobilisation substrate onto the solid agar plates and observing the formation of lysis rings around the substrate after an incubation period. Furthermore, to characterise bacteriophage and bacterial binding on the substrate, scanning electron microscopy (SEM) was utilised. However, it is crucial to note that identifying bacteriophages on substrates can be challenging without proper experimental controls.

Therefore, we took into consideration various factors outlined in previous studies (Chai et al., 2012; Ertürk & Lood, 2018; Gervais et al., 2007; Hiremath et al., 2015; Lee et al., 2013; Li et al., 2010; Singh et al., 2009) to ensure the accuracy of the results. Finally, we employed confocal microscopy, utilising fluorescently tagged cells, to confirm bacteriophage immobilisation through bacterial binding, as detailed in the literature (Richter et al., 2016; Richter et al., 2017).

### 5.3.1 The disk-diffusion technique

To test the viability of chemically immobilized bacteriophages, IDEs were placed on BHI agar overlay plates containing either *E. coli* BL21 (DE3) or the commensal *S. epidermidis* strain. It was found that cysteamine and glutaraldehyde did not hamper the viability of the immobilised phage as Figure 35 shows areas of lysis around the IDE with *E. coli* BL21 (DE3). These areas of lysis show that the bacteriophages can perform their life cycle despite being immobilised to the IDE surface, thus indicating that bacteriophage-bacteria binding is still viable.

As shown in Figure 35a: An *E. coli* overlay agar plate was divided into four sections; A positive control of bacteriophage was spotted on the plate creating a zone of lysis. Physically absorbed and immobilised bacteriophage IDEs produced area of lysis (Red arrow) whilst one without phage produced no lysis.

As shown in Figure 35b: A *S. epidermidis* overlay agar plate was divided into four sections, but IDEs with physically absorbed and immobilised bacteriophages produced no lysis. This reflects the host specificity of the bacteriophage to *E. coli* BL21 (DE3). As a result, we concluded that the immobilisation worked as expected, with the bacteriophages binding only to *E. coli*, and the next step was to examine the IDE surface with scanning electron microscopy (SEM) to look for the bacteriophages.

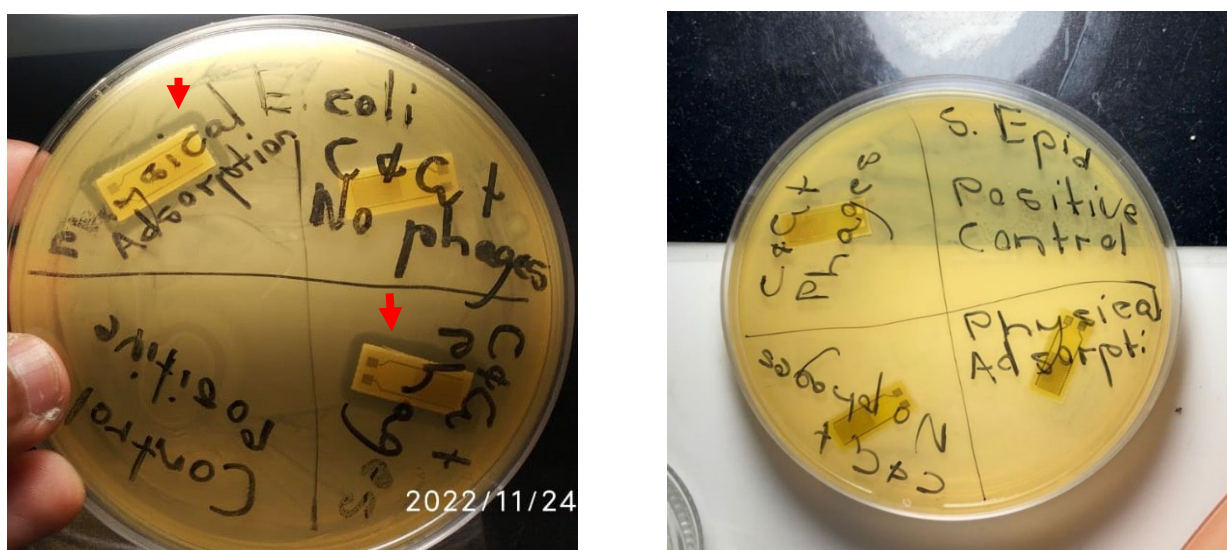


Figure 35: Disk-diffusion test with a) *E. coli* and b) non-specific *S. epidermidis*.

### 5.3.2 Scanning Electron Microscopy (SEM)

The upper image in Figure 36 shows the effect of treating IDEs with covalently bound bacteriophages and due to the nature of bacteriophages being <200 nm the SEM could not detect bacteriophage structures. On this basis, *E. coli* BL21 (DE3) was added to the IDE for detection instead, and the *E. coli* cells were detectable.

The lower image of Figure 36 depicts the IDE with *E. coli* adhering to covalently bound bacteriophages, as expected. In addition, we were able to image an IDE with physically bound bacteriophages and observed a few *E. coli* cells adhering to the surface. We were also expecting to see lysed *E. coli* cells, which were not

Drone adaptation and configuration to sensor apparatus for on-site, real-time digitalised water quality test application.

seen. Furthermore, because we could only focus on a very limited region of the IDE and *E. coli* cells did not evenly distribute across the IDE surface, the results were inconclusive in confirming complete binding and, thus, successful immobilisation.

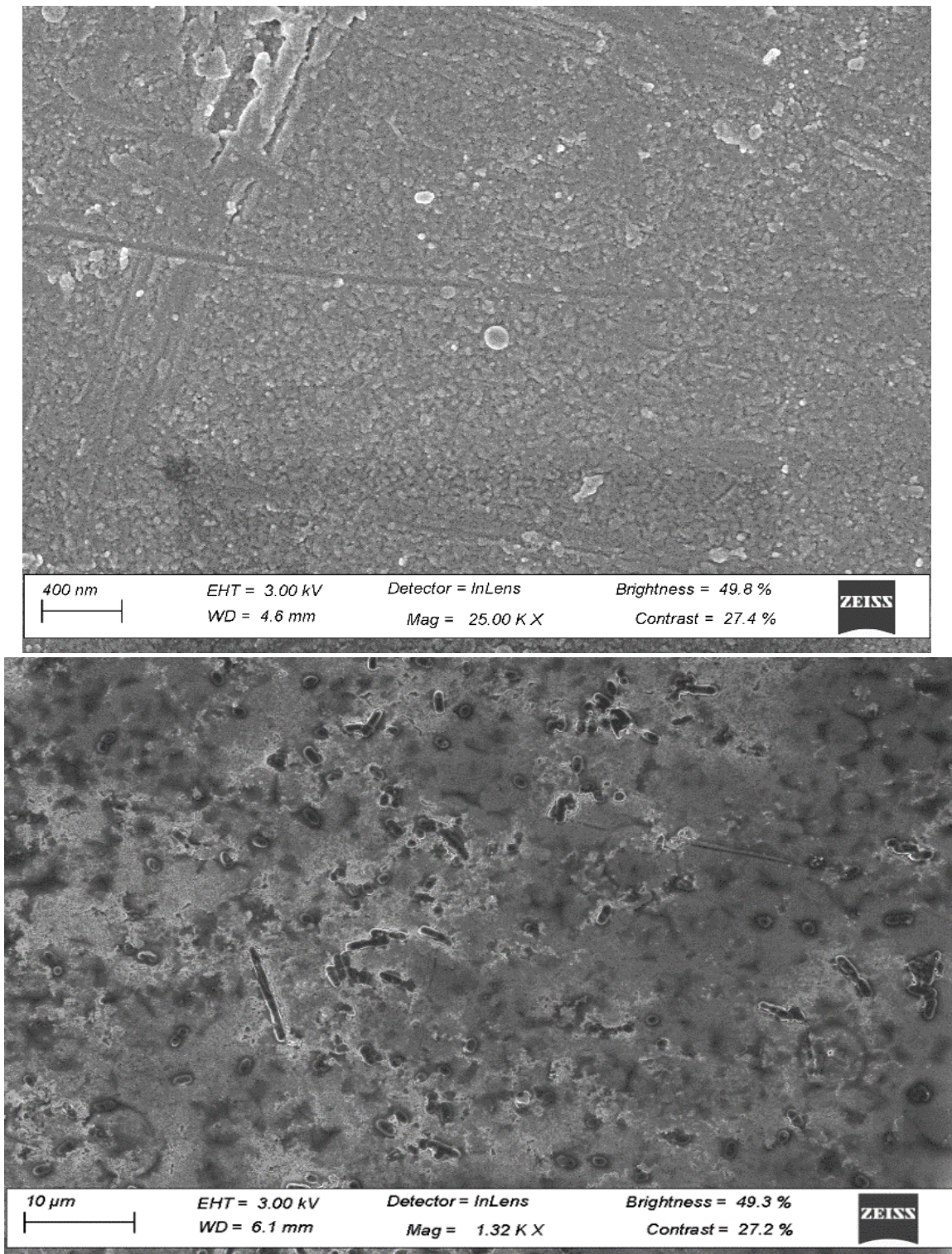


**Figure 36:** SEM images of treated IDE: a) Before exposure, and b) After exposure to *E. coli* BL21 (DE3).

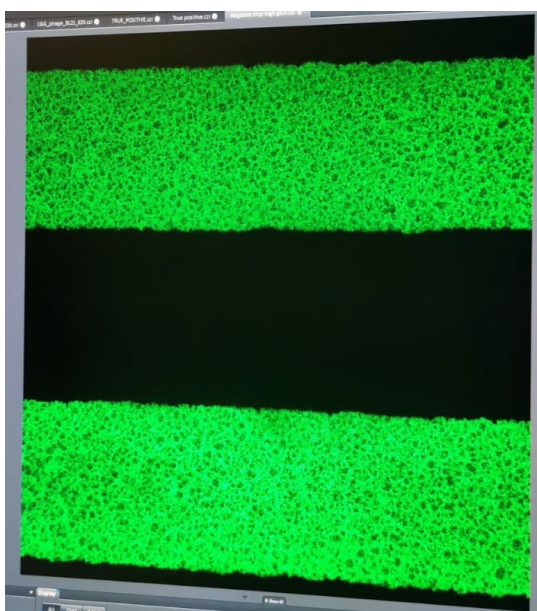
### 5.3.3 Confocal microscopy analysis

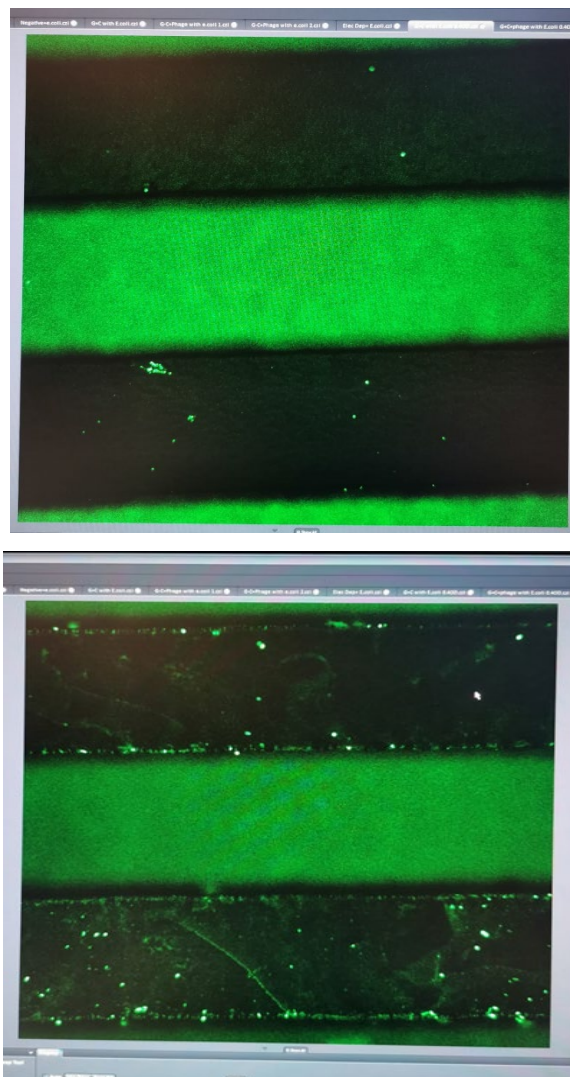
After conducting initial tests on the immobilisation method, we employed confocal microscopy to establish a robust comparison among the treated IDEs, thereby confirming successful bacteria capture and validating the biosensor's effective functionality. In Figure 37, all three IDEs were allowed to bind for 10 minutes with *E. coli* BL21 (DE3) expressing the GFP gene, which fluoresces. Subsequently, the IDEs were rinsed to remove excess and unbound bacteria. This test was performed at OD<sub>600</sub> values of 0.4 and 0.1, and the results reported here are at 0.4; however, a similar trend was observed at 0.1. It is also noteworthy that before this analysis, bacteriophages were tested for their specificity to the modified *E. coli* cells, and they demonstrated continued effectiveness, as anticipated.

Figure 37 a) shows a blank IDE that underwent the cleaning step only, revealing, as anticipated, very limited bacteria binding onto the surface.

Figure 37 b) depicts a C&G + no phage IDE that underwent cysteamine and glutaraldehyde incubation without phage addition, demonstrating limited bacteria capture due to glutaraldehyde's expected non-specific binding to proteins.

Figure 37c) showcases a C&G + phage IDE that underwent the complete covalent immobilisation process with added bacteriophage. Clearly, this IDE exhibits a higher level of bound bacteria, consistent with the expected bacteria binding to the immobilised bacteriophages on the IDE surface. This verifies the intended functionality of the biosensor, a validation to be further examined through EIS measurements.





**Figure 37:** Validation of bacteria capture efficacy using confocal microscopy - a) Blank (top), b) C&G without phage treatment (middle), and c) C&G with phage treatment (bottom).

#### 5.3.4 Electrochemical Impedance Spectroscopy (EIS) measurements

The IDEs prepared above were replicated in triplicate and analysed to confirm changes in IDE capacitance, indicative of successful bacteriophage immobilisation. As depicted in Figure 38, the capacitance of the IDE was plotted across a wide frequency range to determine the optimal frequency for subsequent measurements, with 100 kHz being selected for further analysis. The capacitance profile of the IDE demonstrates variation when transitioning from a blank surface to an immobilised state, confirming effective bacteriophage immobilisation. Baseline measurements of blank IDEs were utilised to calculate percentage changes, as demonstrated in Figure 38, thus confirming immobilisation. Analysis was conducted at a frequency of 100 kHz, as detailed in Table 7, for consistency and comparison.

In Table 7, three samples of variously treated IDEs were analysed to confirm immobilisation. These included:

1. **C&G without bacteriophages** (blank IDEs treated with cysteamine and glutaraldehyde only).
2. **C&G + bacteriophages** (blank IDEs treated with cysteamine and glutaraldehyde, followed by addition of a bacteriophage stock at a known concentration).

3. **C&G + Electric Field + Bacteriophage** (blank IDEs treated with cysteamine and glutaraldehyde, followed by addition of a bacteriophage stock at a known concentration in the presence of an electric field).

This analysis was conducted in triplicate, with the treated IDEs labelled 1 to 3, as shown in Table 7. Baseline measurements were taken of the blank IDEs before any treatment, serving as a baseline from which percentage changes were calculated to assess treatment effects. Figure 38 displays three different IDEs, each subjected to different treatments, with the entire frequency range depicted to illustrate how capacitance varies with frequency across these IDEs. Measurements were conducted over two separate days, revealing that immobilised bacteriophages consistently increased the capacitance of an IDE, with those containing bacteriophages consistently exhibiting higher capacitance compared to those without, on both days. It is noteworthy that these IDEs underwent treatment on the same day as those in the confocal experiment, utilising the same number of diluted bacteriophages. This confirmation underscores the observed differences in confocal microscopy results.

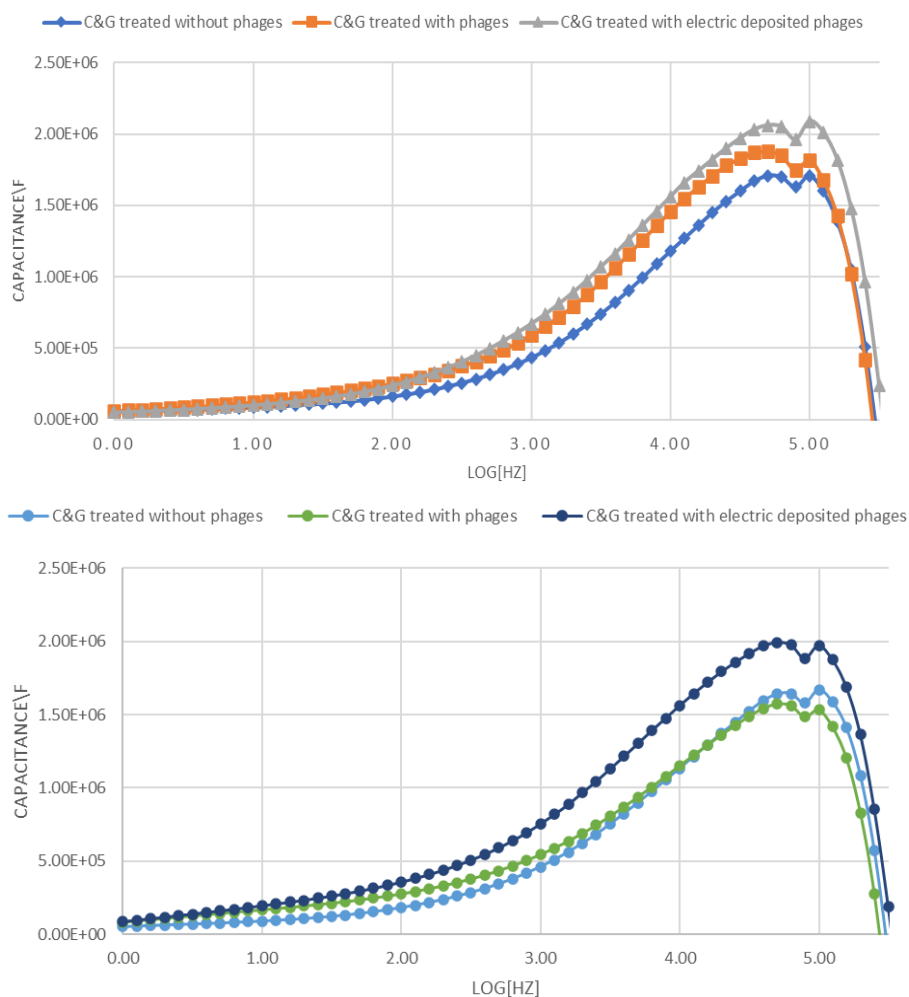


**Figure 38:** Raw EIS measurements to confirm immobilisation: a) First day (upper graph) and b) Second day (lower graph).

In Table 7, three samples of variously treated IDEs were analysed to confirm immobilisation. The first sample, C&G without bacteriophages, exhibited percentage changes below 60%, accompanied by a large variance. This variability could potentially be attributed to inconsistent coverage of the IDE surface. The second sample, C&G + bacteriophages, demonstrated significantly higher and consistent percentage changes, around 75%,

compared to the IDEs without bacteriophages. This suggests a more uniform covering of the IDE surface with bacteriophages, potentially explaining the observed difference.

The third sample, C&G + Electric Field + Bacteriophage, also showed high percentage changes, around 70%. However, the method proved to be challenging to perform without contaminating the IDE surface, as evidenced by the last IDE where measurements could not be obtained. In conclusion, the analysis successfully distinguished the immobilised IDEs with bacteriophages from those without. It is noteworthy that the IDE surface was maximised with the highest concentration of bacteriophages, without any dilutions, to ensure maximum bacteriophage presence on the IDE surface. This contrasts with previous experiments where IDEs were not maximised due to dilution of the bacteriophage solution to achieve a specific bacteriophage concentration on the IDE surface.

**Table 5: EIS measurements analysis to confirm immobilisation**

<i>Treatment</i>	<i>Sample</i>	<i>Base measurement / (F)</i>	<i>Capacitance Change / (F)</i>	<i>% Change</i>	<i>Comment</i>
C&G without bacteriophages	1	1.14E+07	6.70E+06	58.7 %	
	2	1.10E+07	3.68E+06	33.4 %	
	3	8.38E+06	-4.89E+05	-5.8 %	<b>Outlier</b>
C&G + bacteriophages	1	1.02E+07	7.77E+06	76.4 %	
	2	7.93E+06	6.32E+06	79.7 %	
	3	1.24E+07	9.42E+06	75.7 %	
C&G + Electric Field + bacteriophages	1	1.14E+07	7.71E+06	67.9 %	
	2	1.20E+07	8.68E+06	72.1 %	
	3	9.49E+06	Wrong	#VALUE!	<b>Outlier</b>

### 5.3.5 Conclusion

While our initial intention was to visualise bacteriophages using SEM to optimise their orientation and assess surface coverage, we successfully immobilised them on the IDE's active surface. This successful immobilisation was indirectly confirmed by observing bacterial capture using SEM imaging and measuring capacitance changes due to immobilisation through EIS measurements. All these methods confirmed the success of the immobilisation process. The next step involved measuring the bacteria capture efficiency of the biosensor, which is crucial for determining its correct functioning.

Future work from this biosensor development project will concentrate on this section regarding immobilisation protocols and their confirmation to ensure the proper orientation and uniform immobilisation of bacteriophages on solid substrates. The aim will be to develop protocols that enable visualisation and verification of this claim, as these protocols have wide-ranging applications beyond bacterial biosensors. Therefore, future work will focus on refining these protocols and establishing confirmation methods to meet various requirements.

## 5.4 INITIAL BIOSENSOR TESTING

To test the function of the biosensor, the commercially available potentiostat, PalmSens 4, was utilized. Various treated IDEs were prepared, and the controls were the C&G IDEs without bacteriophages to verify the correct functioning of the biosensor. The first treated IDEs were the C&G + bacteriophages IDEs, which were chemically treated to immobilise bacteriophages. Lastly, the C&G + Electric Field + bacteriophages were tested, where the bacteriophages were chemically immobilised in the presence of an electric field. It is crucial to note that the IDEs were treated with *E. coli BL21 (DE3)* bacteriophages whenever bacteriophages are

mentioned. These bacteriophages are specific to *E. coli*, which is the bacteria of interest tested and whenever other bacteria are mentioned they are used as negative controls. The following exact procedure was followed for these measurements:

1. The measuring setup was performed as shown in Figure 21 in the previous chapter, where the PalmSens is connected to the PC and to the IDE via a holder for easy electrical connections.
2. The IDE capacitance baseline of the treated IDE was measured for each IDE before testing the sample. Soon after testing the sample, another measurement was taken. These two measurements were then used to calculate the change in capacitance directly related to the number of cells in the sample.
3. The sample testing was conducted as follows: the treated IDE was immersed in an Eppendorf with the desired sample for roughly 5 minutes. Soon after, the IDE was washed with excess PBS buffer solution to remove excess unbound cells from the sample.
4. A PBS buffer solution was used as the measuring solution for all measurements taken with the PalmSens. Wells were used as liquid holder on the IDE to expose the testing surface to this solution during a measurement.

#### 5.4.1 Confirmation of bacteria capture using electrochemical impedance spectroscopy (EIS)

Figure 39 illustrates the average of three measurements taken with different IDEs in each set. From the graph, it is evident that the C&G + no phage (C&G without bacteriophages) IDEs exhibit the lowest capacitance, as anticipated, serving as the baseline for the measurements. Conversely, the graph representing C&G + phage (C&G with bacteriophages) is positioned above this line, indicating a higher bacteria capture compared to the IDEs without the bacteriophages, consistent with the expected bacterial binding to the immobilised bacteriophages. Additionally, the C&G + electrically deposited phages (C&G with bacteriophages immobilised in the presence of an electric field) graph surpasses both previous graphs, suggesting the highest bacteria capture, aligning with expectations and demonstrating the successful functionality of the biosensor in distinguishing between specific and non-specific binding on this occasion. This behaviour was observed across almost all tested frequency ranges of the IDE, validating the chosen frequency for further analysis.

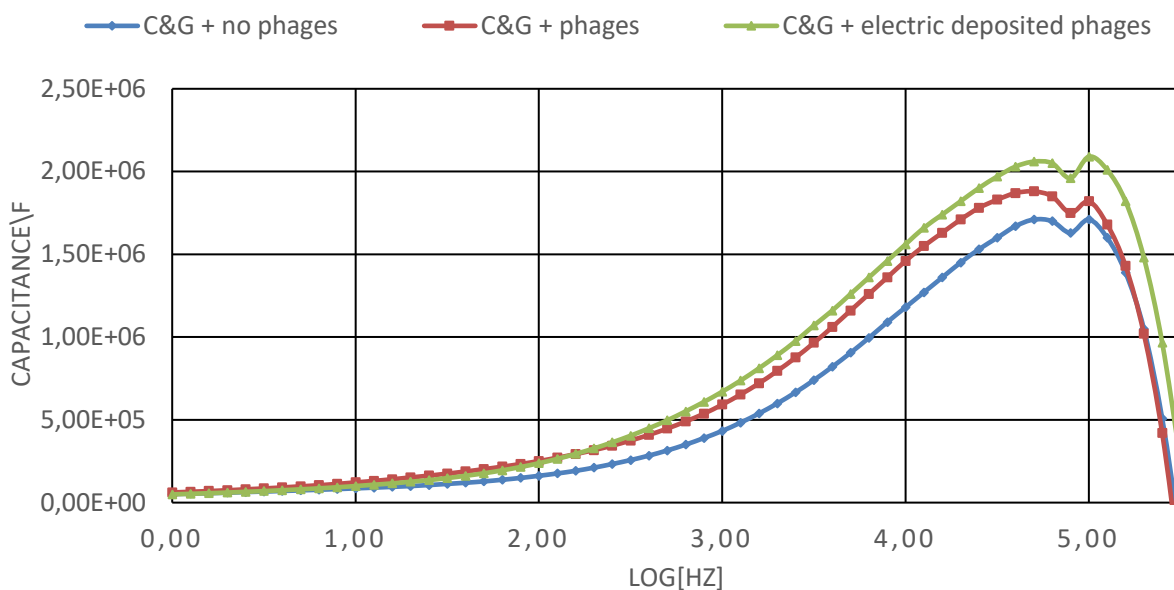


Figure 39: EIS measurements to confirm bacteria capture.

Drone adaptation and configuration to sensor apparatus for on-site, real-time digitalised water quality test application.

After distinguishing the differently treated IDEs, additional sets of IDEs were prepared to test for bacteria capture at a specific frequency of 100 kHz, which is the operating frequency of the developed biosensor. At this specific frequency, it was possible to distinguish between the different IDEs. It is noteworthy that the tabulated results in Table 8 are based on the baseline chosen as the IDE treated with C&G but without bacteriophages. This IDE was measured after bacteria capture, and therefore, the percentage changes indicate the difference in bacteria capture among these different IDEs. For instance, the C&G with bacteriophages, even in the presence of an electric field, captured a relatively higher number of bacteria, as evidenced by the increase in capacitance.

**Table 6: EIS measurements to confirm bacteria capture**

Sample	Base measurement / (F)	Measured capacitance / (F)	% Change	Comment
C&G <i>without</i> bacteriophage	$1.71 \times 10^6$	$1.71 \times 10^6$	0	Baseline measurement
C&G + bacteriophage	$1.71 \times 10^6$	$1.82 \times 10^6$	6.34 %	Relatively higher
C&G + Electric Field + bacteriophages	$1.71 \times 10^6$	$2.09 \times 10^6$	22.22 %	Effective bacterial capture

Table 9 presents the same IDEs; however, in this case, a binding blocking agent, skim milk, was utilised. The IDEs were incubated in 5% skim milk for 30 minutes at room temperature following immobilisation, and subsequently, these IDEs were tested for bacteria capture. The data demonstrated the expected results, showing a similar trend to the previous experiment but with a lower standard deviation compared to the ones without the blocking agent. Nevertheless, there is a drawback associated with reducing the signal, as indicated in Table 9. It is noteworthy that all IDEs in this subsection were treated with diluted bacteriophages to match the maximum number of bacteriophages theoretically allowed on the IDE surface without overlap. The number of these bacteriophages needed to achieve the theoretical maximum output of the IDE was previously calculated and estimated at  $1 \times 10^9$  PFU. This was done by adding 100 uL of the original bacteriophage stock to 900 uL of PBS and suspending the IDEs in this solution.

**Table 7: EIS measurement to confirm bacteria capture using a non-specific binding blocking agent**

Sample	Base measurement / (F)	Measured capacitance / (F)	% Change
C&G without bacteriophage	$1.62 \times 10^6$	$1.62 \times 10^6$	0
C&G + bacteriophage	$1.62 \times 10^6$	$1.69 \times 10^6$	4.20 %
C&G + Electric Field + bacteriophages	$1.62 \times 10^6$	$1.78 \times 10^6$	9.94 %

After successfully confirming bacteria capture, the focus shifted to testing the biosensor for sufficient signals to develop an actual biosensor. The experiments in this section were further developed with minor changes made to the overall procedures to obtain maximum signal differences for the biosensor. The subsequent subsection will focus on this.

#### 5.4.2 Electrochemical Impedance Spectroscopy (EIS) results discussion

The bacteriophage immobilisation protocol was optimised, and the biosensor was tested at different sample concentrations. The IDEs were prepared in cysteamine in the dark at 37°C for 18 hours, followed by treatment in glutaraldehyde in the dark at room temperature for two hours. Subsequently, the IDEs were prepared for

the different samples as outlined in Table 10. It is worth noting that the IDEs were immobilised with an excess of the original bacteriophage stock (concentration of  $7 \times 10^{10}$  PFU/ml) to ensure the maximum number of bacteriophages on the IDE surface. This excess saturation of the IDE surface had a significant impact on the biosensor's performance, resulting in improved performance.

A positive sample was spiked with *E. coli* BL21 (DE3) to reach an OD<sub>600</sub> of 0.280. Using the OD<sub>600</sub> calibration curve prepared earlier and provided below, the concentration of *E. coli* at this OD<sub>600</sub> value was estimated to be  $5.70 \times 10^7$  CFU/ml. The biosensor was then tested with serial dilutions of this sample to determine its limit of detection (LOD). Additionally, a baseline was established for each biosensor's IDE by measuring the capacitance after treatment but before sample testing. Sample detection is carried out by calculating changes in capacitance from this baseline.

$$\text{Conce [CFU/ml]} = (\text{OD600\_val} \times 2\text{E8}) + 1\text{E6} = (0.280 \times 2\text{E8}) + 1\text{E6} = 5.70\text{E7}$$

**Table 8: EIS measurements to confirm biosensor functionality**

Treatment	Sample	Base measurement (F)	E-2 dilution	E-1 dilution	No dilution	Comment
			% Change	% Change	% Change	
C&G without bacteriophages	1	1.14E+07	30.5 %	52.6 %	23.1 %	
	2	1.10E+07	17.9 %	4.7 %	7.6 %	
	3	8.38E+06	34.4 %	-5.1 %	14.5 %	
C&G with bacteriophages	1	1.02E+07	7.7 %	48.3 %	18.9 %	
	2	7.93E+06	-11.7 %	42.8 %	-7.0 %	<b>Outlier</b>
	3	1.24E+07	17.0 %	50.8 %	25.0 %	
C&G + Electric Field + bacteriophages	1	1.14E+07	11.0 %	33.8 %	10.5 %	
	2	1.20E+07	4.7 %	37.1 %	18.3 %	
	3	9.49E+06	6.4 %	40.0 %	13.3 %	

The results obtained at these concentrations of *E. coli* BL21 (DE3) are summarised in Table 10. Three different treatments were applied to the IDEs as follows:

1. C&G without bacteriophages: This exhibited non-specific binding, as evidenced by significant variations in capacitance changes. This variability confirmed non-specific binding of the bacteria to the IDEs, possibly due to the binding effect of exposed cysteamine and glutaraldehyde. The binding was uneven across the IDEs in this group.
2. C&G with bacteriophages: This showed specific binding, with capacitance changes being more consistent and increasing with higher *E. coli* concentrations, indicating that the biosensor was functioning as intended.
3. C&G + Electric Field + bacteriophages: This set displayed very consistent behaviour, even more so than the set without the electric field. However, it had the drawback of requiring meticulous preparation to avoid contaminating the IDEs.

From the overall results, it was observed that the IDEs treated with C&G but without the bacteriophages exhibited non-specific binding, rendering them unsuitable for the biosensor. Conversely, those treated with the bacteriophages demonstrated specific and consistent binding, indicating the intended functionality of the biosensor, with signal increasing proportionally to the concentration of *E. coli*. The IDEs treated with C&G + Electric Field + bacteriophages exhibited the desired behaviour for our intended biosensor with very minimum variance for the IDEs tested in a similar manner.

As summarised in Table 11: At the lowest tested concentration, the biosensor showed a minimum signal of approximately 7.4% with minimal variation across the three IDEs. As the concentration increased tenfold, the signal rose to around 37% and in some cases to 50 %, before decreasing to approximately 14% with a further tenfold increase in concentration, defining the maximum limit of detection. Therefore, the biosensor operates by initially detecting signals from the minimum limit of detection (LOD) up to a certain maximum, beyond which no further capacitance changes are observed. This indicates that no binding occurs, as bacteria can be easily washed off from the IDE surface.

**Table 9: Defining the non-linear limit of detections of the biosensor**

	<b>Sample concentration [CFU/ml]</b>	<b>Signal % Change</b>
Minimum LOD	$5.7 \times 10^5$	7.4 %
Non-linear maximum	$5.7 \times 10^6$	37.0 %
Maximum LOD	$5.7 \times 10^7$	14.0 %

### 5.4.3 Conclusion

The biosensor successfully demonstrated its capability as a proof-of-concept for detecting the presence of *E. coli BL21 (DE3)* in laboratory settings. However, further refinement is necessary to develop a biosensor with a linear response, indicating linear changes in signal. Achieving this will require additional work and the development of protocols to immobilise bacteriophages uniformly on the IDE surface. This uniform immobilisation will ensure consistent capture of bacteria on the surface. We plan to conduct further research on these immobilisation protocols. By optimising these protocols, we aim to enhance the performance and versatility of the biosensor.

## 5.5 CONCLUSIONS

This section concludes the work done on the biosensor. The following conclusions are based on the results of the experiments and testing performed on this work:

- It is very evident that there is need for a rapid microbial water quality testing biosensor for field testing applications as shown by the literature review that all the current methods are time consuming and require trained technicians to conduct the test with results available after at least 8 hours with the rapid and expensive methods.
- More simulations are needed to understand the surface interactions of interdigitated electrodes in biosensor applications and how the design can be optimised to produce more sensitive and consistent IDEs.
- It is important to prove that bacteriophages can be used as a cheap alternative to expensive antibodies as a bioreceptor for biosensor applications. Study results also proved that bacteriophages have high specificity for bacterial strains and show a rapid lysis time.
- The results indicated a bacteriophage immobilisation protocol using cysteamine and glutaraldehyde as well as the electric field that resulted in improved bacterial capture compared to simple physical adsorption of phage.

- The study proved the efficiency of the immobilisation protocols using different methods, including confocal microscopy, which clearly showed potential for such a biosensor if signals are measured.
- Demonstrated that PBS can be used as a measuring solution for electrochemical impedance spectroscopy measurements, as evidenced by the absence of lysis seen by observing its lysis profile in this buffer.
- We were able to measure distinguishable signals for the differently treated IDEs and establish baselines to prove the concept of a phage-based EIS biosensor despite poor sensitivity and consistency due to non-uniform bacteriophage coverage of the IDE.
- We tested electronic circuits that can be used on such a proof-of-concept biosensor.

## CHAPTER 6: DROBOTICS DEVELOPMENT OF WINCH/HOIST SYSTEM FOR THE DRONE – LITERATURE REVIEW

### 6.1 INTRODUCTION

Drobotics have resolved to design and build their own integrated drone adapted winch/system as opposed to acquire and reconfigure a generic, off-the-shelf system. The winch/hoist system shall be designed and configured for launch of digital water quality test probes.

### 6.2 SCOPE

The task is to deploy bacteria test digital probe apparatus using winch and sling systems of a drone platform requiring a more integrated approach than just transport of drone from point to point in that operations protocols require release/deploy, stable hover ability, and lift encompassing real-time data received and record.

#### 6.2.1 Basic winch/hoist system

A basic winch/hoist system comprises a battery-powered electric motor that will turn an attached spool inserted shaft both clockwise and anti-clockwise to release or wind wire, line, or rope on the spool. We were fortunate in that we secured a basic winch concept design from extensive research that we will redesign for drone adaptation and further sub-system installations to accommodate expanded scope defined herein under System Design Protocols (Figure 40).

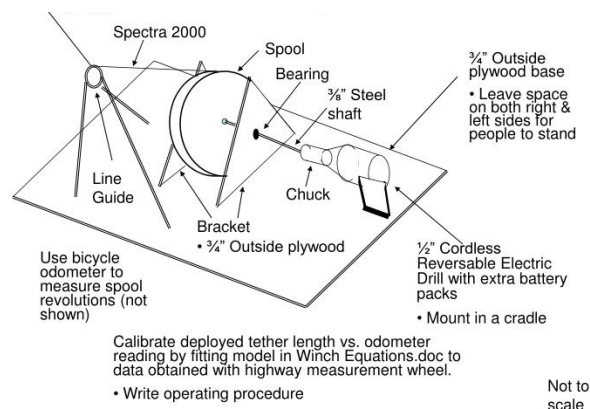


**Figure 40:** Illustration of the winch conceptual (Winch conceptual sketch, 2022).

We will develop our winch as per conceptual design herein above except that we will use a stepper motor (Structural Diagram herein below) with a minimum torque of 0,75 nm in place of a cordless electrill drill motor proposed (Figure 41).

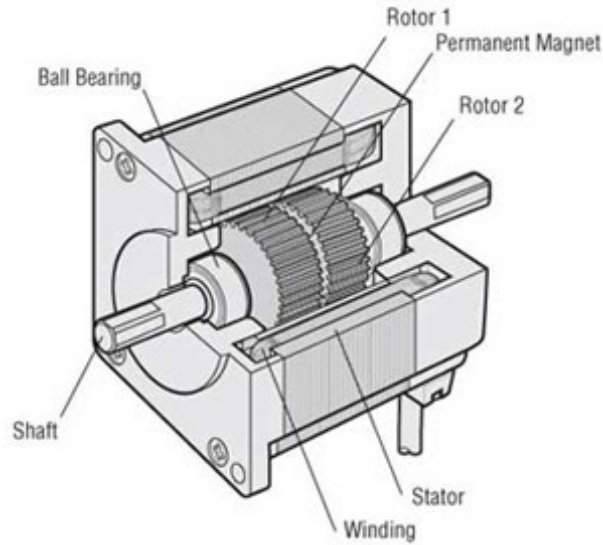


**Figure 41:** Illustration of the motor structural diagram: cross section parallel to shaft (Structure of stepper motors, 2022).

### 6.2.2 System design protocols

The following protocols are contingent on the operation of the winch for the scope as defined.

1. All up lift weight capacity of 10 kg
2. Capacity to winch/hoist minimum 5 m deploy/lift
3. Minimum Battery (Winch Battery) 60 min operational battery life
4. Installed radio communication capacity minimum 1 km receive/transmit
5. Winch installed capacity camera application (Figure 42 a)
6. Winch installed capacity for laser range/distance between winch and test surface (Figure 42 b)
7. Winch installed remote control (Figure 42 c)
8. Winch installed capacity to receive and transmit binary data (Universal Recorder) (Figure 42 d).

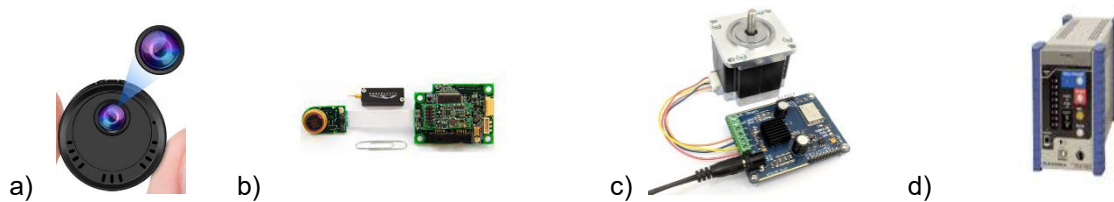


**Figure 42:** Figure showing a) Camera, b) laser range finder, c) remote control, d) universal recorder.

### 6.2.3 Winch/hoist system development

Our approach to the development of the system shall be methodical, and conducted in phases to ultimately deliver capacity as envisaged in the design protocols.

#### Phase 1

Our first phase is to build a basic winch system that we will test our operational lift, weight, and battery capacity hypothesis from elevated platform.

The basic winch system is made up of the following components: stepper motor, battery pack, shaft, bearings, spool mounted on 1 mm aluminium base plate.

Drone adaptation and configuration to sensor apparatus for on-site, real-time digitalised water quality test application.

---

### Phase 2

After successfully testing the hypothesis for phase 1, The following shall be installed and integrated on to the winch system:

1. Remote control of winch system
2. Installation of laser range finder
3. Installation of camera
4. Installation of universal recorder
5. Installation and integration communication hardware and software

The system will be tested as an integrated automated system off an elevated platform.

### Phase 3

The final phase is the integration of the nanosensor to the standalone winch/hoist system. The universal recorder/receiver installed on winch needs to be ingrated to the nanosensor as an alternate to hand-held data reciever attached to the sensor.

## **6.2.4 Drone adaptation**

The winch/hoist is developed as a standalone system that may be attached to any drone capable to lift all up weight of 10 kg. The winch/hoist is attached to the drone via gimble to provide stabilisation for test applications during flight operations. The drone proposed is the Dji Matrice 600 PRO. This drone has a bearing capacity of minimum 5 kg, which will be able to lift the proposed winch/hoist system including probe that will weigh a maximum of 3 kg.

## **6.2.5 Drone adaptation protocols**

Our development of the winch/hoist system is generic in its adaptation to a drone. Our outcome is informed by the need not to be prescriptive and allow prospective users the choice of drone with the following recommended capabilities:

1. Minimum all up lift weight capacity of 10kg
2. Installed anti collision system
3. Installed flotation gear
4. Installed automated flight system
5. Visual line of sight (VLOS) and beyond visual line of sight (BVLOS) flight ops

We will partner with a UAV operator with recommended capabilities that meet all the South African Civil Aviation Authority (SACAA) statutory and regulatory compliances for Remote Pilot Air Service winch/hoist flight operations.

## **6.2.6 Mobile laboratory installed winch/hoist and drone support system**

Notwithstanding the fact that our stand-alone winch/hoist system is designed for adaptation to any drone with recommended capabilities, the drone and winch/hoist operational support systems must be installed within a mobile laboratory that may be integrated and/or uploaded for drone specific operations. The embedded droneport-type system developed by Drobotics shall be installed in the mobile laboratory to support both drone and winch operations as well as digitized test applications. This system will integrate the technologies and sub systems as indicated in Chapter 7.

## CHAPTER 7: FINAL ASSESSMENT OF WINCH/JIG/COMS SYSTEMS IN OPERATIONAL ENVIROMENT

---

### 7.1 INTRODUCTION

Drobotics Systems scope of responsibility related to the current project is the design, development and build of a winch/jig/coms system configured for the launch of digital probes and water sampling within water monitor and oversight processes and operations. An assessment of technologies was carried out against Drobotics design protocols and operational hypotheses, and the following results were achieved: (√ = **Achieved**) (**X = in development**)

- I. Design and development of winch/hoist system √ (**LS Telkom built prototype**)
- II. Design and development of multiple probe JIG √ (**UJ 3D printed prototype**)
- III. Mobile lab installed communication suite √ (**DRB laptop simulation**)
- IV. Probe, winch, laboratory, cloud coms integration √ **Com's hardware/software enabled, X - to Cloud Integration outstanding (LS Telkom/ SUN Development)**
- V. Opticgammetry, lab, cloud coms integration √ (**LST/DRB**)
- VI. Cloud data aggregated dashboard integration (**Phase 2**) (**INFOSYS/DRB**)

Drobotics was reasonably satisfied that based on demonstrations simulating various operational activity, that the winch/jig system with some modifications will meet the threshold for success in demonstrating and validating the system and technologies for *in situ* water quality test applications in an operational environment. The one area that was not achieved was real-time communications from an offshore *in situ* locality to the onshore mobile laboratory. This was attributed to the SUN-developed biosensor that had to remain submerged in water for between 3 and 5 minutes for effective processing of data. Unfortunately, the Drobotics winch and jig design protocols did not stipulate this critical criterion. Thus, the Drobotics Winch and Jig system was designed to carry off the shelf digital probes that send data in real time when in contact with water.

### 7.2 SCOPE

The objective was to provide full validation of technologies and systems for water quality test applications. This would require the following demonstrations in an operational environment:

- I. Launch of probes of drone/static platform for *in situ* water quality testing (WQT) applications at a georeferenced locality.
- II. Launch of water sampling of drone/static platform at georeferenced locality.
- III. Real-time communications from *in situ* offshore location to mobile laboratory to cloud.

### 7.3 METHODOLOGY

The final assessment terms of reference and criterion must represent water quality test applications in an operational environment. The defined operational environment and localities are:

- Lake/Dam (X-Factor Trout Farm, Edenvale).
- River [Klipriver, (Eikenhof)].
- Well/Boreholes [Khoisan Village (Eikenhof)].

Drone adaptation and configuration to sensor apparatus for on-site, real-time digitalised water quality test application.

---

The defined methodology is as follows:

- Matrice 300 drone sampling operations carried out at X-Factor Farm.
- Matrice 600 Pro Drone digital probes *in situ* operations carried out at X-Factor Farm
- Matrice 300 Drone sampling operations carried out at Klipriver.
- Matrice 600 Pro Drone digital probes *in situ* operations carried out at Klipriver.
- Rail track platform water sampling operations for well located at Khoisan Village.
- Rail track platform digital probes *in situ* operations for well located at Khoisan Village.
- Real-time communications from digital probes to onshore mobile laboratory.
- Video of operations live streamed.

### 7.3.1 Drone platform

Very early on in the project we opted to accept the Matrice 600 Pro drone after successful demonstration of critical criteria and design protocols. The drone was tested for 5 kg weight lift, hover, real time kinematics (RTK) and 20 min battery life capacity at Victoria Yards in Lorenzville, Johannesburg. The LS Multicopter was a responsible entity for all drone operations and met skill criteria and SACAA Compliances (Figure 43B).

Contingent considerations and protocols in drone operations are:

- 1) Drone must be able to operate in weight category.
- 2) Configured for expanded scope (Photogrammetry and other GIS related Operations).
- 3) Installed safety redundancy features.
- 4) SACAA and other related statutory and regulatory compliances.
- 5) Skilled pilot licensed in VLOS and BLOS operations.
- 6) Auto pilot.

A)



B)



**Figure 43:** A) Matrice 600 Pro Drone; B) 5 kg weighted hover test using RTK at 5 m .

Drone adaptation and configuration to sensor apparatus for on-site, real-time digitalised water quality test application.

---

### 7.3.1.1 DRONE FINAL DEMO



**Figure 44:** LS Multicopter Matrice 600 Pro Drone fully winch/jig loaded on take-off and water sampling operations.

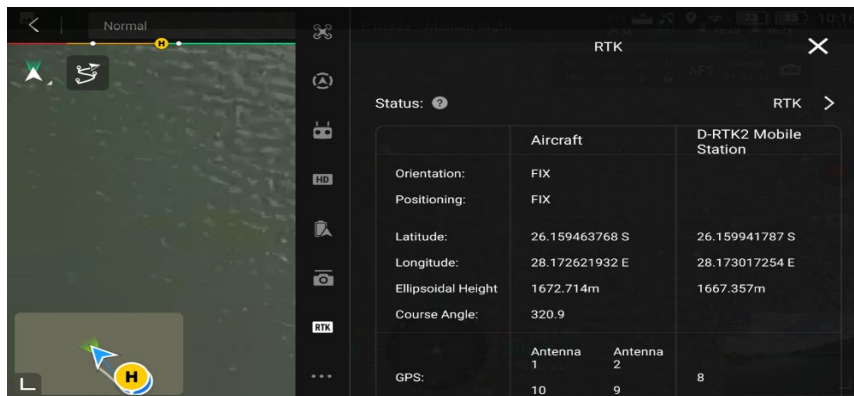


**Figure 45:** Control panel screen shot of Geo-located sampling and *in situ* test operations at X-Factor Trout Farm/dam.

On 31 January 2024, the LS Multicopter Operated Matrice 600 Pro drone was put through its paces in the launch of water sampling and digital probes at two sites that simulated lake/dam and river open water operations (Figure 44 and 45). The final demonstration provides insight and observations in the operational capacity of drone.

#### Observations and insights to the following:

**Water sampling operations:** Two water sampling operations were carried out at each location (X-Factor Trout Farm, Edenvale and Klipriver at the Khoisan village in Eikenhof). All four flight operations at both destinations were successfully conducted. The operations required that the drone transport UJ water sampling bag attached to the drone to geo-referenced location within the water source, fill the water sampler and return. In each locality a 500 ml and 300ml water sampler was transported, filled and returned successfully ([PICS AND VIDEOS\31st Jan Field sampling and showcase\Drone adaptation and configure Teaser 1.mp4](#)).

***In situ* digitalised test operations:** *In situ* test operations were carried out at X-Factor Trout Farm and Klipriver. The scope required that a LS Multicopter Matrice 600 Pro Drone transport pH and oxidation/reduction potential (ORP) probes to geo-referenced nodal point for determination of relevant test values in real time. The operation at X-Factor dam was successful. The pilot skilfully manoeuvred his drone overcoming interference from downwash to successful insert probes for sufficient period to illicit data in real time. The operation at Klipriver had to be postponed without achieving objectives due to technical issues related to the jig. ([PICS AND VIDEOS\31st Jan Field sampling and showcase\Drone adaptation and configure Teaser 2.mp4](#)).

Drone adaptation and configuration to sensor apparatus for on-site, real-time digitalised water quality test application.

Notwithstanding the challenges experienced, Drobotics proposes that the demonstration of the Multicopter Matrice 600 Pro drone as a platform for launch of probes into open waters was a success. Drobotics will adopt the following protocols for all future drone operations:

1. Pilot skill is critical (pilot must be company-accredited for proposed operations).
2. There must be total harmony and understanding between pilot and winch/hoist operator.
3. Redesign of JIG for launch into hostile water conditions.
4. Ensure loading of JIG does not create a lopsided effect in flight and deployment.
5. All components located on Jig must be totally waterproofed.

### 7.3.2 Winch/hoist system

Drones have been identified as a viable platform from which water sampling and water quality test sensors for *in situ* applications may be launched. This prompted the need to design and develop lift and deploy equipment adaptable to drone platform. It was also resolved that lift/deploy equipment be hybrid in that it may be installed to a land-based frame for onshore scope of activity (boreholes, wells, urban water tank storage). Drobotics presented the following design and protocols for winch/hoist system to meet lift and deploy scope and expectations (Figure 46).

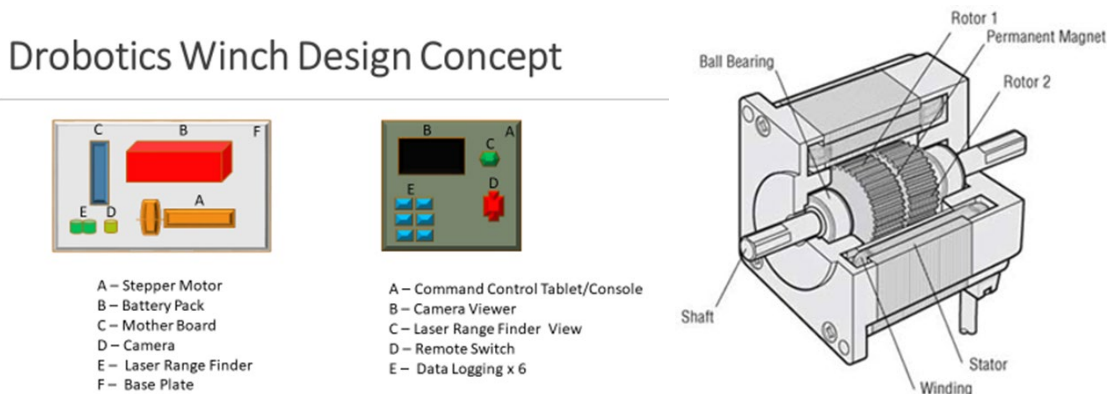


**Figure 46:** Drobotics winch design concept; and illustration of the motor structural diagram: cross section parallel to shaft (Structure of stepper motors, 2022).

#### Design Protocols

- I. Total weight of winch including lift capacity of minimum 3 kg must not exceed 7 Kg.
- II. Winch deploy and lift at minimum 5 m.
- III. Winch installed autonomous battery.
- IV. Winch installed computer.
- V. Winch installed capacity to receive and transmit binary data.
- VI. Winch installed remote control.

#### 7.3.2.1 Winch/hoist prototype build

The most important consideration in the building of the prototype was the design and manufacture of the drone adaptable winch/hoist component housing unit which attaches the lift deploy capacity to the drone. The LS Multicopter design is shown in Figure 47 and the 3D printed housing unit is shown in Figure 48.

Drone adaptation and configuration to sensor apparatus for on-site, real-time digitalised water quality test application.

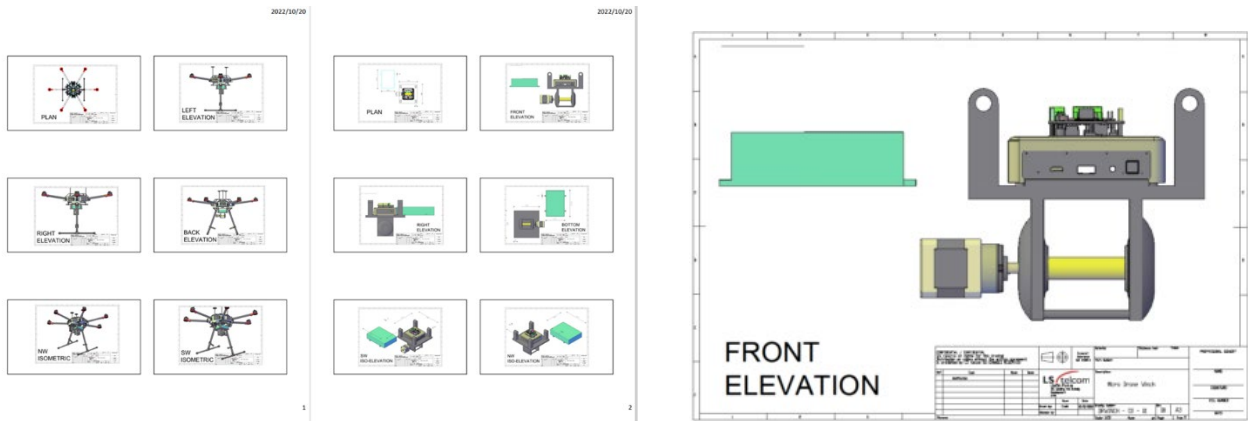


**Figure 47:** CAD Drawings for the development of the winch/hoist system



**Figure 48:** Winch 3D Printed Housing

The building of the housing prototype led to the development of a mock-up winch unit for the initial design protocols scope efficacy test. Initial tests proved that the system would, in principle, work.

As indicated in Figures 49 to 53, the LS Multicopter successfully designed, built, assembled and integrated a winch system comprising the following:

- Drone adapted housing.
- Winch/hoist drum system.
- On board computer.
- Winch/hoist remote control.
- Battery system.
- Telemetry links.

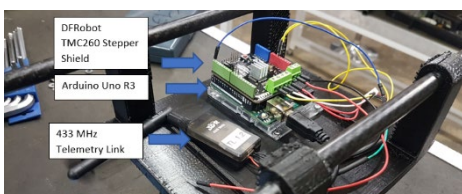


**Figure 49:** On-board winch computing



**Figure 50:** Winch battery unit

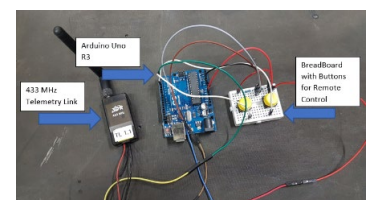


**Figure 51:** Telemetry board

Drone adaptation and configuration to sensor apparatus for on-site, real-time digitalised water quality test application.

---



**Figure 52:** Installed Winch lift components.

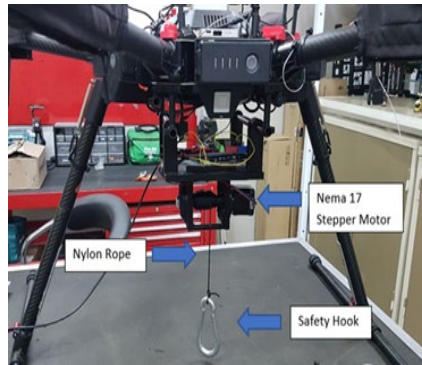


**Figure 53:** Prototype 2 (aluminium).

The LS Multicopter has met almost all the original design protocols that were submitted. The battery life stipulated is not currently possible as battery technologies provide for an average of a 15-minute flight time, and this is impacted by various factors such as load, ambient temperature, etc.

LS Multicopter successfully designed, built, assembled an integrated winch system comprising the following:

- Drone adapted Housing
- Winch/Hoist drum system
- On board Computer
- Winch/Hoist Remote control
- Battery system
- Telemetry Links

### 7.3.2.2 Winch/Hoist Final Demo



**Figure 54:** LS Multicopter multiple platform adapted winch/hoist system and remote-control unit.

The winch/hoist system was installed on a Multicopter Matrice 600 Pro to transport a jig loaded with 2x digital probes for insertion at geo-referenced location for a water quality test application. The winch was required to take off with the jig attached to the winch suspended between 50 cm and 1 m. At the location, the jig was lowered up to 5 m via remote control into water and communications were relayed in real time from the jig-installed probe to the on-board winch-installed computer transmitting data received in real time to the mobile laboratory located on land. Notwithstanding the hiccup at Klipriver, we can conclusively assert the following:

1. That the winch/hoist lifted and transported a loaded jig to the geo-referenced nodal point.
2. That the winch/hoist lowered the loaded jig into the water at the nodal point.

Drone adaptation and configuration to sensor apparatus for on-site, real-time digitalised water quality test application.

3. That data were received by the on-board computer and transmitted to onshore mobile lab in real time.
4. That the winch/hoist lifted the loaded jig and returned to shore.

The above constitutes a successful demonstration of winch/hoist in an operational environment.

### 7.3.3 Jig development

The need for a flotation-type contraption was identified to protect against total immersion and stability of sensor apparatus when the winch launched from the drone platform. Robotics presented the following design concept Figure 55 and Figure 56 as salient solutions to the building of a probe-holding jig.

#### Design Concept

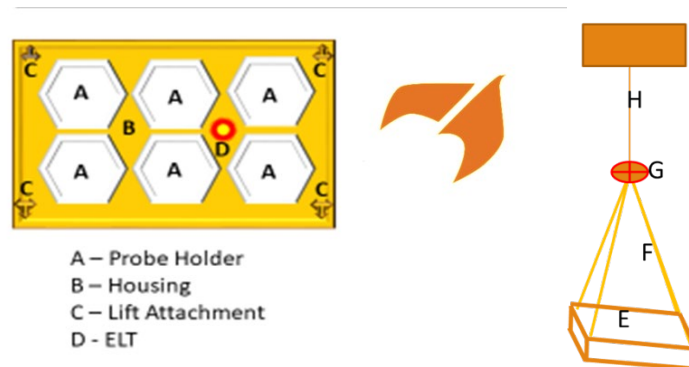


**Figure 55:** Schematic of jig and UJ 3D printed jig prototype.



**Figure 56:** Prototype of multiprobe-holding jig.

Proposed 1 Manufacture:

- Improved and tested buoyancy.
- Configured for specific probe fit.
- Configured for water sampling.

Robotics initial attempt at designing a jig produced from the UJ 3D printed prototype made from high-density foam fell short in meeting its flotation/buoyancy design protocol. Adjustments are also needed for the various size probes. After various tests in an operational environment, it was resolved that a new jig that's wider and consists of different material (Styrofoam) be developed that will be configured for digital probe-specific

Drone adaptation and configuration to sensor apparatus for on-site, real-time digitalised water quality test application.

dimensions and with improved buoyancy. It was further resolved that the jig be configured to accommodate Stellenbosch University biosensors, mindful of the fact that consideration be given for the installation of a dry compartment on the jig for a biosensor microprocessor, battery, and coms. Drobotics designed and developed two biosensor housing units, one for applications in a dry environment and the other for total immersion in water (Figure 57D). To accommodate SUN biosensor supporting hardware, Drobotics designed and built crude Jig opting for wider square shaped Jig that would hold four regular probes/sensors and 110x 160 mm in the dry compartment centre. Together with UJ's biosensor housing unit, these biosensor housing units require to be tested once SUN has optimised its testing protocols in open water sources.

The wide body jig has been configured for specific pH and ORP probes launched for real-time demonstration as well as two dummy probes at the four corners with biosensor hardware compartment taking up centre space as indicated by blue area on concept design (Figure 57B). Final assembly shall be concluded on receiving biosensor connected hardware from SUN.

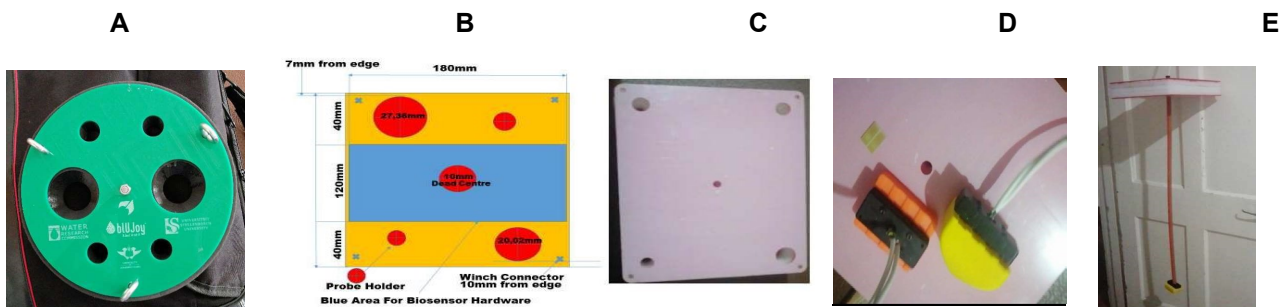


**Figure 57:** (A) UJ's Multi Probe-holding jig (B) New design protocols (C) Probe specific jig (D) SUN biosensor housing (E) SUN biosensor attachment to jig.

### 7.3.3.1 JIG Final Demo

The expected scope for the jig is to house digital probes securely in its deployment for *in situ* water quality testing operations. The jig holding pH and ORP probes was launched at the X-Factor Trout dam and Klipriver. It achieved its objective at the dam but fell short of expectations by tipping over when deployed into a strong river current. As previously alluded to in the section related to drone operations, going forward, Drobotics proposes to redesign the Jig to a more circular tubular configuration that should significantly reduce friction and resistance when entering strong water current. Another consideration will be to equitably balance the weight of the jig so as to avoid lopsided lift in flight which inevitably impacts when deployed. The following has been achieved in validating this technology:

1. Transport of drone-adapted jig for *in situ* pH and ORP test application.
2. Buoyancy test.
3. Apple Tag located on jig simulated ELT to track and locate the position of the jig.

Drone adaptation and configuration to sensor apparatus for on-site, real-time digitalised water quality test application.

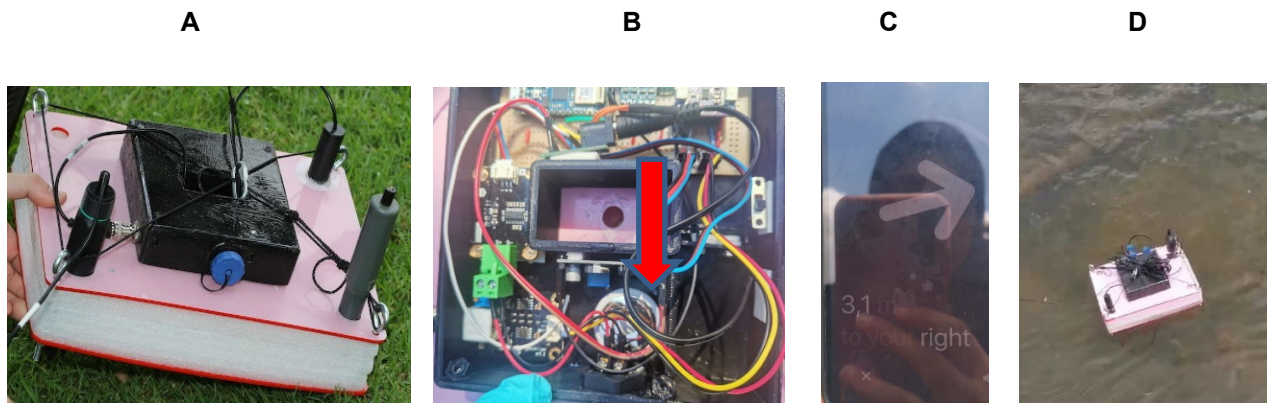


**Figure 58: (A) Drobotics multi probe Jig with onboard aggregate sensor microprocessor (B) Air tag locator (C) Air tag track on iPhone (D) Buoyancy Test.**

### 7.3.4 Communications

Real time and/or near real time communications is a contingent project deliverable. To achieve this constitutes a paradigm shift within water resource monitor and oversight activity. Drobotics presented the following protocols (Figure 59) in the design and development of communication architecture and system:



**Figure 59: Drobotics communication protocols and architecture.**

On 28 March 2023, Drobotics carried out some provisional tests on communications and reported to reference group meeting at the end of July 2023 recorded herein in Figure 60.

Drone adaptation and configuration to sensor apparatus for on-site, real-time digitalised water quality test application.

## Real and/or Near Real Time Scope Data Coms Assessment.

**Drobotics presented the following protocols in design of Scope Data Coms**

1. Real and/or Near Real Time Receive/Transmit results/data (**Achievable**)
2. Coms between drone and mobile laboratory up to 10km range (**Achievable**)
3. WIFI Coms between mobile laboratory and Cloud (**Achievable**)
4. Binary data aggregation between Cloud and Stakeholder (**Phase 2**)
5. Storage of Binary Data (**Achievable**)
6. Test points and Flight Grid Recorded and Stored (**Achievable**)

**Coms Infrastructure Established**

1. On-board Computer
2. Base Station Computer Simulation
3. Winch Remote Control

**Coms Link tested**

1. On-board Computer (receive/transmit)
2. Base Station Laptop (receive/transmit)
3. Winch Remote Control (Winch Ops)
4. Probe to Cell Phone App

**Coms Link in development**

1. Probe to On-board Computer to Base



18

**Figure 60:** Communications assessment, LS Multicopter winch remote, on-board computer.

Communications remain a critical contingent deliverable. In March 2023, we achieved SUN biosensor communications integration to the winch installed on-board computer. However, this could not be demonstrated in its *in situ* operational environment. The communications integration was achieved through onshore simulation whereby SUN sent dummy data from its biosensor that was received by the winch-installed on-board computer. It was already apparent that SUN may not be ready for direct *in situ* operations for its biosensor, prompting a decision to secure alternate off-the-shelf technologies to demonstrate real-time communications.

LS Multicopter conducted some provisional research and advised on specific pH and ORP chemical sensors that may be integrated to provide real-time communications as stipulated. Some insight into its design and technical considerations are indicated in Figure 61.

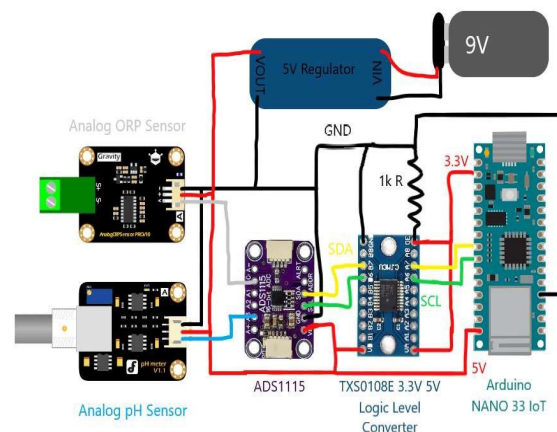


**Figure 61:** LS Multicopter ORP and pH coms integration design architecture.

LS Multicopter provided the following on its processes thus far:

- Base station and drone software. This has not changed since March 2023.
- Arduino Wi-Fi NINA access point configuration coding.
- Arduino to drone communication protocol.
- Arduino ORP probe integration.
- Arduino pH probe integration.

Drone adaptation and configuration to sensor apparatus for on-site, real-time digitalised water quality test application.

- Formal winch circuit diagram.
- 3D design and print of winch remote control.
- 3D design of Arduino probe enclosure.

The outstanding issues bulleted below are minor and are more related to update and fine tuning. We are confident that it will all be completed and in no way impede our successful demonstration of real-time communications.

- Update the formal winch remote control circuit diagram to include the newly procured logic level converter. This will replace the voltage splitter seen in the current formal circuit diagram.
- Migrate winch remote control components to a new enclosure.
- Update the formal probe wiring diagram to include a voltage.
- Print probe enclosure.

#### 7.3.4.1 Final Communications Demo

The demonstration of real-time communications had to be emphatic and so it was opted to substitute real-time transmission from an offshore *in situ* location to the onshore laboratory to Cloud. With offshore *in situ* location to onshore laboratory to three external locations (Johannesburg, Venda, and New Zealand) (Figure 62) via live stream YouTube link (Drone video footage <https://youtube.com/@kylevanheyde4423?si=qrehq40AJf6wnm0T> and data at <https://youtube.com/live/MJ3NeGv31CM?feature=share>).

We provide the following assessment:

1. Real time communications were achieved from pH and ORP sensors from *in situ* offshore location to onshore mobile laboratory live streamed via YouTube link to external destinations in real time (Figure 64).  
The chemical analysis data from the digital pH (Analog ORP sensor pro – for Arduino) versus handheld probe (Hannah pocket meter), respectively, indicated the following values (Table 12):

Sample	Conventional testing		Jig/Drone	
	pH	ORP (mV)	pH	ORP (mV)
Khoisan river	6.86	-312	7.29	-314
Khoisan well	7	-307	7.43	-309
Edenvale Dam Drone	-	-	6.25	-305
Edenvale shore	8.43	-306	-	-

**Table 10: Digital chemical testing via Drone platform versus conventional testing.**

2. Near real time (within 5 minutes) was achieved with SUN biosensor from onshore test location to mobile lab via winch installed on board computer.
3. The winch installed on-board computer met performance expectations in operational environment.
4. The winch remote control met performance expectations in operational environment (Figure 63B).
5. 10 km range was not tested; however, we are confident with correct communication apparatus this is achievable.

Drone adaptation and configuration to sensor apparatus for on-site, real-time digitalised water quality test application.

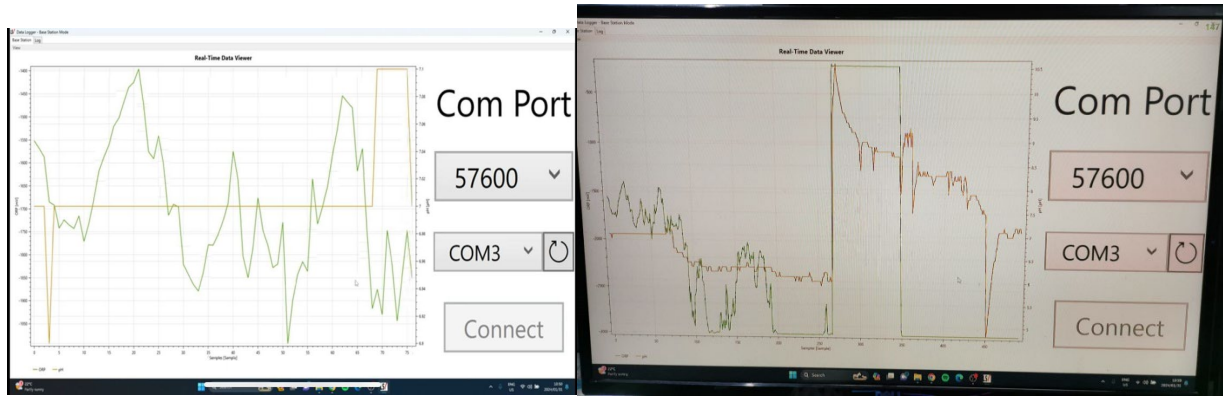


Figure 62: Pictures of live stream data captured via YouTube link in Johannesburg, Venda and New Zealand.

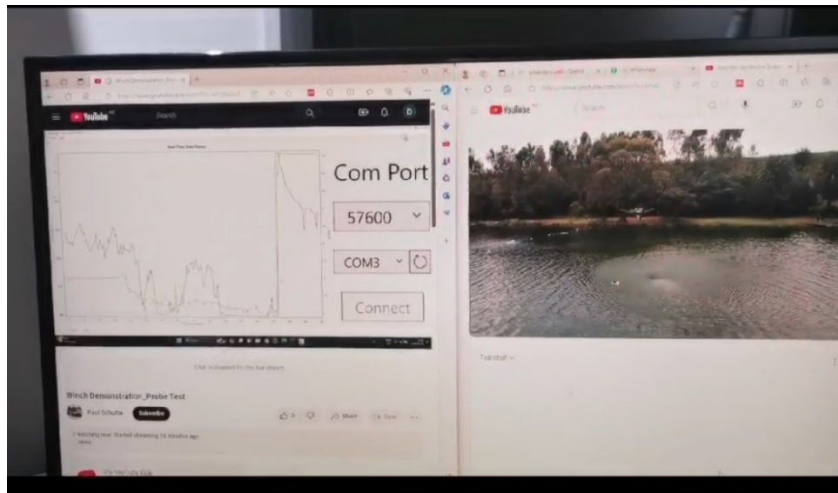


Figure 63: Picture of live stream data from chemical sensors and video footage from the drones.

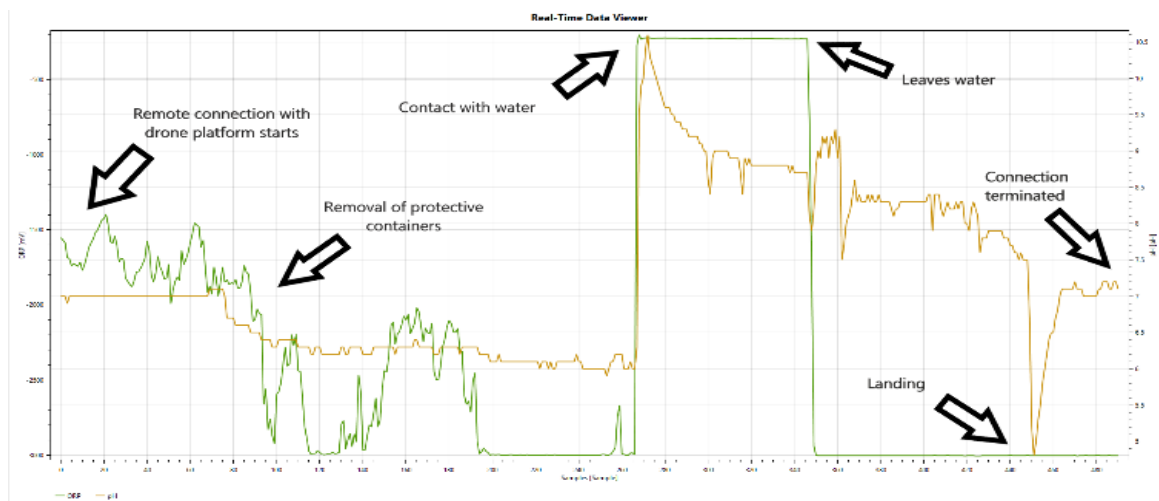
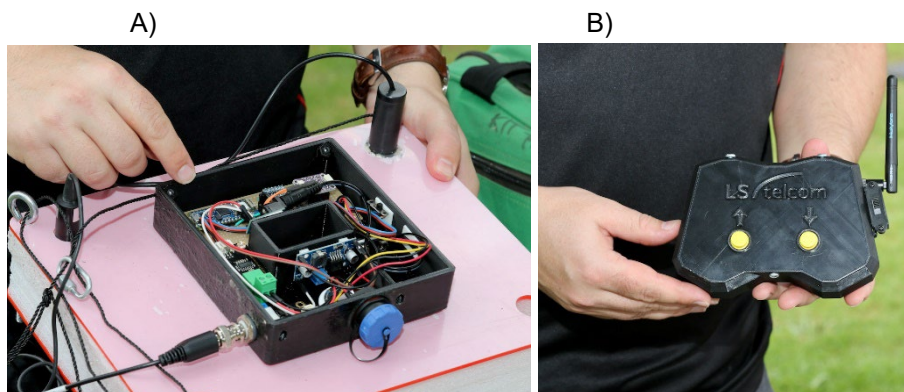


Figure 64: Real time communications received from ORP and pH sensors simultaneously on contact with water.

Drone adaptation and configuration to sensor apparatus for on-site, real-time digitalised water quality test application.

---

The technology was successfully demonstrated in X-Factor Dam and at the Klipriver, with some adjustments to be made to the jig, i.e. to avoid tip over of jig and getting the pH and ORP components wet, which is in the box on top of the jig (Figure 65A); to seal the box and be water resistant.



**Figure 65:** ORP, pH integrated coms hardware and improved winch remote control.

### 7.3.5 EXPANDED PLATFORM

The winch/hoist design protocols stipulated adaptation to multiple platforms for expanded scope of activity configured to launch the probes from urban-located bridges, urban water reservoirs and plants, boreholes, as well as marine and other static stations. Robotics designed and built a mock-up prototype of a platform that may be installed and adapted to multiple static localities and infrastructure (Figure 66). The modular design provides for simulation of applications on all other water sources where use of the drone may not be practical. The expanded platform has been adapted to accommodate the LS Multicopter drone-adapted winch prototype. The platform shall provide aerial access restricted to its static operational area.



**Figure 66:** A) Printed winch housing attached to alternate platform (left). B) Winch system attached to modular rail cart platform (middle). C) Modular rail cart platform for static water sources and infrastructure.

The objective of the alternate platform was to demonstrate winch/hoist adaptability for expanded scope of operations and the images above serve as evidence of winch adapted to static platform poised to carry out well operations. Unfortunately, a full demo was not carried out due to Jig capsizing in River ops resulting in minor flooding of on-board jig installed communications unit. We are satisfied in that the winch and jig have been successfully field tested. The critical demonstration was the winch-adapted alternate platform as opposed to working of the winch.

Drone adaptation and configuration to sensor apparatus for on-site, real-time digitalised water quality test application.

---

### 7.3.6 FINAL VALIDATION SYNOPSIS

#### Lake/Dam Operational Environment

1. Successful launch of ORP and pH sensor in geo-referenced locality X-Factor Trout Dam in Edenvale, GP, RSA transmitting results in real time to laptop located at mobile laboratory, video/data livestreamed to UJ Campus Johannesburg, located in Venda, South Africa and located in New Zealand.
2. Water sampling using sampling bags of drone platform at precise geo-referenced point as ORP and pH *in situ* test localities.

#### River Operational Environment

1. Launch of ORP and pH sensor in geo-referenced locality in Klip River transmitting results in real time to laptop located at mobile laboratory. (Operation stalled due to tip over of jig in strong current).
2. Water sampling using sampling bags of drone platform at precise geo-referenced point as ORP and pH *in situ* test localities.

#### Well water source operational environment and simulation of urban reservoir/water treatment facilities operational environment

1. Launch of ORP and pH sensor static platform into well located in Khoisan Village
2. Water sampling using bags at the well for conventional microbiology testing.

It must be noted that our objective involves technology demonstrations where we want to show the following:

1. Onsite conventional test at remote locations **(Achieved)**
2. Real and/or near real time communications to mobile laboratory forward to external parties and locations **(Achieved)**
3. Launch of digital probes of multiple platforms for *in situ* test applications **(Achieved)**
4. Water sampling of drone platform **(Achieved)**
5. Application live-stream to mobile view deck and external stakeholder **(Achieved)**

## CHAPTER 8: UNIVERSITY OF JOHANNESBURG SAMPLING BAG AND BIOSENSOR SAMPLING CARTRIDGE UNIT DEVELOPMENT

---

### 8.1 BACKGROUND

After the reference group meeting held in 2022, the University of Johannesburg undertook to produce a water sampling/collection bag to be hoisted by the drone and the digital bacterial probe disinfectant unit to disinfect the digital probe in flight. The university is considering submitting patents for these two products and so is unable to provide detailed information and graphics of the products. Designs for the sampling bag and the biosensor sampling cartridge unit are complete and currently we are busy with tests and analysis and modifications. A successful demonstration was held on the 28<sup>th</sup> of March 2023, at UJ Vaal Dam Island, whereby UJ, Drobotics and SUN demonstrated and realised limitations and issues relating to communication between the digital bacterial probe, the winch and the mobile laboratory (Figure 67). The sampling bag depth capabilities was also tested.



Figure 67: Demonstration at UJ Vaal Dam Island, Vereeniging

## 8.2 BIOSENSOR SAMPLING CARTRIDGE UNIT

### 8.2.1 Design Considerations / Goals

The design of the Biosensor sampling cartridge (BSSC) aimed to produce a user-friendly economic product that met the criteria listed below, including the bacteriophage assay requirements of the Stellenbosch University Digital Phage Probes (SUN Probes). The considerations included:

- Eliminate the chances of contamination (Achieved)
- Have the device be easy to operate and transport (Achieved)
- Reuse or recycling of at least 80% of the components (Achieved)
- Allow multiple modular units (Achieved)
- Incorporate failsafe power and communications (Achieved)
- Satisfy the technical operating requirements for the SUN Probes (Achieved)
- Operate within all the design limitations (Achieved)

### 8.2.2 Design Methodology

The design was modelled in McNeel Rhinoceros 8 resulting in the design shown in Figures 68 and 69. Specific design limitations were considered during the design process of the biosensor sampling cartridge (BSSC) and included the maximum winch payload (2 kg), drone flight time (20 min), probe sample reading time (3-5 min) and the available area underneath the drone when landed.

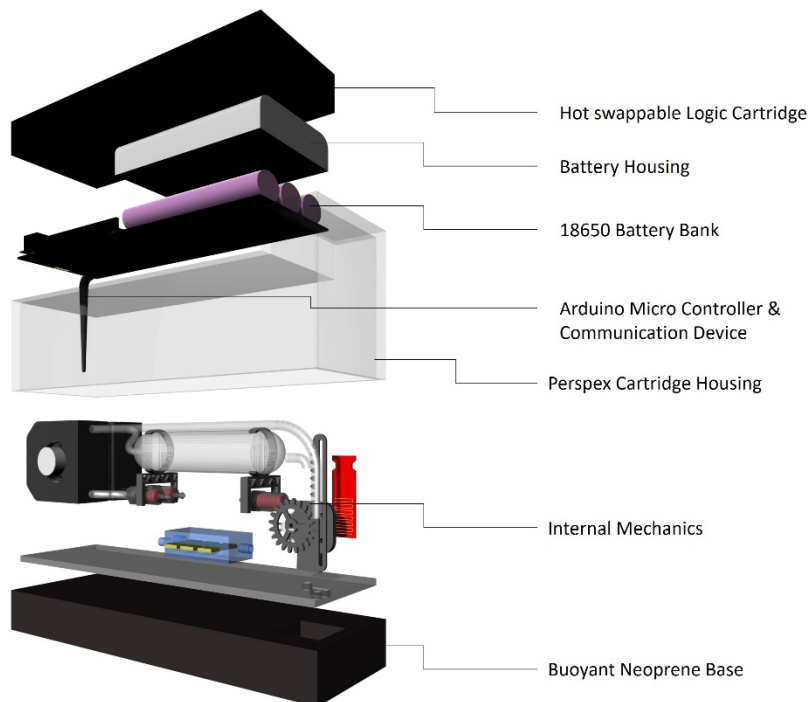


**Figure 68:** Exploded axonometric of all the sample and logic cartridge components creating the biosensor sampling cartridge

An assembled cartridge is composed of two main parts: the logic cartridge and the sample cartridge. The logic cartridge is a reusable component and so users can pair a smaller number of logic cartridges with a recurring order of higher quantities of sampling cartridges. The sampling cartridge is a single-use consumable component with the option for the components can be recycled after use.

Drone adaptation and configuration to sensor apparatus for on-site, real-time digitalised water quality test application.

---

The sample cartridges designs considered potential contamination issues, hence the choice of a single test to avoid contamination. This supply model allows customers to return their used sample cartridges for recycling. The replacement cartridges are supplied at a discounted rate.

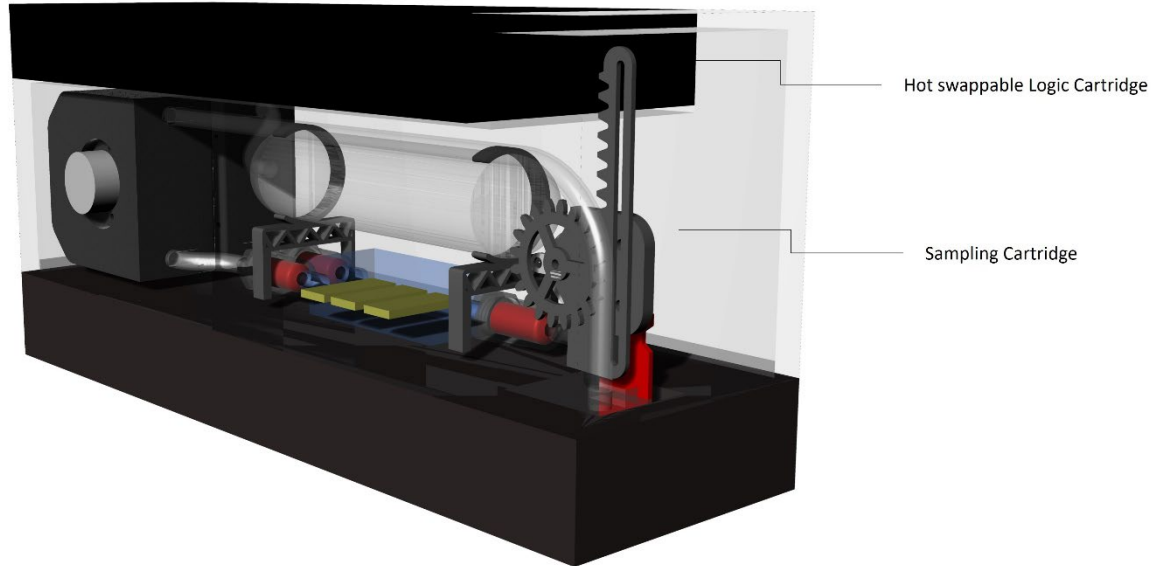


**Figure 69:** Rendering of the assembled Biosensor Sampling Cartridge

The design allows for each cartridge to operate autonomously and as a single device. They can be grouped in cluster arrays, allowing for multiple sampling capabilities. The benefit of this is that they still operate independently, providing an inherent fail-safe system. Each cartridge is individually isolated, however, when clipped together in a multiple-array format they are synced via the operating software and can be monitored and controlled as a group or individually within the cluster.

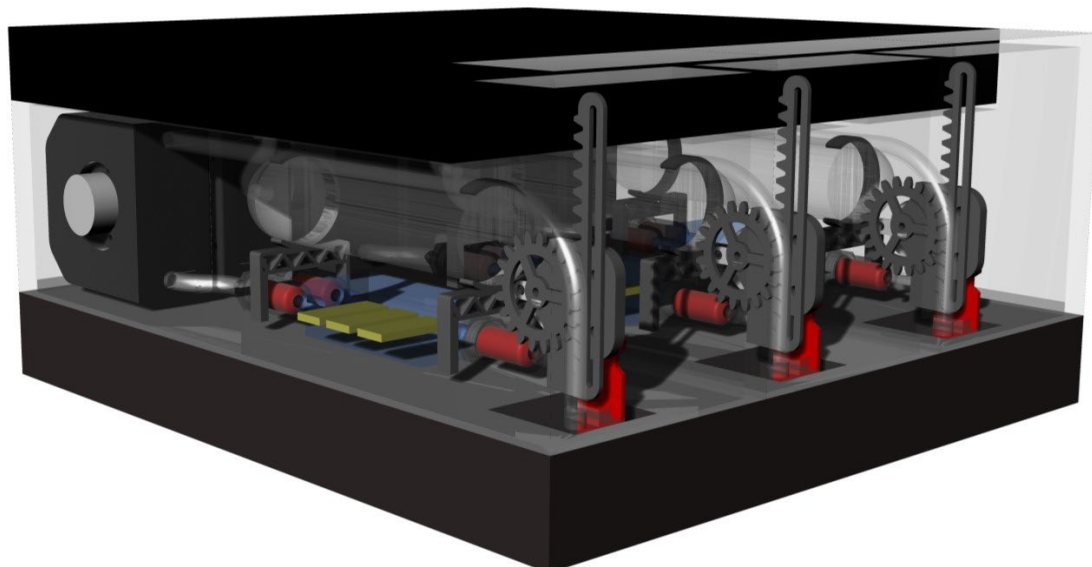


**Figure 70:** Rendering of the proposed assembly of multiple Biosensor Sampling Cartridges

Each cartridge is still hot-swappable. This is due to the 16-pin quick contact connection that is responsible for connecting the internal mechanisms to the microcontroller and power source. This system allows for efficient changing of cartridges and easy charging cycles.

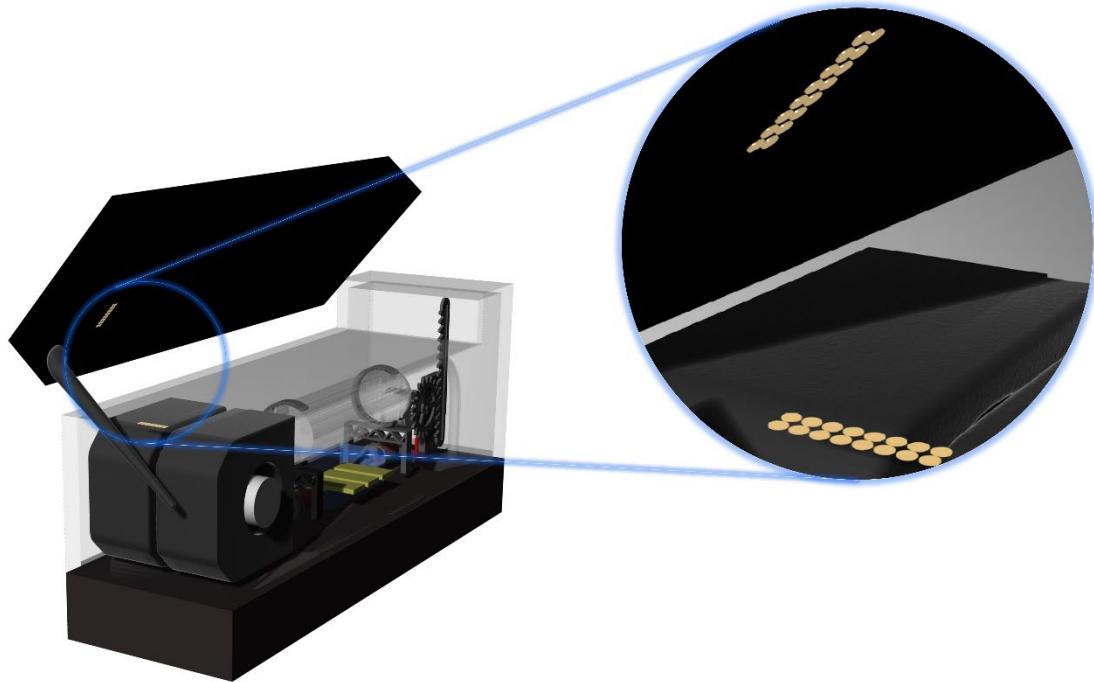


**Figure 71:** Rendering of the 16 Pin quick connect detail used for hot swapping of the assembly and logic cartridges in the Biosensor Sampling Cartridge

### 8.2.3 System Operations

The cartridge operates as follows:

1. A drone flight plan is prepared alongside a sampling plan. Once the sites are geo-located and programmed in, the drone can go out.
2. The autonomous operation sequence is initiated once the drone reaches a sampling destination.
3. The cartridge begins its sequence by discarding the PBS storage solution. It then performs a ten-second PBS rinse cycle, to wash the probes.
4. Once the cartridge contacts the water, the water level sensor triggers the rack & pinion sample tube lift, which lowers the collection tube into the water.
5. The peristaltic sampling pump then performs a ten-second rinse of the probes with the sample water. A five-second pressurization of the probe chamber then follows this. This pressurization puts the sample chamber in equilibrium, meaning the sample liquid will remain still in flight.
6. The sampling cartridge is then winched back up to the drone which then moves on to the remaining sampling sites.
7. After a holding time of three minutes, the sample is discarded, and a second PBS rinse cycle is initiated. A pressurization of PBS solution then follows this.

- Once the drone completes its sampling run it can return to the base where the sample cartridges can be swapped out for new ones.

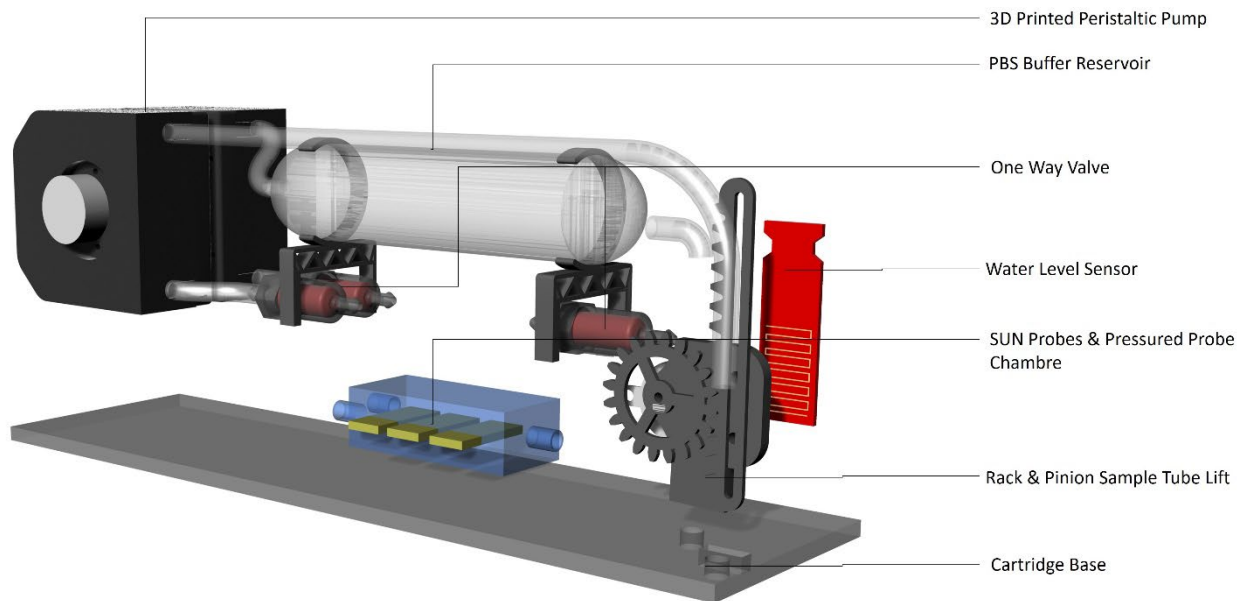


**Figure 72:** Rendering of the internal mechanism of the complete Biosensor Sampling Cartridge

### 8.3 TESTING FLOW OF DRONE SAMPLING WATER COLLECTION BAG

- Water sampling bags of 600 ml and 300 ml capacity have been developed.
- The water sampler bag can collect 200 ml and 500 ml of water and then be placed on the ground maintaining these water volumes without leaking.
- The water sample bag has a wiretap that can 100% seal the bag during transport.
- The water sampler bag was tested with a drone to see how it reacts to the downward wind the drone produces.
- The weight of the bag was tested as to its direct entry in the water without floating.
- Depth testing was conducted to determine the water depth the bag must reach to collect the water sample.

### 8.4 METHOD FOR SAMPLING

On 31 January 2024 the holistic concept was demonstrated, that is, digital chemical and biosensors versus conventional methods. Three methods were tested as indicated in Figure 73, whereby only one method, that is, the bacterial sensors to be attached to the drone and dipped into the water source, was not tested. The concept was demonstrated at two sites: 1) X-Factor Trout Farm/dam in Edenvale, 2) Khoisan community adjacent to the Klipriver where the community has an open well source.

Drone adaptation and configuration to sensor apparatus for on-site, real-time digitalised water quality test application.

**Four variations of method validation**

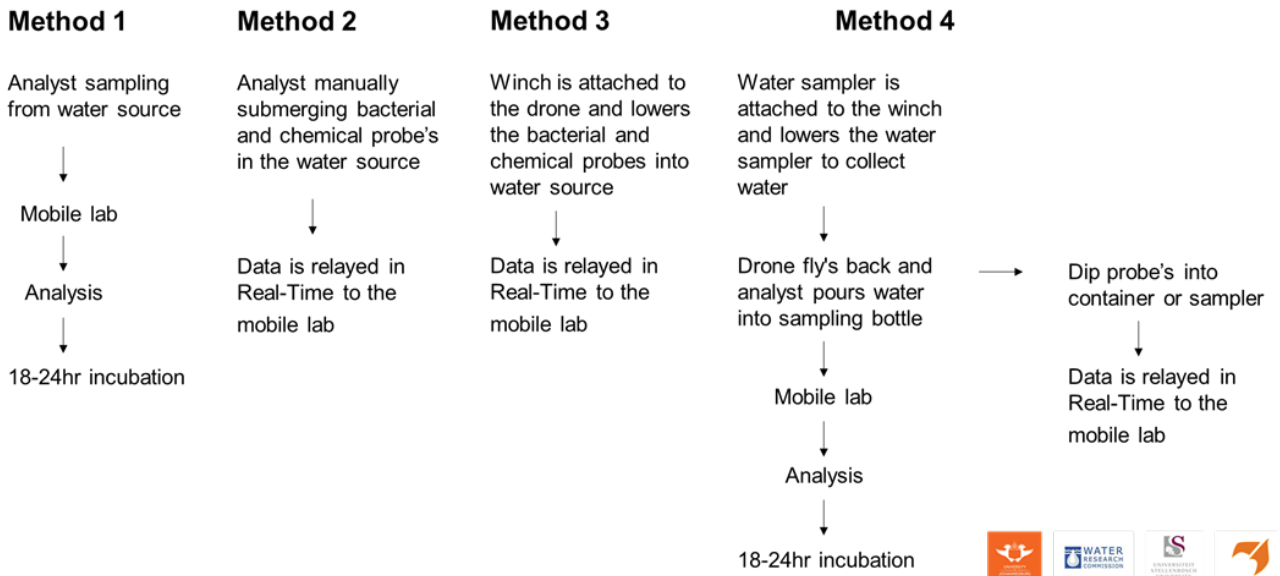


**Figure 73:** Process of sampling to validate the methods.

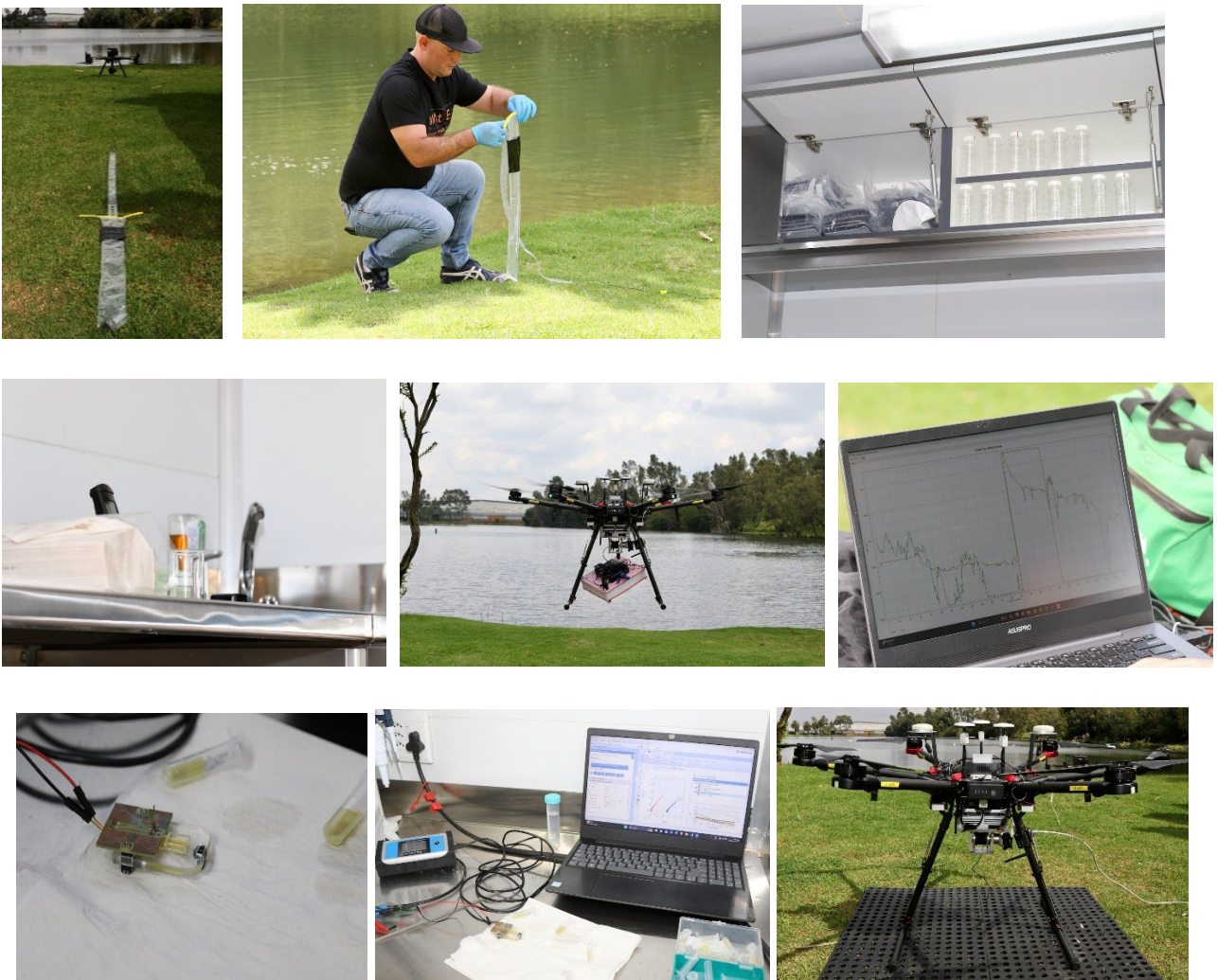


**Figure 74:** Demonstration of sampling methods at X-Factor Trout Farm and Khoisan Village.



**Figure 75:** Group picture of members from Water Research Commission, UJ Water and Health Research Centre, Stellenbosch University, Drobotics and LS Coms.

## CHAPTER 9: WRC DEMO MICROBIOLOGY RESULTS DISCUSSION

### 9.1 INTRODUCTION

The integration of the biosensor with the drone system was scheduled to be demonstrated on 31 January 2024 in Johannesburg. The plan was to test the biosensor in water during a drone flight, simulating real-time and on-site microbial water quality testing. Unfortunately, the biosensor demonstration was hindered by unforeseen challenges in the manufacturing process. The crucial printed circuit board (PCB), necessary for the device's functionality, was expected to be ready by 26 January 2024, in time for the scheduled demonstration. However, a delay in the production timeline meant that the PCB could only be supplied on 29 January, the day we were supposed to travel to Johannesburg for the project demonstration. This delay posed a logistical challenge as it left insufficient time for adequate testing and preparation, ultimately preventing the device from being showcased as planned.

The specific purpose of this PCB was to replace the existing PalmSens in the measurement setup, enabling automatic sampling and adapting the system for drone use. Despite this setback, the current setup remains crucial for acquiring more comprehensive data to fine-tune the biosensor's calibration on real samples and demonstrating the biosensor. During our visit in early 2023 to the Vaal Dam, we tested the communication protocols for the biosensor by transmitting dummy data via a Wi-Fi connection. The biosensor utilises the same protocol, and we simulated real-time measurements using previously collected data, which was transmitted from the drone to the base station on the day of the demonstration, January 31<sup>st</sup>, 2024. Additionally, the functionality of the biosensor was tested separately with samples collected by the drone using the University of Johannesburg's water sample collection system.

The goal of the demonstration was to compare the performance of the biosensor with conventional methods, which was successfully achieved by comparing with the Colilert® Quanti-Tray/2000® and HPC for Quanti-Tray (IDEXX, Westbrook, ME, USA). The biosensor was allowed to incubate with the sample for 5 minutes, followed by measurements, whereas conventional methods required overnight incubation, with results reported the next day. For accurate results, the biosensor required three 100 µl volumes per sample, whereas conventional methods required 100 ml per sample for testing. Additionally, conventional methods necessitated a laboratory setup for testing, while the biosensor only required a simple workbench. There was also potential for direct testing of the water source with a biosensor, although this feature was not ready for demonstration.

### 9.2 DIGITAL PROBE METHODOLOGY AND RESULTS DISCUSSION

The water samples were collected using the water collection samplers from UJ, and 300 µl from each site was collected for testing with the biosensor. The biosensor's IDEs were pre-treated with bacteriophages specific to *E. coli*, specifically the *E. coli* BL21 (DE3) strain, before travelling to Johannesburg. The C&G + bacteriophages IDEs were prepared, as their immobilisation process was easy to perform for many IDEs at once while obtaining relatively consistent results. To verify the effectiveness of the treated IDEs, an *E. coli* BL21 (DE3) stock was inoculated the day before as a positive control for testing on the demonstration day. A water sample spiked with this *E. coli* BL21 (DE3) to an OD600 of 0.03 was tested alongside the collected samples.

The IDEs were incubated for 5 minutes each with 100 µl of each sample after baseline measurement of the IDEs were performed. Immediately after this incubation, measurements were taken, and the capacitance change was calculated. Biosensor measurements were conducted in triplicate, and the results are presented

Drone adaptation and configuration to sensor apparatus for on-site, real-time digitalised water quality test application.

in Table 13. In the table, the red boxes indicate outlier IDE measurements that did not align with others. These IDEs were considered incorrect and were subsequently discarded.

**Table 13: Digital probe results for each volume of sample tested for *E. coli***

Sample	Volume used (ml)	% Changes			Implications
		1 <sup>st</sup>	2 <sup>nd</sup>	3 <sup>rd</sup>	
Khoisan river	0.1	162.40 %	-3.76 %	-6.72 %	No changes
Khoisan well	0.1	27.86 %	-4.54 %	-12.88 %	No changes
Edenvale dam	0.1	21.26 %	8.92 %	17.38 %	Possibly contaminated
Edenvale shore	0.1	3.97 %	-13.29 %	0.06 %	No changes
Spiked (positive control)	0.1	64.25 %	10.99 %	126.07 %	Contaminated

The spiked sample, serving as the positive control for testing, exhibited a significant change in signal levels, indicating the expected contamination. Samples collected from the Khoisan river, well, and the Edenvale shore did not show signal changes, suggesting no contamination of these water sources. However, the sample from the Edenvale Dam displayed a signal change, hinting a potential source contamination.

It's worth noting the considerable variance in measurements at each sample site, likely due to the suboptimal immobilisation of bacteriophages on IDEs, which was non-uniform and unoriented. Despite this limitation, we proceeded with this relatively poor immobilisation as a proof of concept. Future efforts will concentrate on enhancing immobilisation for improved biosensor reliability and accuracy. Additionally, it's essential to consider how a 100 µl sample may accurately represent the water source compared to conventional methods that collect larger sample volumes, potentially offering a more accurate representation of the source.

### 9.3 CONVENTIONAL METHODS METHODOLOGY AND RESULTS DISCUSSION

The samples were analysed for bacteria quality using Colilert® Quanti-Tray/2000® and HPC for Quanti-Tray (IDEXX, Westbrook, ME, USA) within 24 hours. Aliquots of 100 ml of water sample were analysed for the detection of total coliforms and *E. coli* as per the manufacturer's instructions. The Quanti-Trays were incubated at 35°C (± 0.5) for 18 hours. Samples that were positive for coliforms turned yellow and samples that were positive for *E. coli* fluoresced under UV light (366nm). All analysis included quality controls which were *E. coli* ATCC: 25922 (positive control), *Klebsiella pneumonia* ATCC: 31488 (positive control for total coliforms), *Pseudomonas aeruginosa* ATCC: 27853 (negative control for coliforms) and deionised water for media sterility. Broth from the positive samples was collected for downstream processes.

In addition, 100 ml of the same samples was analysed to detect heterotrophic organisms using the HPC for Quanti-tray (IDDEX, Westbrook, ME, USA) as per manufacturer's instructions and incubated 36°C (± 2) for 44–72 hours. Samples positive for heterotrophs fluoresced under UV light. The quality control for HPC included the *Enterococcus faecalis* ATCC: 29212 (positive control) and deionised water for media sterility.

The data from the laboratory tests conducted on the samples are presented in Table 14. The table displays the most probable number (MPN) determined for each volume tested without adjusting for dilution. We included data for both total coliforms and *E. coli* as we believe it could impact the biosensor readings.

**Table 14: Most probable numbers determined for each volume of sample tested**

Sample	Volume used (ml)	Actual count (MPN)		Comment
		Total coliforms	<i>E. coli</i>	
Khoisan river	100	>2419.6	>2419.6	10x serial dilutions done and analysed 1 ml
	10	>2419.6	>2419.6	
	1	>2419.6	2419.6	
	0.1	>2419.6	727	
Khoisan well	100	>2419.6	1413.6	10x serial dilutions done and analysed 1 ml
	10	866.4	118.7	
	1	77.6	13.4	
	0.1	7.5	2	
Edenvale Dam	100	>2419.6	686.7	10x serial dilutions done and analysed 1 ml
	10	>2419.6	83.9	
	1	290.9	8.5	
	0.1	26.2	<1	
Edenvale shore	100	>2419.6	613.1	10x serial dilutions done and analysed 1 ml
	10	1732.9	47.3	
	1	228.2	3	
	0.1	21.6	<1	

The data indicate that for the Edenvale samples, the *E. coli* counts in a 0.1 ml sample are below the detection limit of the test, implying that there are fewer than 1 *E. coli* cell in the sample volume. This conclusion is supported by the theoretical data, which shows 0.85 (Edenvale Dam) and 0.3 (Edenvale shore) *E. coli* cells in the samples, a scenario that is not feasible. In these cases, obtaining variable data with the biosensor is understandable, as it depends on the possibility of an *E. coli* cell being present in the collected sample.

When examining the Khoisan River and well samples, the biosensor should theoretically detect *E. coli*, especially in the river sample. However, there's a possibility that excess other bacteria might interfere or mask the bacteriophages, preventing *E. coli* binding. This interpretation needs to consider the biosensor's detection limit in spiked samples to determine if this is the case. Additionally, it's essential to consider if the bacteriophages used have any *E. coli* strain specificity, binding only to specific strains.

#### 9.4 COMPARISON BETWEEN THE DIGITAL PROBE AND CONVENTIONAL METHODS

The data from the laboratory tests and biosensor conducted on the samples are presented in Table 13. The table displays the Most Probable Number (MPN) determined for the 0.1 ml volume, as it is the equivalent volume tested for the biosensor. Data for both total coliforms and *E. coli* is included, as it might affect the biosensor readings.

**Table 15: Comparison between the conventional methods and digital probe**

Sample	Sample volume (ml)	Conventional method (MPN)		Digital probe % Changes	Comment
		Total coliform	<i>E. coli</i>		
Khoisan river	0.1	>2419.6	727	-5.24 % (Ave)	Below LOD
Khoisan well	0.1	7.5	2	-8.71 % (Ave)	Extremely low
Edenvale Dam	0.1	26.2	<1	19.32 % (Ave)	Contradiction
Edenvale shore	0.1	21.6	<1	2.02 % (Ave)	Extremely low

The data suggest that for the Edenvale samples, the count of *E. coli* in a 0.1 ml sample falls below the detection limit of either method, as indicated by the conventional method, which implies fewer than 1 *E. coli* cell in the sample volume. The biosensor supports this conclusion for Edenvale shore but provides conflicting results for Edenvale Dam. The biosensor indicates a potential contamination in the sample, evidenced by a significant percentage change within the biosensor's operational range. This inconsistency could be attributed to the need to ensure the sample is free from dirt that might obscure the biosensor surface, leading to inaccurate results. Moreover, this dirt might have been non-biological, considering the extremely low total coliform count for this sample.

When examining the Khoisan River and well samples, the conventional method indicated that the river is highly contaminated with both total coliforms and *E. coli*, while the well is relatively less contaminated. Theoretical predictions suggest that the biosensor should be capable of detecting *E. coli*, particularly in the river sample. However, considering the range of the limit of detection encountered in the laboratory during biosensor development, this amount is significantly below the biosensor's limit of detection. After testing the samples from this site, the biosensor did not exhibit any signal changes suggesting contamination. These observations were supported by the actual counts of these sites, which indicated that the actual amount of *E. coli* was well below the biosensor's limit of detection. Additionally, the results from the Khoisan River showed that the biosensor was not affected by the high volume of total coliform counts, suggesting again that something non-biological was interfering with the sample from the Edenvale Dam.

To address the high limit of detection of the biosensor to meet the levels found in natural water sources, we recommend enhancing the production of bacteriophages that can bind more effectively to the natural water *E. coli* strains. Additionally, improving the immobilisation protocol to increase the number of bacteriophages on the biosensor surface and ensuring their correct orientation are very important steps to reduce the limit of detection of the biosensor. Subsequently, concentration methods for the *E. coli* in the samples can be prioritised.

## 9.5 CONCLUSION

The biosensor performed relatively well as intended, successfully testing the water quality in the samples in less than 5 minutes. While it still requires further refinement to improve accuracy and reliability, it operated exceptionally well during its initial real sample testing. We recommend focusing on enhancing the immobilisation protocols to produce a more reliable biosensor with a lower limit of detection for contamination levels in real water sources. This includes developing bacteriophages that are more effective against natural water *E. coli* strains.

Drone adaptation and configuration to sensor apparatus for on-site, real-time digitalised water quality test application.

---

Once a highly reliable biosensor is developed, the next step is to create an automated system for water quality testing. This involves utilising an IDE holder immersed in the water source, with measurements conducted by biosensor electronics housed on a drone. A fluid mechanic system would wash the IDEs after sampling and manage the movement in and out of the PBS solution during measurements. Upon the drone's return to shore, the biosensor IDEs would be replaced for testing the next sample, all while transmitting live data to the base station for onward transmission to the required destinations.

## CHAPTER 10: CONCLUSIONS, RECOMMENDATIONS AND KNOWLEDGE DISSEMINATION

---

### 10.1 CONCLUSIONS

The aim of the project was 1) to develop a drone winch system for the lifting and the transport of digital probes and water sample collection; 2) to develop a remote test platform for onsite real time digitalised water quality test application.

The University of Johannesburg has designed and developed a water sampling/collection bag to be attached to the drone to sample water from various water sources. It was tested for strength, weight and depth collection of water samples. Together with Drobotics and LS communications it was further tested for attachment, and release from the drone. This was successfully achieved. In conjunction with developing the water collection bag a housing unit for the biosensor is being developed for the digital bacterial probe. Tests and analysis are underway to produce the final housing unit. Drobotics has successfully demonstrated its winch/hoist/jig/communications systems within operational environments in real and or near real-time water quality test applications as per project objectives.

Stellenbosch University thus far has achieved that the biorecognition element of the digital probe will be bacteriophages, and the correct immobilisation of these bacteriophages improves the sensitivity and performance of the probe. At the time of writing the digital probe's transduction mechanism was being optimised and tested. The digital probe's communication protocol to the system (winch and mobile laboratory) is being designed and tested with Drobotics and University of Johannesburg. This communication link via WI-FI has been completed.

In parallel two water source sites have been identified and selected to be used for the comparison of the digital bacterial probe data to standard IDEXX Colilert® Quanti-Tray® method. On 31 January 2024 the testing and validation was implemented at these sites, whereby the successful launch of chemical sensor probes via the Drone platform in geo-referenced locality transmitting results in real-time to the laptop located at the mobile laboratory. Successful water sampling using sampling bags of the Drone platform was conducted at precise geo-referenced points as chemical sensor probes *in situ* test localities. Successful testing of the biosensor for the water quality in the samples occurred in less than 5 minutes and providing results offshore. Despite the inability to test the biosensor directly via the drone, the project's goals have been met, with recommendations for further enhancements proposed.

### 10.2 RECOMMENDATIONS

- 1) The biosensor has successfully demonstrated its capability as a proof of concept for detecting the presence of *E. coli*. However, further refinement is necessary to develop a biosensor with better repeatability (currently, we are using three IDE chips per test, which leads to outliers, but the goal is to use one IDE chip per test). Also aim to achieve a very linear response and a low detection limit for water source samples. To achieve this, we recommend the following steps:
  - a. Additional work is needed on the development of protocols to uniformly immobilise bacteriophages on solid substrates. By optimising these protocols, we aim to enhance the performance and versatility of the biosensor. This will enable us to control the immobilisation process better, resulting in a more consistent biosensor without the outliers.

- b. Enhancing the production of bacteriophages that can bind more effectively to the natural water *E. coli* strains.
  - c. Increasing the biosensor sensitivity by increasing the effective surface area of the IDEs to allow for more bacteriophages to immobilise on the IDE fingers.
  - d. The relative accuracy of a 100 µl sample representing the water source compared to conventional methods that collect larger sample volumes, potentially offers a more accurate representation of the source.
  - e. Subsequently, this prioritises concentration methods for the *E. coli* in the samples.
- 2) Develop and implement a uniform protocol for the calibration of digital chemical probes and handheld probes. This should include standardised procedures for calibration, maintenance, and validation to ensure accuracy and reliability across different environments and operators.
  - 3) Developments in drone technology to improve the efficiency of water sample collection and biosensor testing. This could include longer flight times, enhanced stability in diverse weather conditions, and autonomous navigation systems for more accurate sample collection locations.
  - 4) Formulate strategies for scaling the technology for widespread use, including cost reduction techniques, training programs for potential users, and deployment logistics. Collaboration with governmental and non-governmental organisations could be pivotal in this aspect.

### 10.3 KNOWLEDGE DISSEMINATION

#### Conferences

- SUN presented at SASM, SA 2023
- UJ submitted abstract to IWA Canada 2024
- UJ submitted abstract to WISA 2024 Biennial Conference & Exhibition 2024.

#### Magazine

- Published article in the WRC's Water Wheel magazine in June 2023.

#### Articles to be submitted for publications

- A literature review article on water sampling techniques and the use of biosensors as on-site diagnostic method.
- A literature review article on the use of drone technology in water sampling.

## REFERENCES

---

- Aaron, J., van Zyl, L. J., & Dicks, L. M. T. (2022). Isolation and characterization of lytic proteus virus 309. *Viruses*, *14*(6). <https://doi.org/10.3390/v14061309>
- Ahovan, Z. A., Hashemi, A., De Plano, L. M., Gholipourmalekabadi, M., & Seifalian, A. (2020). Bacteriophage based biosensors: Trends, outcomes and challenges. *Nanomaterials*, *10*(3). <https://doi.org/10.3390/nano10030501>
- Ahuja, S. (2017). Chapter One - Overview: Sustaining Water, the World's Most Crucial Resource. In S. Ahuja (Ed.), *Chemistry and Water* (pp. 1–22). Elsevier. <https://doi.org/10.1016/B978-0-12-809330-6.00001-5>
- Albert, J. (2000). Rethinking the management of transboundary freshwater resources: A critical examination of modern international law and practice. *Natural Resources Forum*, *24*(1), 21–30. <https://doi.org/10.1111/j.1477-8947.2000.tb00926.x>
- Arya, S. K., Singh, A., Naidoo, R., Wu, P., McDermott, M. T., & Evoy, S. (2011). Chemically immobilized T4-bacteriophage for specific *Escherichia coli* detection using surface plasmon resonance. *Analyst*, *136*(3), 486–492.
- Atiq, M., Naeem, I., Sahi, S. T., Rajput, N. A., Haider, E., Usman, M., Shahbaz, H., Fatima, K., Arif, E., & Qayyum, A. (2020). Nanoparticles: a safe way towards fungal diseases. *Archives of Phytopathology and Plant Protection*, *781–792*. <https://doi.org/10.1080/03235408.2020.1792599>
- Aquagenx. (n.d.). How to use CBT E. coli Water Test Kit. Available from: <https://www.aquagenx.com/how-to-use-cbt-ectc/>
- Babacan, S., Pivarnik, P., Letcher, S., & Rand, A. G. (2000). Evaluation of antibody immobilization methods for piezoelectric biosensor application. *Biosensors and Bioelectronics*, *15*(11–12), 615621. [https://doi.org/10.1016/S0956-5663\(00\)00115-9](https://doi.org/10.1016/S0956-5663(00)00115-9)
- Balasubramanian, S., Sorokulova, I. B., Vodyanoy, V. J., & Simonian, A. L. (2007). Lytic phage as a specific and selective probe for detection of *Staphylococcus aureus* - a surface plasmon resonance spectroscopic study. *Biosensors and Bioelectronics*, *22*(6), 948–955.
- Basili, M., Perini, L., Zaggia, L., Luna, G. M., & Quero, G. M. (2023). Integrating culture-based and molecular methods provides an improved assessment of microbial quality in a coastal lagoon. *Environmental Pollution*, *334*, 122140. <https://doi.org/10.1016/J.ENVPOL.2023.122140>
- Batani, G., Bayer, K., Böge, J., Hentschel, U., & Thomas, T. (2019). Fluorescence *in situ* hybridization (FISH) and cell sorting of living bacteria. *Scientific Reports*, *9*(1). <https://doi.org/10.1038/s41598-019-55049-2>
- Bhalla, N., Jolly, P., Formisano, N., & Estrela, P. (2016). Introduction to biosensors. *Essays in Biochemistry*, *60*(1), 1–8. doi:10.1042/EBC20150001
- Boretti, A., & Rosa, L. (2019). Reassessing the projections of the World Water Development Report. *Npj Clean Water*, *2*(1). <https://doi.org/10.1038/s41545-019-0039-9>
- Cesewski, E., & Johnson, B. N. (2020). Electrochemical biosensors for pathogen detection. *Biosensors and Bioelectronics*, *159*. doi:10.1016/j.bios.2020.112214
- Chai, Y., Li, S., Horikawa, S., Park, M. K., Vodyanoy, V., & Chin, B. A. (2012). Rapid and sensitive detection of *Salmonella typhimurium* on eggshells by using wireless biosensors. *Journal of Food Protection*, *75*(4), 631–636. <https://doi.org/10.4315/0362-028X.JFP-11-339>
- Chang, L., Li, J., & Wang, L. (2016). Immuno-PCR: An ultrasensitive immunoassay for biomolecular detection. *Analytica Chimica Acta*, *910*, 12–24. <https://doi.org/10.1016/J.ACA.2015.12.039>
- Covert, T. C., Shadix, L. C., Rice, E. W., Haines, J. R., & Freyberg, R. W. (1989). Evaluation of the auto analysis Colilert test for detection and enumeration of total coliforms. *Applied and Environmental Microbiology*, *55*(9), 2443–2447.

- Covert, T. C., Rice, E. W., Johnson, S. A., Berman, D., Johnson, C. H., & Mason, P. J. (1992). Comparing defined-substrate coliform tests for the detection of *Escherichia coli* in water. *Journal of the American Water Works Association*, 84(2), 98–104.
- Dąbrowiecki, Z., Dąbrowiecka, M., Olszański, R., & Siermontowski, P. (2019). Developing a methodology for testing and preliminary determination of the presence of *Legionella* Spp. and *Legionella pneumophila* in environmental water samples by immunomagnetic separation combined with flow cytometry. *Polish Hyperbaric Research*, 68(3), 71–92. <https://doi.org/doi:10.2478/phr-2019-0013>
- DeSarno, M., Warden, P. S., Eldred, B. J., & Fricker, C. R. (2018). Multicentre study of the performance of methodologies for the detection of coliforms and *E. coli* In drinking water. *Water Institute of South Africa*, Paper 157.
- Dixon, P. F. (1987). Detection of *Renibacterium salmoninarum* by the enzyme-linked immunosorbent assay (ELISA). *Journal of Applied Ichthyology*, 3, 77-82. <https://doi.org/10.1111/j.1439-0426.1987.tb00456.x>
- Ebrahim, T. (2023). *The development of a biosensor for the early detection of pancreatic cancer*. Doctoral dissertation, Stellenbosch University. Retrieved from <http://hdl.handle.net/10019.1/127182>.
- Eccles, J. P., Searle, R., Holt, D., & Dennis, P. J. (2004). A comparison of methods used to enumerate *Escherichia coli* in conventionally treated sewage sludge. *Journal of Applied Microbiology*, 96, 375-383. <https://doi.org/10.1046/j.1365-2672.2004.02165>.
- Eckner, K. F. (1998). Comparison of membrane filtration and multiple-tube fermentation by the Colilert and Enterolert methods for detection of waterborne coliform bacteria, *Escherichia coli*, and enterococci used in drinking and bathing water quality monitoring in southern Sweden. *Applied and Environmental Microbiology*, 64(8), 3079–3083.
- Edberg, S. C., Allen, M. J., Smith, D. B., & the National Collaborative Study. (1988). National field evaluation of a defined substrate method for the simultaneous enumeration of total coliforms and *Escherichia coli* from drinking water: Comparison with the standard multiple tube fermentation method. *Applied and Environmental Microbiology*, 54(6), 1595–1601.
- Erena, M., Atenza, J. F., Garcia-Galiano, S., Dominguez, J. A., & Bernabe, J. M. (2019). Use of drones for the topo-bathymetric monitoring of the reservoirs of the Segura River basin." *MDPI Water*, 11(445), 1-16. doi: 10.3390/w11030445.
- Ertürk, G., & Lood, R. (2018). Bacteriophages as biorecognition elements in capacitive biosensors: Phage and host bacteria detection. *Sensors and Actuators, B: Chemical*, 258, 535–543. <https://doi.org/10.1016/j.snb.2017.11.117>
- Gervais, L., Gel, M., Allain, B., Tolba, M., Brovko, L., Zourob, M., Mandeville, R., Griffiths, M., & Evoy, S. (2007a). Immobilization of biotinylated bacteriophages on biosensor surfaces. *Sensors and Actuators B: Chemical*, 125(2), 615–621. <https://doi.org/10.1016/J.SNB.2007.03.007>
- Gonzalez, A., Gaines, M., Gallegos, L. Y., Guevara, R., & Gomez, F. A. (2018). Enzyme-linked immunosorbent assays (ELISA) based on thread, paper, and fabric. *Electrophoresis*, 39(4), 476-484. <https://doi.org/10.1002/elps.201700354>
- González, I., Martín, R., García, T., Morales, P., Sanz, B., & Hernández, P. E. (1993). A sandwich enzyme-linked immunosorbent assay (ELISA) for detection of *Pseudomonas fluorescens* and related psychrotrophic bacteria in refrigerated milk. *Journal of Applied Bacteriology*, 74, 394-401. <https://doi.org/10.1111/j.1365-2672.1993.tb05144.x>
- Gunda, N. S. K., & Mitra, S. K. (2016). Rapid water quality monitoring for microbial contamination. *The Electrochemical Society Interface*, 25(4), 73. <https://dx.doi.org/10.1149/2.F06164if>
- HACH, South Africa. (n.d.). Hydrogen Sulfide Test Kit, Model HS-C1. Retrieved January 13, 2023 from <https://za.hach.com/hydrogen-sulfide-test-kit-model-hs-c1/product?id=55240876302>
- Halámek, J., Přebyl, J., Makower, A., Skládal, P., & Scheller, F. W. (2005). Sensitive detection of organophosphates in river water by means of a piezoelectric biosensor. *Analytical and Bioanalytical Chemistry*, 382(8), 1904–1911. <https://doi.org/10.1007/s00216-005-3260-y>

- Hameed, S., Xie, L., & Ying, Y. (2018). Conventional and emerging detection techniques for pathogenic bacteria in food science: A review. *Trends in Food Science & Technology*, *81*, 61–73. <https://doi.org/10.1016/J.TIFS.2018.05.020>
- Hiremath, N., Guntupalli, R., Vodanyoy, V., Chin, B. A., & Park, M. K. (2015). Detection of methicillin-resistant *Staphylococcus aureus* using novel lytic phage-based magnetoelastic biosensors. *Sensors and Actuators, B: Chemical*, *210*, 129–136. <https://doi.org/10.1016/j.snb.2014.12.083>
- Hoefel, D., Grooby, W. L., Monis, P. T., Andrews, S., & Saint, C. P. (2003). Enumeration of water-borne bacteria using viability assays and flow cytometry: A comparison to culture-based techniques. *Journal of Microbiological Methods*, *55*(3), 585–597. [https://doi.org/10.1016/S0167-7012\(03\)00201-X](https://doi.org/10.1016/S0167-7012(03)00201-X)
- Hussain, B., Yüce, M., Ullah, N., & Budak, H. (2017). Bioconjugated nanomaterials for monitoring food contamination. *Nanobiosensors*, 93–127. <https://doi.org/10.1016/B978-0-12-804301-1.00003-5>
- Ionescu, R. E. (2022). Use of cysteamine and glutaraldehyde chemicals for robust functionalization of substrates with protein biomarkers - an overview on the construction of biosensors with different transductions. *Biosensors*, *12*(8), 581. <https://doi.org/10.3390/bios12080581>
- Jones, J. L. (2015). High throughput screening of seafood for foodborne pathogens. *High Throughput Screening for Food Safety Assessment: Biosensor Technologies, Hyperspectral Imaging and Practical Applications*, 491–505. <https://doi.org/10.1016/B978-0-85709-801-6.00020-4>
- Kadadou, D., Tizani, L., Wadi, V. S., Banat, F., Alsafar, H., Yousef, A. F., Barceló, D., & Hasan, S. W. (2022). Recent advances in the biosensors application for the detection of bacteria and viruses in wastewater. *Journal of Environmental Chemical Engineering*, *10*(1), <https://doi.org/10.1016/j.jece.2021.107070>
- Kaya, H. O., Cetin, A. E., Azimzadeh, M., & Topkaya, S. N. (2021). Pathogen detection with electrochemical biosensors: Advantages, challenges and future perspectives. *Journal of Electroanalytical Chemistry*, *882*. <https://doi.org/10.1016/j.jelechem.2021.114989>
- Kuo, J. T., Chang, L. L., Yen, C. Y., Tsai, T. H., Chang, Y. C., Huang, Y. T., & Chung, Y. C. (2021). Development of fluorescence *in situ* hybridization as a rapid, accurate method for detecting coliforms in water samples. *Biosensors*, *11*(1). <https://doi.org/10.3390/bios11010008>.
- Kusangaya, S., Warburton, M. L., Van Garderen, E. A., & Jewitt, G. P. W. (2021) Impacts of climate change on water resources in Southern Africa: A Review. [online], Available from: <https://researchspace.csir.co.za/dspace/bitstream/handle/10204/7382/Archer%20van%20Gardere%202013.pdf?sequence=3>, [Accessed 2022].
- Lagier, J. C., Edouard, S., Pagnier, I., Mediannikov, O., Drancourt, M., & Raoult, D. (2015). Current and past strategies for bacterial culture in clinical microbiology. *Clinical Microbiology Reviews*, *28*(1), 208–236. <https://doi.org/10.1128/CMR.00110-14>
- Lazcka, O., Del Campo, F. J., & Muñoz, F. X. (2007). Pathogen detection: A perspective of traditional methods and biosensors. *Biosensors and Bioelectronics*, *22*(7), 1205–1217. <https://doi.org/10.1016/j.bios.2006.06.036>
- Leclerc, H., Mossel, D. A. A., Edberg, S. C., & Struijk, C. B. (2001). Advances in the bacteriology of the coliform group: Their suitability as markers of microbial water safety. *Annual Review of Microbiology*, *55*(1), 201–234. <https://doi.org/10.1146/annurev.micro.55.1.201>
- Lee, J. W., Song, J., Hwang, M. P., & Lee, K. H. (2013). Nanoscale bacteriophage biosensors beyond phage display. *International Journal of Nanomedicine*, *8*, 3917–3925. <https://doi.org/10.2147/IJN.S51894>
- Li, D., Liu, L., Huang, Q., Tong, T., Zhou, Y., Li, Z., Bai, Q., Liang, H., & Chen, L. (2021). Recent advances on aptamer-based biosensors for detection of pathogenic bacteria. *World Journal of Microbiology and Biotechnology*, *37*(3), 45. <https://doi.org/10.1007/s11274-021-03002-9>
- Li, S., Li, Y., Chen, H., Horikawa, S., Shen, W., Simonian, A., & Chin, B. A. (2010). Direct detection of *Salmonella typhimurium* on fresh produce using phage-based magnetoelastic biosensors. *Biosensors and Bioelectronics*, *26*(4), 1313–1319. <https://doi.org/10.1016/j.bios.2010.07.029>

- Li, X., Li, X., Guo, Y., Liu, Y., Mei, S., Song, X., Li, J., Grugbaye, A. G., Li, J., & Xu, K. (2019). Development and assessment of a paper-based enzyme-linked immunosorbent assay for the colorimetric diagnosis of human brucellosis. *Analytical Letters*, 52(10), 1614-1628. <https://doi.org/10.1080/00032719.2018.1563939>.
- Liu, S., Zhao, K., Huang, M., Zeng, M., Deng, Y., Li, S., Chen, H., Li, W., & Chen, Z. (2022). Research progress on detection techniques for point-of-care testing of foodborne pathogens. In *Frontiers in Bioengineering and Biotechnology*, 10. <https://doi.org/10.3389/fbioe.2022.958134>
- Luo, X., & Davis, J. J. (2013). Electrical biosensors and the label free detection of protein disease biomarkers. *Chemical Society Reviews*, 42(13), 5944–5962. <https://doi.org/10.1039/c3cs60077g>
- Maas, M. B., Perold, W. J., & Dicks, L. M. T. (2017). Biosensors for the detection of *Escherichia coli*. *Water SA*, 43(4), 707–721. South African Water Research Commission. <https://doi.org/10.4314/wsa.v43i4.17>
- Maas, M. B., Maybery, G. H. C., Perold, W. J., Neveling, D. P., & Dicks, L. M. T. (2018). Borosilicate glass fiber-optic biosensor for the detection of *Escherichia coli*. *Current Microbiology*, 75(2), 150–155. <https://doi.org/10.1007/s00284-017-1359-y>
- Maas, M., Brischwein, M., Los, P., Perold, W., & Dicks, L. (2018). Evaluating nonlinear impedance excitation as detection method for biosensors. *IEEE Transactions on Nanotechnology*, 17(5), 1069–1076. <https://doi.org/10.1109/TNANO.2018.2864572>
- Mairal, T., Cengiz Özalp, V., Lozano Sánchez, P., Mir, M., Katakis, I., & O'Sullivan, C. K. (2008). Aptamers: Molecular tools for analytical applications. *Analytical and Bioanalytical Chemistry*, 390(4), 989–1007. <https://doi.org/10.1007/s00216-007-1346-4>
- Matner, R. R., Fox, T. L., McIver, D. E., & Curiale, M. S. (1990). Efficacy of Petrifilm™ *E. coli* count plates for *E. coli* and coliform enumeration. *Journal of Food Protection*, 53(2), 145-150. <https://doi.org/10.4315/0362-028X-53.2.145>
- McClure, M. (2021). What are the causes and effects of water pollution in Africa? *Greenpeace* [online]. Available from: <https://www.greenpeace.org/africa/en/blogs/49015/what-are-the-causes-and-effects-of-water-pollution-in-africa/>, [Accessed 2022].
- MERCK. (n.d.). "ELISA protocols." Available from: <https://www.sigmaaldrich.com/ZA/en/technical-documents/protocol/protein-biology/elisa/elisa-protocols>. [Accessed 2024].
- Murcott, S., Keegan, M., Hanson, A., Jain, A., Knutson, J., Liu, S., Tanphanich, J., & Wong, T. K. (2015). Evaluation of microbial water quality tests for humanitarian emergency and development settings. *Procedia Engineering*, 107, 237-246. <https://doi.org/10.1016/j.proeng.2015.06.078>
- Nanduri, V., Sorokulova, I. B., Samoylov, A. M., Simonian, A. L., Petrenko, V. A., & Vodyanoy, V. (2007). Phage as a molecular recognition element in biosensors immobilized by physical adsorption. *Biosensors and Bioelectronics*, 22(6), 986–992.
- Neveling, D. P., Van Den Heever, T. S., Perold, W. J., & Dicks, L. M. T. (2014). A nanoforce ZnO nanowire-array biosensor for the detection and quantification of immunoglobulins. *Sensors and Actuators, B: Chemical*, 203(December), 102–110. <https://doi.org/10.1016/j.snb.2014.06.076>
- Niemela, S. I., Lee, J. V., & Fricker, C. R. (2003). A comparison of the International Standards Organisation reference method for the detection of coliforms and *Escherichia coli* in water with a defined substrate procedure. *Journal of Applied Microbiology*, 95(6), 1285–1292. <https://doi.org/10.1046/j.1365-2672.2003.02099>
- Nikkhoo, N., Cumby, N., Gulak, P. G., & Maxwell, K. L. (2016) Rapid bacterial detection via an all-electronic CMOS biosensor." *PLoS ONE*, 11(9), e0162438. doi:10.1371/journal.pone.0162438
- Nnachi, R. C., Sui, N., Ke, B., Luo, Z., Bhalla, N., He, D., & Yang, Z. (2022). Biosensors for rapid detection of bacterial pathogens in water, food and environment. *Environment International*, 166, 107357. <https://doi.org/10.1016/J.ENVINT.2022.107357>
- Offenbaume, K. L., Bertone, E., & Stewart, R. A. (2020). Monitoring approaches for faecal indicator bacteria in water: Visioning a remote real-time sensor for *E. coli* and enterococci. *Water (Switzerland)*, 12(9). <https://doi.org/10.3390/w12092591>

- Olsen, E. V., Sorokulova, I. B., Petrenko, V. A., Chen, I. H., Barbaree, J. M., & Vodyanoy, V. J. (2006). Affinity-selected filamentous bacteriophage as a probe for acoustic wave bio detectors of *Salmonella typhimurium*. *Biosensors and Bioelectronics*, 21(8), 1434–1442.
- Olsson, S. (2018). *Drones in arctic environments: Development of automatic water sampler for aerial drones*. Research dissertation in fulfilment of Master's thesis in Mechanical Engineering, KTH Royal Institute of Technology School of Industrial Engineering and Management.
- Paczesny, J., Cuervo, A., Burrowes, B., Orlova, E. V., Richter, R., Kutateladze, M., & Letarov, A. V. (2020). *Bacteriophages: Biology, Technology, Therapy*. Springer.
- Pang, B., Zhao, C., Li, L., Song, X., Xu, K., Wang, J., Liu, Y., Fu, K., Bao, H., Song, D., Meng, X., Qu, X., Zhang, Z., & Li, J. (2018). Development of a low-cost paper-based ELISA method for rapid *Escherichia coli* O157:H7 detection. *Analytical Biochemistry*, 542, 58–62. <https://doi.org/10.1016/j.ab.2017.11.010>
- Patil, P. N. (2012). Physico-chemical parameters for testing of water - A review IPA-Under Creative Commons license 3.0. *International Journal of Environmental Sciences*, 3(3). <https://www.researchgate.net/publication/344323634>
- Pilevar, M., Kim, K. T., & Lee, W. H. (2021). Recent advances in biosensors for detecting viruses in water and wastewater. *Journal of Hazardous Materials*, 410, 124656. doi:10.1016/j.jhazmat.2020.124656
- Pisciotta, J. M., Rath, D. F., Stanek, P. A., Flanery, D. M., & Harwood, V. J. (2002). Marine bacteria cause false-positive results in the Colilert-18 rapid identification test for *Escherichia coli* in Florida waters. *Applied and Environmental Microbiology*, 68(2), 539–544. <https://doi.org/10.1128/AEM.68.2.539-544.2002>
- Popli, S. (2023). The molecular techniques to identify plant host-virus interactions and their implications on transmission. *Plant RNA Viruses: Molecular Pathogenesis and Management*, 285–296. <https://doi.org/10.1016/B978-0-323-95339-9.00026-0>
- PubChem Compound Summary for CID 3485, Glutaraldehyde. (2023).
- PubChem Compound Summary for CID 6058, Cysteamine. (2023).
- Ramees, T. P., Dhama, K., Karthik, K., Rathore, R. S., Kumar, A., Saminathan, M., Tiwari, R., Malik, Y. S., & Singh, R. K. (2017). Arcobacter: An emerging food-borne zoonotic pathogen, its public health concerns and advances in diagnosis and control - A comprehensive review. *Veterinary Quarterly*, 37(1), 136–161. <https://doi.org/10.1080/01652176.2017.1323355>
- Richter, L., Matula, K., Leśniewski, A., Kwaśnicka, K., Los, J., Paczesny, J., & Holyst, R. (2016). Ordering of bacteriophages in the electric field: Application for bacteria detection. *Sensors and Actuators B: Chemical*, 224, 233–240.
- Richter, L., Bielec, K., Lesniewski, A., Los, M., Paczesny, J., & Holyst, R. (2017). Dense layer of bacteriophages ordered in alternating electric field and immobilized by surface chemical modification as sensing element for bacteria detection. *ACS Applied Materials & Interfaces*, 9(23), 19622–19629.
- Rompré, A., Servais, P., Baudart, J., De-Roubin, M. R., & Laurent, P. (2002). Detection and enumeration of coliforms in drinking water: Current methods and emerging approaches. *Journal of Microbiological Methods*, 49(1), 31–54. [https://doi.org/10.1016/S0167-7012\(01\)00351-7](https://doi.org/10.1016/S0167-7012(01)00351-7)
- Rosner, D., & Clark, J. (2021). Formulations for bacteriophage therapy and the potential uses of immobilization. *Pharmaceuticals*, 14(4), 359.
- Roth Bioscience. (2022). Evaluation of Easygel Card (now renamed to R-Card®) for Detection of Aerobic Bacteria Counts. Available from: <https://www.rothbioscience.com/blogs/news/evaluation-of-easygel-card-now-renamed-to-r-card-for-detection-of-aerobic-bacteria-counts>. [Accessed 2024].
- Sartory, D. P., & Howard, L. (1992). A medium detecting  $\beta$ -glucuronidase for the simultaneous membrane filtration enumeration of *Escherichia coli* and coliforms from drinking water. *Letters in Applied Microbiology*, 15(6), 273–276. <https://doi.org/10.1111/j.1472-765X.1992.tb00782.x>
- Sartory, D. P., & Watkins, J. (1999). Conventional culture for water quality assessment: Is there a future? *Journal of Applied Microbiology Symposium Supplement*, 85(28). <https://doi.org/10.1111/j.1365-2672.1998.tb05302.x>

- Shan, S., Liu, D., Guo, Q., Wu, S., Chen, R., Luo, K., Hu, L., Xiong, Y., & Lai, W. (2016). Sensitive detection of *Escherichia coli* O157:H7 based on cascade signal amplification in ELISA. *Journal of Dairy Science*, 99(9), 7025-7032. <https://doi.org/10.3168/jds.2016-11320>
- Singh, A., Glass, N., Tolba, M., Brovko, L., Griffiths, M., & Evoy, S. (2009). Immobilization of bacteriophages on gold surfaces for the specific capture of pathogens. *Biosensors and Bioelectronics*, 24(12), 3645–3651
- Skládal, P. (2016). Piezoelectric biosensors. *TrAC - Trends in Analytical Chemistry*, 79, 127–133. <https://doi.org/10.1016/j.trac.2015.12.009>
- ThermoFisher Scientific. (n.d.). Antibodies and immunoassays for pathway research: ELISA kits and ELISA components. Available from: <https://www.thermofisher.com/za/en/home/life-science/antibodies/immunoassays/elisa-kits.html> [Accessed 2024].
- Thévenot, D. R., Toth, K., Durst, R. A., & Wilson, G. S. (2001). Electrochemical biosensors: Recommended definitions and classification. *Biosensors and Bioelectronics*, 16(1–2), 121–131. [https://doi.org/10.1016/S0956-5663\(01\)00115-4](https://doi.org/10.1016/S0956-5663(01)00115-4)
- Tombelli, S., & Mascini, M. (2000). Piezoelectric quartz crystal biosensors: Recent immobilisation schemes. *Analytical Letters*, 33(11), 2129–2151. <https://doi.org/10.1080/00032710008543179>
- Välilä, A. L., Tilsala-Timisjärvi, A., & Virtanen, E. (2015). Rapid detection and identification methods for *Listeria monocytogenes* in the food chain – A review. *Food Control*, 55, 103–114. <https://doi.org/10.1016/J.FOODCONT.2015.02.037>
- Viazis, S., Akhtar, M., Feirtag, J., Brabban, A. D., & Diez-Gonzalez, F. (2011). Isolation and characterization of lytic bacteriophages against enterohaemorrhagic *Escherichia coli*. *Journal of Applied Microbiology*, 110(5), 1323–1331. <https://doi.org/10.1111/j.1365-2672.2011.04989.x>
- Viviers, C., Du Toit, A., Perold, W., Loos, B., & Hofmeyr, J. H. (2020). A resistive biosensor for the detection of LC3 Protein in autophagy. *IEEE Sensors Journal*, 20(10), 5119–5129. <https://doi.org/10.1109/JSEN.2020.2970479>
- Vo-Dinh, T., & Cullum, B. (2000). Biosensors and biochips: Advances in biological and medical diagnostics. *Fresenius' Journal of Analytical Chemistry*, 366(6–7), 540–551. <https://doi.org/10.1007/s002160051549>
- World Health Organization. (2017). *Guidelines for Drinking-water Quality: Fourth Edition Incorporating the First Addendum*. Geneva. WHO Guidelines Approved by the Guidelines Review Committee. PMID: 28759192. Bookshelf ID: NBK442376.
- UNICEF, Office of Innovation (2022) [online]. Available from: <https://www.unicef.org/innovation/rapid-water-quality-testing> [Accessed 2022].
- Wagtech projects (2022) [online]. Available from: [www.wagtech.com](http://www.wagtech.com). [Accessed 2023].
- Yun, Y. H., Eteshola, E., Bhattacharya, A., Dong, Z., Shim, J. S., Conforti, L., Kim, D., Schulz, M. J., Ahn, C. H., & Watts, N. (2009). Tiny medicine: Nanomaterial-based biosensors. *Sensors*, 9(11), 9275–9299. <https://doi.org/10.3390/s91109275>
- Zhou, Y., Marar, A., Kner, P., & Ramasamy, R. P. (2017). Charge-directed immobilization of bacteriophage on nanostructured electrode for whole-cell electrochemical biosensors. *Analytical Chemistry*, 89(11), 5734–5741. <https://doi.org/10.1021/acs.analchem.6b03751>

## APPENDIX A: SIMULATION PARAMETERS

**Table 11: Simulation parameters**

1. D (diffusion coefficient of the redox pair)	7e-10 [m <sup>2</sup> /s]
2. C <sub>red</sub> (bulk concentration of Fe(CN) <sub>6</sub> <sup>4-</sup> )	1 [mol/m <sup>3</sup> ]
3. C <sub>ox</sub> (bulk concentration of Fe(CN) <sub>6</sub> <sup>3-</sup> )	0 [mol/m <sup>3</sup> ]
4. ko1 (standard heterogeneous rate on a bare gold electrode)	2.5e-4 [m/s]
5. ko2 (standard heterogeneous rate on an immobilized gold electrode)	6.7e-7 [m/s]
6. α (dimensionless transfer coefficient)	0.5 [ ]
7. C <sub>dl</sub> (double layer interfacial capacitance)	20 [uF/cm <sup>2</sup> ]
8. I <sub>oref</sub> (Exchange current density at the reference state)	ko1*F_const*1[M]
9. freq <sub>min</sub> (minimum chosen EIS simulation frequency)	0.01 [Hz]
10. freq <sub>max</sub> (maximum chosen EIS simulation frequency)	1e6 [Hz]
11. log_freq <sub>min</sub> (Log of min frequency)	log <sub>10</sub> (freq <sub>min</sub> [1/Hz])
12. log_freq <sub>max</sub> (Log of max frequency)	log <sub>10</sub> (freq <sub>max</sub> [1/Hz])
13. x <sub>diff_max</sub> (mean diffusion layer thickness at min frequency)	sqrt(D/(2*pi*freq <sub>min</sub> ))
14. x <sub>diff_min</sub> (mean diffusion layer thickness at max frequency)	sqrt(D/(2*pi*freq <sub>max</sub> ))
15. H (height of the simulation model)	x <sub>diff_max</sub> *10
16. W (width of 1 electrode times 4)	400 [um]
17. L <sub>we</sub> (length of the working electrode)	(W/4)
18. L <sub>ce</sub> (length of the counter electrode)	(W/4)
19. L <sub>gap</sub> (length of the gap between electrodes)	(W/4)